

DEVELOPMENT OF AN ELECTROSTATIC AIR SAMPLER AS AN ALTERNATIVE
METHOD FOR AEROSOL IN VITRO EXPOSURE STUDIES

Jose Zavala

A dissertation submitted to the faculty of the University of North Carolina at Chapel Hill in partial fulfillment of the requirements for the degree of Doctor of Philosophy in the Department of Environmental Sciences and Engineering in the Gillings School of Global Public Health.

Chapel Hill
2014

Approved by:

J. Jason West

Kenneth G. Sexton

Harvey E. Jeffries

Ilona Jaspers

Johnny L. Carson

© 2014
Jose Zavala
ALL RIGHTS RESERVED

ABSTRACT

Jose Zavala: Development of an Electrostatic Air Sampler as an Alternative Method for
Aerosol In Vitro Exposure Studies
(Under the direction of J. Jason West)

There is growing interest in studying the toxicity and health risk of exposure to multi-pollutant mixtures found in ambient air, and the U.S. Environmental Protection Agency (EPA) is moving towards setting standards for these types of mixtures. Additionally, the Health Effects Institute's strategic plan aims to develop and apply next-generation multi-pollutant approaches to understanding the health effects of air pollutants. There's increasing concern that conventional *in vitro* exposure methods are not adequate to meet EPA's strategic plan to demonstrate a direct link between air pollution and health effects. To meet the demand for new *in vitro* technology that better represents direct air-to-cell inhalation exposures, a new system that exposes cells at the air-liquid interface was developed. This new system, named the Gillings Sampler, is a modified two-stage electrostatic precipitator that provides a viable environment for cultured cells. The performance of the sampler was evaluated under controlled laboratory conditions. Fluorescent polystyrene latex spheres were used to determine deposition efficiencies (38-45%), while microscopy and imaging techniques verified particle deposition. Negative control cell exposures indicated the sampler can be operated for up to 4 hours without inducing any significant toxic effects on the cells. A novel positive aerosol control exposure method was also developed to test this system. This new positive control test confirmed that reproducible biological results can be obtained

when exposing cultured cells with the Gillings Sampler. Further testing exposing cells to various test atmospheres included diesel exhaust, kerosene soot, secondary organic aerosols, and ozone. Results showed various cell types (human and mouse) can be used with the Gillings Sampler and estimated doses less than $1 \mu\text{g}/\text{cm}^2$ can elicit acute biological effects on cultured cells. These tests demonstrated the advantages of the sampler and also highlighted limitations to be addressed in the future. The Gillings Sampler is intended to be used as an alternative research tool for aerosol *in vitro* exposure studies and while further testing and optimization is still required to produce a "commercially ready" system, it serves as a stepping-stone in the development of cost-effective *in vitro* technology that can be made accessible to researchers in the near future.

To my family, for all their support, motivation, and words of encouragement that have helped me get to where I am today. ¡Si Se Pudo!

To my wife, for believing in me and accompanying me in this journey. Thank you for always being there for me. I couldn't have done this without you. Te Amo!

ACKNOWLEDGEMENTS

I would like to thank all of those that have helped me throughout the years, both personally and academically during my tenure at UNC-Chapel Hill.

My research advisor - Dr. Kenneth Sexton; I am grateful that I had the opportunity to work side-by-side with you and learn from your knowledge. I have learned tremendously from you. Thank you!

My committee – Drs. Harvey Jeffries, Jason West, Ilona Jaspers, and Johnny Carson; Thank you for all of your guidance, contributions, and willingness to always help me in any way possible.

Funding; This work was supported in part by grants from the National Institute of Environmental Health Sciences (T32 ES007018, R01 ES15241-S1, and R01 ES013611) and the Gillings School of Global Public Health's Gillings Innovation Laboratory Program for Research and Innovations Solutions.

Collaborators; I would like to thank Dr. Glenn W. Walters and D.J. Fedor from the Environmental Sciences and Engineering (ESE) Design Center for their collaboration in the design and manufacturing of the Gillings Sampler. My research couldn't have been possible without their great work. I thank Dr. David Leith for his guidance and involvement in my research. I also thank Missy Brighton from the Center for Environmental Medicine, Asthma,

and Lung Biology (CEMALB), for all of their technical help. Lastly, I thank Dr. William Vizuete, for all of his guidance and assistance throughout the years.

My Co-workers/Mentors; I would like to thank Drs. Kim Lichtveld and Seth Ebersviller for all of their guidance and support over the years, even after graduating they continued to provide much help and support. Thank you for everything that you have taught me and for setting the bar so high. I couldn't have asked for better co-workers/mentors/friends.

My Friends; To the friendships that I have made while at UNC, thank you for your support and the great memories that I will always have. To Angel Rodriguez and Claudia Morua, thank you for your support and all the great wishes you have sent me all the way from California.

My Family; To my parents, brothers, sisters, nieces, and nephews, I couldn't have accomplished any of this without your love and support. It's been difficult being all the way across the country, but it has been worth it. Every visit and every phone call always renewed my desire to continue pursuing my goal and never giving up. To my in-laws, you have been a great motivation. Thank you for believing in me.

My wife Alexandra; We have grown up together these past 9 years. It has been a great journey thanks to you being by my side this whole time. You're the one who taught me about research when I had no clue what research was. Seeing how passionate you were about doing research when we were at UC Davis is what motivated me to try it out. You passed along that passion to me and I will always be grateful for that.

TABLE OF CONTENTS

LIST OF TABLES	x
LIST OF FIGURES	xi
LIST OF ABBREVIATIONS.....	xvii
CHAPTER 1: BACKGROUND AND SIGNIFICANCE.....	1
Rationale	1
Cellular Response of In Vitro Models	2
Exposure Methods under Submerged Culture Conditions.....	3
Exposure Methods at an Air-Liquid Interface	4
Research Objective	5
Engineering Design Process	6
Conclusion	9
CHAPTER 2: THE GILLINGS SAMPLER – DESIGN AND TESTING OF A PORTABLE IN VITRO AEROSOL EXPOSURE SYSTEM	10
Introduction.....	10
Materials and Methods.....	12
Results.....	20
Discussion.....	28

CHAPTER 3: A POSITIVE AEROSOL CONTROL METHOD FOR QUALITY ASSURANCE TESTING OF IN VITRO EXPOSURE SYSTEMS	32
Introduction.....	32
Materials and Methods.....	36
Results.....	40
Discussion.....	51
CHAPTER 4: PERFORMANCE TESTING OF THE GILLINGS SAMPLER UNDER VARIOUS TEST ATMOSPHERE	55
Introduction.....	55
Materials and Methods.....	58
Results and Discussion	66
Conclusion	87
CHAPTER 5: OVERALL CONCLUSIONS, LIMITATIONS, AND FUTURE WORK ...	89
Summary of Research Objective	89
Summary of Findings.....	90
Limitations	95
Future Work	104
Overall Conclusion	107
REFERENCES	110

LIST OF TABLES

Table 3-1: Comparison of Positive Controls used for Testing Air-Liquid Interface (ALI) Exposure Systems.....	34
Table 4-1: Exposure times, cell types used and biological endpoints measured for the exposures conducted.....	66
Table 4-2: Exposure conditions from burning a kerosene lamp for soot generation.....	71

LIST OF FIGURES

Figure 1-1: The phases in the engineering design process	6
Figure 2-1: Side-view schematic of the Gillings Sampler. A vacuum pump on the sampler outlet pulls air through the device. Air first enters the Heated Humidification System where the air is warmed and humidified. The air then enters the Cell Exposure System where two perforated screens disperse the air into the charging region. In the charging region, a corona wire sitting below the flow path produces positive ions to electrically charge the incoming particles. The charged particles then enter the precipitation region where they are subjected to a positive electric field that forces the particles downwards onto the deposition plate. The particles deposit inside the wells of the deposition plate where cultured cells are exposed. The air then leaves via the outlet.....	13
Figure 2-2: A demonstration of how one precipitation pattern occurs with an "air parcel" containing particles is shown here. One precipitation cycle in this 2-part, pulsed-precipitation pattern consists of having the electric field turned off for 4 seconds to allow the precipitation region to be filled with particles, followed by turning on the electric field for 1.5 seconds to force down the particles onto the collection area. At 0 seconds, all the particles are in the charging section, above the corona wire. At 2 seconds into the cycle, the charged particles are flowing over the deposition plate. At 4 seconds, the charged particles have "filled up" the volume over the deposition plate. At 5.5 seconds, the end of the cycle, all particles have been deposited on the deposition plate. Most particles have deposited inside the wells where cultured cells will sit and some particles will deposit on the masking lid.	15
Figure 2-3: The standard curve was generated by making serial dilution standards from the YG-PSL sphere stock solution and obtaining their fluorescent output. This curve was then used to convert the raw fluorescence measurements obtained in the deposition efficiency tests into mass collected.....	21
Figure 2-4: TEM micrographs of YG-PSL spheres collected on a TEM grid using the Gillings Sampler. Micrograph A shows the size of individual YG-PSL spheres was observed to be 214 nm, while micrographs B and C show various clusters of YG-PSL spheres.....	21
Figure 2-5: Number size distribution of the nebulized YG-PSL spheres obtained with the SMPS.....	22

Figure 2-6: Calculated deposition efficiency using YG-PSL spheres with the 6-well and 9-well deposition plates. Statistical comparison via t-test indicates no statistical significant difference between the two deposition plates..... 22

Figure 2-7: An illustration of 1000 deposition cycles to calculate the deposition efficiency on a Millicell-CM insert. 24

Figure 2-8: Infrared, episcopic fluorescence, and TEM images are observed here: A) View of a new Millicell-CM membrane without magnification. B) View of an infrared image of the IR-PSL spheres collected on a Millicell-CM membrane without magnification. The gray shades indicate fluorescence of the IR-PSL spheres. C) An episcopic fluorescence image of YG-PSL spheres collected on a Millicell-CM membrane at 20X magnification over a randomly selected area of the membrane. The top-right and top-left corners of this image lack brightness due to the microscope lighting itself, and not the lack of YG-PSL deposition in those areas. D) A TEM micrograph of YG-PSL spheres collected on TEM grid placed on top of Millicell-CM membrane over a randomly selected area of the TEM grid. The smallest dots are the single YG-PSL spheres, while the larger dots are the multiplets. The larger the dots, the larger the number particles present in the clusters. 25

Figure 2-9: Ozone measured at the outlet of the Gillings Sampler during a 4-hour clean air exposure where the charging section was powered on only. An average of 69 ppb of ozone was generated by the corona wire. 26

Figure 2-10: Fold increase in cytotoxicity, as measured by LDH, from 4-hour long (2,620 cycles) exposures to clean air using the Gillings Sampler at various operational conditions. No statistical difference observed when comparing exposed cells to unexposed controls under any conditions..... 27

Figure 2-11: Fold increase in inflammation, as measured by IL-6, from 4-hour long (2,620 cycles) exposures to clean air using the Gillings Sampler at various operational conditions. No statistical difference observed when comparing exposed cells to unexposed controls under any conditions. 27

Figure 2-12: Fold increase in inflammation, as measured by IL-8, from 4-hour long (2,620 cycles) exposures to clean air using the Gillings Sampler at various operational conditions. No statistical difference

observed when comparing exposed cells to unexposed controls under any conditions.	28
Figure 3-1: A schematic of the experimental set up used for mineral oil aerosol exposures. A clean air generator serves as the source of air. The mineral oil (with and without TOLALD) is first nebulized using a Collison nebulizer. Clean air is added to dilute the aerosol output which then enters a personal cascade impactor. The mineral oil aerosol is then introduced into a 3.8-liter glass chamber. The air sampled by the Gillings Sampler, the SMPS, and the midget impinger is drawn from the glass chamber.	37
Figure 3-2: Number size distribution of the mineral oil aerosol was measured with and without a personal cascade impactor as a size selective inlet in the experimental setup.	41
Figure 3-3: Number size distribution of the mineral oil aerosol for all experiments was measured with an SMPS for all experiments conducted. Repeatable size and concentrations were achieved.	41
Figure 3-4: GC-MS chromatograph from all three experiments containing TOLALD. The unreacted PFBHA is observed at retention time of 17 minutes. The TOLALD peak is detected at the retention time of about 30.5 minutes.	43
Figure 3-5: Fold increase in LDH and IL8 mRNA levels of exposures to mineral oil only and mineral oil with TOLALD compared to their respective controls. The asterisk symbol (*) indicates a statistically significant difference (t-test; $p < 0.05$) over unexposed controls. The pound sign (#) indicates a statistically significant difference (t-test; $p < 0.05$) between the mineral oil only exposure and the mineral oil with TOLALD exposure. The caret symbol (^) indicates results obtained from the clean air exposures presented in Chapter 2.	45
Figure 3-6: Images captured with a 10X objective lens of cells at 9-hours post-exposure for (A) unexposed controls and (B) exposed cells to the mineral oil aerosol containing TOLALD. Changes in the cell morphology are observed after cells have been exposed to the toxic mineral oil aerosol.	46
Figure 3-7: Fold increase in LDH levels of exposures mineral oil with TOLALD compared to their respective controls for every ng/cm ² of TOLALD dose delivered to the cells. ANOVA analysis indicates no statistical difference in replicate exposures.	48

Figure 3-8: Fold increase in IL8 mRNA levels of exposures mineral oil with TOLALD compared to their respective controls for every ng/cm ² of TOLALD dose delivered to the cells. ANOVA analysis indicates no statistical difference in replicate exposures.	48
Figure 3-9: IL-8 protein in the supernatant was measured via ELISA in all cell exposures conducted to the mineral oil aerosol. Results show that IL-8 protein levels are suppressed after exposure, however these results show interference with the biochemistry of the assay. After conducting qRT-PCR (results shown in Figures 3-5, 3-7, and 3-8), it was observed that IL-8 mRNA levels increased. This indicates that ELISA interference is occurring.	49
Figure 3-10: GC-MS chromatograph from the "cocktail" mineral oil aerosol containing acetone, acrolein, methacrolein, and TOLALD.	51
Figure 4-1: Injection of diesel exhaust into the rooftop chamber and sampling of the chamber contents in the laboratory.	60
Figure 4-2: Schematic of experimental setup for generating secondary organic aerosols as a result of reacting ozone with limonene.	63
Figure 4-3: Number size distribution of diesel exhaust particles sampled from the UNC rooftop chamber while cell exposures were being conducted with the Gillings Sampler.	67
Figure 4-4: GC/MS chromatograph of the measured carbonyls of the diesel exhaust in the morning (Fresh) and evening (Photochemically-aged) inside the UNC rooftop chamber while cell exposures were being conducted with the Gillings Sampler.	68
Figure 4-5: TEM micrograph of photochemically-aged diesel exhaust particles collected on a TEM grid placed on the deposition plate inside the Gillings Sampler during cell exposure.	69
Figure 4-6: Biological analysis of cytotoxicity (LDH), inflammation (IL-6 mRNA and IL-8 mRNA), and oxidative stress (HO-1 mRNA) from A549, EpiAirway, BALB/cJ, and C57BL/6J exposed cell cultures to photochemically-aged diesel exhaust. The * denotes statistical significance ($p < 0.05$).	70
Figure 4-7: Number size distribution of kerosene soot produced from igniting a double-wick kerosene lamp measured with an SMPS for the three concentrations tested.	72

Figure 4-8: GC/MS chromatograph of the measured carbonyls from the kerosene soot sampled from the indoor chamber while cell exposures were being conducted with the Gillings Sampler.	73
Figure 4-9: Biological analysis of inflammation (IL-6 mRNA, IL-8 mRNA, and COX-2 mRNA) from A549 exposed cell cultures to kerosene soot. Data is presented as fold change over control. The * denotes statistical significance ($p < 0.05$).	74
Figure 4-10: Images captured with a 10X objective lens of cells at 9-hours post-exposure for (A) unexposed controls and (B) exposed cells to 0.6 mg/m ³ of kerosene soot. Changes in the cell morphology are observed after cells have been exposed to kerosene soot.....	75
Figure 4-11: Electron micrograph of an unexposed A549 cell, outlined in red, observed under SEM. The "hair-like" membranes seen on the surface of the cell is microvilli, which helps to increase the surface area of the cell and are involved in a variety of functions.	76
Figure 4-12: Electron micrograph of an exposed A549 cell, outline in red, to kerosene soot observed under SEM. The morphology of the cell has completely changed compared to the unexposed cells.	77
Figure 4-13: TEM micrograph of kerosene soot particles collected on a TEM grid placed on the deposition plate inside the Gillings Sampler during cell exposure.	78
Figure 4-14: Number size distribution of secondary organic aerosols produced from reacting ozone with limonene during the exposures conducted.	79
Figure 4-15: GC/MS chromatograph of the measured carbonyls produced from reacting ozone with limonene during the "Gases Only" exposure (top) and "Gases + Particles" exposure (bottom).	80
Figure 4-16: Biological analysis of cytotoxicity (LDH) and inflammation (IL-6 mRNA and IL-8 mRNA) from A549 exposed cell cultures to secondary organic aerosols produced from reacting ozone with limonene. The asterisk symbol (*) indicates a statistically significant difference (t-test; $p < 0.05$) over unexposed controls. The pound sign (#) indicates a statistically significant difference (t-test; $p < 0.05$) between the Gases Only exposure and the Gases + Particles exposure. The caret symbol (^) indicates results obtained from the clean air exposures presented in Chapter 2.	82

Figure 4-17: IL-8 protein in the supernatant was measured via ELISA in both cell exposures conducted in Chapter 4 to the secondary organic aerosols. Results show that IL-8 protein levels are suppressed after exposure, however these results show interference with the biochemistry of the assay. After conducting qRT-PCR (results shown in Chapter 4), it was observed that IL-8 mRNA levels increased. This indicates that ELISA interference is occurring.....	84
Figure 4-18: Analysis of cytotoxicity (LDH) and inflammation (IL-8 protein) from A549 exposed cell cultures to ozone. The asterisk symbol (*) indicates a statistically significant difference (t-test; $p < 0.05$) over unexposed controls. The pound sign (#) indicates a statistically significant difference (t-test; $p < 0.05$) between the GIVES exposure and the Gillings exposure.....	85
Figure 4-19: Ozone measurements at inlet and outlet of Heated Humidification System. Measurements indicated that ozone concentrations diminish as it flows through the system due to the humid environment present inside.....	86
Figure 5-1: Observed YG-PSL deposition versus the expected deposition pattern as the deposition cycle time change.....	98
Figure 5-2: Calculated deposition efficiencies using the 6-well deposition plate as the pulse-precipitation cycle times are adjusted. HV = High Voltage in the Cell Exposure System	99
Figure 5-3: Example of suggested deposition testing plan by varying each operational variable. First, testing can be conducted by varying the particle size and fixing the other parameters. In a new set of experiments, the charging current can be varied while maintaining the other parameters fixed. In the next two sets of the experiments the charging frequency and electric field strength can then be changed.	105
Figure 5-4: Recommended experimental flow chart for conducting future cell exposure studies with the Gillings Sampler.....	107

LIST OF ABBREVIATIONS

ALI	air-liquid interface
CES	Cell Exposure System
COX-2	cyclooxygenase-2
DE	diesel exhaust
EAVES	Electrostatic Aerosol in Vitro Exposure System
EES	Electrical Enclosure System
ELISA	enzyme-linked immunosorbent assay
GIVES	Gas In-Vitro Exposure System
HHS	Heated Humidification System
HO-1	heme oxygenase-1
IL-6	interleukin-6
IL-8	interleukin-8
IR-PSL	infrared polystyrene latex
LDH	lactate dehydrogenase
L/min	liters per minute
MOA	mineral oil aerosol
O ₃	ozone
PFBHA	o-(2,3,4,5,6-pentafluorobenzyl) hydroxylamine chloride
PM	particulate matter
ppb	parts per billion
PSL	polystyrene latex
qRT-PCR	quantitative real-time reverse-transcription polymerase chain reaction

SMPS	scanning mobility particle sizer
TOLALD	p-tolualdehyde
YG-PSL	Yellow-Green polystyrene latex

CHAPTER 1: BACKGROUND AND SIGNIFICANCE

Rationale

There is growing interest in the scientific community in studying the toxicity of multi-pollutant mixtures found in ambient air, and the U.S. Environmental Protection Agency (EPA) is moving towards setting standards for these types of mixtures.^{1, 2} The EPA strategic plan calls for demonstrating a direct link between air quality and health effects.¹ Additionally, the Health Effects Institute (HEI) strategic plan aims to develop and apply next-generation multi-pollutant approaches to understanding exposure to and health effects of air pollutants.³ While epidemiological studies have shown that some measured air pollutants in cities are highly correlated with tens of thousands of deaths a year, there are many problems in relating ambient monitoring data to health effects.⁴⁻⁷ Laboratory toxicological studies of the single-pollutants often show few health effects from the exposure levels seen in ambient air.⁵⁻⁸ There is currently limited scientific knowledge on how exposures to multi-pollutant mixtures in real-world settings affect human health.² For example, in the atmosphere, it is unclear whether particulate matter (PM) toxicity is being driven by particle size, composition, the chemical transformation and interaction with gas phase molecules, or some synergistic combination of all these factors. This limited knowledge on the health effects associated with multi-pollutant exposures limits the ability of decision-makers to establish multi-pollutant policies.²

Cellular Response of In Vitro Models

Animal exposure studies have been conducted to investigate the health effects associated with multi-pollutant exposures, however they can be costly and require extra labor to conduct these complex studies.² Alternatively, *in vitro* studies are relatively inexpensive and can be used for rapid screening of pollutants or components of complex mixtures.⁹ *In vitro* exposure studies can be a practical approach to identify underlying mechanisms by which air pollutants damage cells, while *in vivo* studies can provide interpretation of the underlying pathophysiological mechanisms.^{9, 10} Molecular tools and "omics" approaches make it possible to understand many of the underlying cellular pathways and biochemical processes which drive a cell's response to a toxicant. The respiratory tract has the potential to contain key markers that document a response to exposures of a specific chemical. There is increasing evidence that certain cytokines play key roles in the initiation of response, cell recruitment, tissue repair, and resolution aspects of inflammation. Determining the effect of a chemical exposure on specific gene expression levels within *in vitro* models should provide useful information to assess potential adverse health effects.¹¹ Measuring inflammatory mediators and cytotoxicity can quantitatively assess the degree of inflammation or injury.

The airway epithelial cells themselves are capable of responding to stimulation by the release of inflammatory mediators, such as, interleukin-6, Interleukin-8, cyclooxygenase-II enzyme, and Tumor Necrosis Factor- α (IL-6, IL-8, Cox-2, and TNF- α), upon exposure to particles and other forms of air pollutants.¹²⁻¹⁵ These inflammatory mediators can be expressed and secreted during the hours after exposure. They can then be measured either in the culture medium or through mRNA analysis. Further Injury to the epithelial cells results cell membrane damage, which in turn results in the release of intercellular lactate

dehydrogenase (LDH). LDH can be considered an indicator of cell injury,¹⁶ and increased release of LDH is considered to be a sign of cellular death. As with the inflammatory mediators, the LDH is secreted into the culture medium after injury and therefore can be quantified. While the measurement of these mediators can provide useful information to assess potential adverse health effects of air pollutant, the challenge of *in vitro* toxicology, however, is that conventional *in vitro* exposure methods do not properly emulate human exposures and are not adequate to meet EPA's strategic plan.

Exposure Methods under Submerged Culture Conditions

Conventional *in vitro* exposure methods to ambient air pollutants rely on submerged culture conditions, whereby the pollutant of interest is added to a culture medium and subsequently placed over the cells.^{9, 10, 17, 18} A common method for collecting air pollutants is to sample the air through filters. Filters collect particulate matter efficiently. After filter collection, PM is resuspended in a liquid medium and subsequently deposited onto the cells. In this recovery process, the particles' physical and chemical characteristics are altered, leading to particle agglomeration and the loss of volatile organic compounds (VOCs).^{19, 20} Impactors can also be used collect large diameter PM on plates relatively efficiently,²¹ but, as with filters, VOCs can be lost during collection and the particle's characteristics are altered when transferred to a liquid medium. In addition, impactors can only be used to sample particles of relatively large diameter due low collection efficiency for small particles.^{22, 23} An alternative method to filter and impactor collection is to use impingers to collect the air mixture. Impingers pass air containing PM through a liquid medium in which portions of particles and gases are collected, however there is a lower PM collection efficiency using this method than filter collection.²⁴⁻²⁷ As with filter collection, the particles' physical and

chemical characteristics are altered, and particle agglomeration can take place. A major limitation to the use of exposure methods under submerged culture conditions is that the number or mass of particles that actually interact with the cells cannot be determined.¹⁰ For these reasons, alternative *in vitro* methods were developed to produce more realistic aerosol exposures.

Exposure Methods at an Air-Liquid Interface

Alternative *in vitro* exposure methods are needed to overcome the shortcomings of conventional methods. Exposing cells at the air-liquid interface (ALI) is the most realistic approach to emulate *in vivo* inhalation exposures. The apical surface of the cells is exposed to the air while the basolateral surface of the cells is fed with a culture medium through a porous membrane.^{10, 28} *In vitro* technologies currently exist, developed both in-house and commercially, whereby cells are exposed at the ALI^{19, 29-38} creating a more realistic air-to-cell inhalation exposure. These exposure systems use different mechanisms to deposit particles onto the cells including diffusion, sedimentation, cloud settling, and electrostatic precipitation. The CULTEX and VITROCELL Systems are the only two commercially available devices which rely on diffusion and sedimentation to deposit particles onto the cells. Studies have reported deposition efficiencies of less than 2% for particles ranging from 50 to 500 nm using the CULTEX glass modules.^{18, 39} Electrostatic precipitation is one of the main mechanisms to improve the deposition efficiencies. In a study by Savi *et al.*, the deposition efficiencies were greatly improved to 15-35% using bipolar charging of particles and an alternating electric field. To improve these results, a high efficiency electrostatic precipitator is needed with a unipolar charger since the particle charging efficiency is near 100% for particles larger than 30 nm¹⁸.

Electrostatic precipitators (ESP) use electrostatic forces to collect charged particles for aerosol sampling and air cleaning.²² Traditionally, ESP have been used as a method for aerosol collection in the control of airborne dust in residential and industrial settings.⁴⁰ When using ESP, the particles in the air are electrically charged and then subjected to a strong electric field that causes the particles to drift across the flow, and ultimately to deposit on a grounded collection plate.^{41, 42} Our research group previously developed a prototype *in vitro* exposure system using electrostatic precipitation as its principle of operation named the Electrostatic Aerosol in Vitro Exposure System (EAVES).¹⁹ A direct particle-to-cell deposition is achieved using the EAVES by exposing cells at the ALI. Particles are electrically charged and then subjected to an electric field that causes them to repel away from a plate of similar charge and subsequently deposit in a collection plate where cultured lung cells are exposed.¹⁹ This electrical charge placed on the particles does not induce any observed toxicological response from the cells.¹⁹ The EAVES deposition efficiency was calculated between 35-47% and was shown to be more sensitive than exposing cells under submerged culture conditions.^{19, 20}

While the development of the EAVES and other ALI exposure systems have contributed to advancing the knowledge of multi-pollutant exposure, these systems are limited to a laboratory setting. Currently, there are no portable *in vitro* systems which can be deployed in a real-world setting.

Research Objective

The objective of this dissertation consists of the development of a portable aerosol sampler to be used for conducting *in vitro* exposure studies at the air-liquid interface.

Engineering Design Process

To meet my research objective of developing a portable aerosol sampler, I followed a systematic engineering design process (Figure 1-1). The portable aerosol sampler will be referred to as the Gillings Sampler.

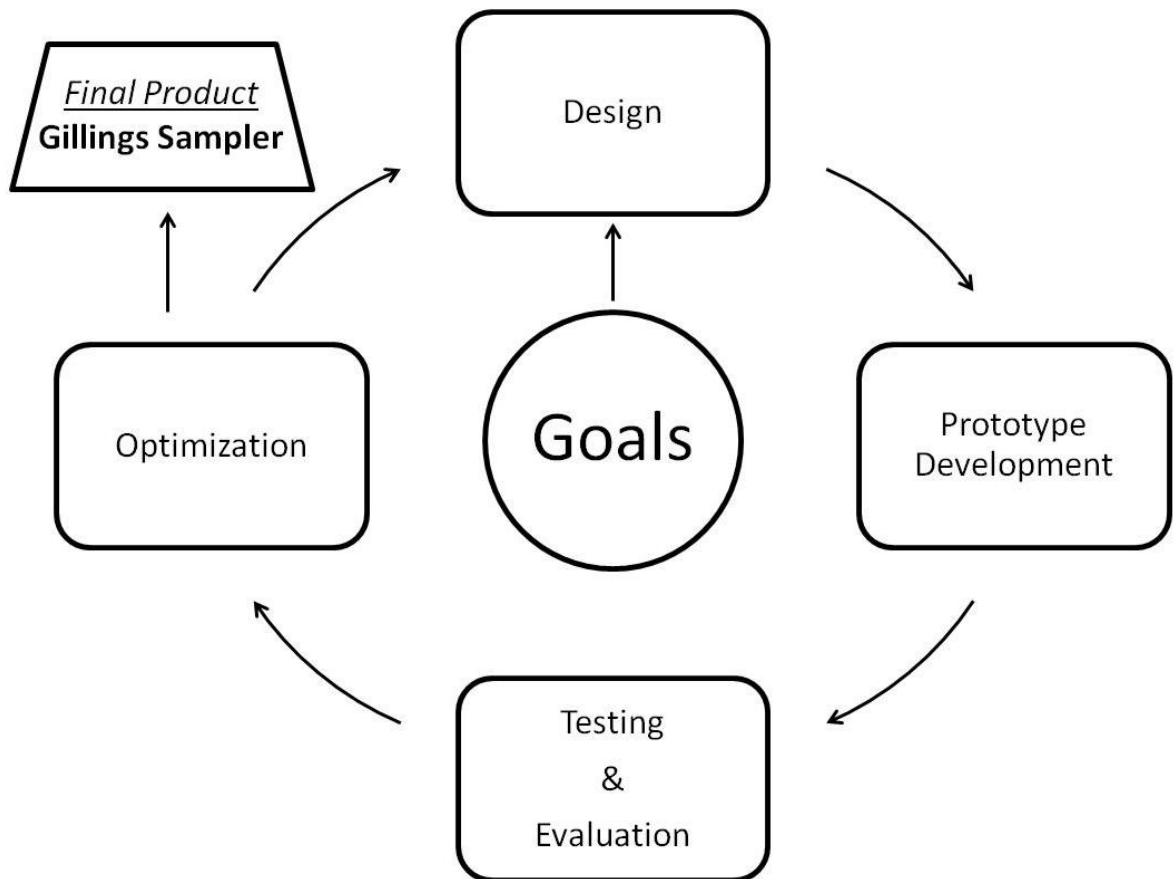


Figure 1-1: The phases in the engineering design process

The first task was to establish a set of goals or requirements that the final product should meet. The portable aerosol sampler should meet the following design goals:

- 1) Maintain the features and principle of operation of the EAVES
- 2) Use commercially available components for ease of manufacturing and assembly

- 3) Incorporate a humidification and heating system to remove the need for a tissue culture incubator
- 4) Provide the flexibility to co-expose up to 9 commercially available tissue inserts without needing to modify them

The portable aerosol sampler should also meet the following operational goals:

- 1) Deposit particles over the entire tissue insert cell growth area
- 2) Deposit particles across all tissue inserts with minimal variation from insert to insert
- 3) Do not induce toxicity to the cells from the use of the *in vitro* system
- 4) Allow an exposure time of up to 4 hours

Once all goals were established, the design and development phases began. With the collaboration of the Environmental Sciences and Engineering (ESE) Design Center located in the Gillings School of Global Public Health, University of North Carolina at Chapel Hill, a prototype of the portable aerosol sampler was manufactured. Wiring of all electronic components of the sampler was conducted in the laboratory. Testing and evaluation of the Gillings Sampler was divided into four sub-phases: electrical, particle deposition, cell viability, and performance.

Electrical Testing:

Electrical connections of power supplies were evaluated using an oscilloscope to observe the electrical signals over time to ensure that voltage characteristics, such as

waveform, frequency, and amplitude, were monitored. All heating elements and sensors were monitored using proportional-integral-derivative (PID) controllers.

Particle Deposition Testing:

The objective of this sub-phase was to ensure that sufficient particle deposition in the desired tissue insert cell growth area occurred. To maximize the particle collection efficiency, the electrical charging of the sampled particles needed to be optimized. Several design iterations of the charging mechanism were manufactured to ensure the Gillings Sampler adequately charged the sampled particles. The collection surface consists of a deposition plate that houses the tissue inserts where cells are cultured for exposure. Several design iterations of the deposition plate were necessary until an optimal design was achieved that yielded high particle collection efficiencies.

Cell Viability Testing:

The operational parameters (flow rate, voltages, currents, etc.) were identified for optimal particle collection efficiency. Cell viability testing was required, however, to ensure that cell cultures could be housed inside the sampler at the operational parameters to be used without inducing adverse effects onto the cells. Possible factors that could adversely affect the cell cultures were: the material of the deposition plate, the sample flow rate, the high electric field the cells are subjected to, and the ozone (O₃) produced by the charging system. Only the material of the deposition plate proved to be an issue. This resulted in several design iterations of the deposition plate until an adequate material was selected.

Performance Testing:

The performance of the Gillings Sampler was evaluated under controlled laboratory conditions. Five test atmospheres containing toxic air pollutants were generated to expose cultured cells using the sampler. The test atmospheres used consisted of a synthetic toxic mineral oil aerosol (MOA), diesel exhaust (DE) particulates, kerosene soot, secondary organic aerosols (SOA), and O₃. Testing of the sampler under various conditions provided valuable insights into the qualities of the system and highlighted various limitations that should be addressed moving forward. A detailed overview of the Gillings Sampler's design, performance and efficacy is described in the following chapters.

Conclusion

The Gillings Sampler was developed to meet the needs to the scientific community to better address the link between air quality and health effects. This new technology is intended to be used as an alternative research tool for aerosol *in vitro* exposure studies, which can help achieve EPA and HEI's strategic plan to towards setting standards for multi-pollutant mixtures and next-generation multi-pollutant approaches.^{1, 3} Successful development and dissemination of this innovative technology can help bridge the gap between toxicology and epidemiology, which in turn can affect policy decision-making by more accurately representing toxic effects and risk of exposure to air pollutants. Further testing and optimization is still required to produce a "commercially ready" *in vitro* system. The Gillings Sampler, however, is a stepping-stone in the development of cost-effective *in vitro* technology that can be made accessible to researchers in the near future.

CHAPTER 2: THE GILLINGS SAMPLER – DESIGN AND TESTING OF A PORTABLE IN VITRO AEROSOL EXPOSURE SYSTEM

Introduction

Scientific studies have shown that exposures to airborne particulate matter (PM) have a negative impact on human health.^{4-6, 10} In a report from the World Health Organization, more than 2 million premature deaths each year can be attributed to air pollution⁴³ and PM is responsible for about 0.8 million of these premature deaths.⁴⁴ Adverse health effects observed have been associated with PM₁₀ and PM_{2.5} (aerodynamic particle diameter < 10 µm and 2.5 µm) exposures in humans.⁴⁵ The smaller particles can penetrate deeper in the airway and have been shown to increase morbidity and mortality.⁴⁶ In addition, PM composition may play a role in particle-associated adverse health effects.¹⁰ In the atmosphere, it is unclear whether toxicity is driven by particle size, composition, the chemical transformation and interaction with gas phase molecules, or some synergistic combination of all these factors.

In vitro studies use cell culture models as a surrogate for biological responses allowing for rapid screening of pollutants. A major limitation of conventional *in vitro* methods is the difficulty of exposing cells to PM in a manner that better emulates direct air-to-cell inhalation exposures. Typical toxicological *in vitro* exposure studies use submerged culture conditions, where PM is added to a culture medium.^{9, 10, 17, 18} In this process, the particles' physical and chemical characteristics are altered, and the number or mass of particles that actually interact with the cells cannot be determined.^{10, 19, 20} What is needed is new *in vitro* technology that

can quantify the dynamic changes in the toxicity of particles while maintaining their size, composition, and interaction with other gasses.

In vitro technologies currently exist whereby cells are exposed at an air-liquid interface (ALI),^{19, 29-38} creating a more realistic air-to-cell inhalation exposure. In this type of exposure, the apical surface of the cells is exposed to air while the basolateral surface is nutritionally supported with culture media through a porous membrane.^{18, 47} Cells grown on membrane inserts can be exposed to PM by depositing particles directly onto the cell surface.¹⁹ Current commercial ALI exposure systems rely on diffusion and sedimentation to deposit particles onto cells.^{30, 31, 35} Studies have reported efficiencies between 0.7-2% for these systems for particle sizes of 50 to 500 nm.¹⁸ Although current commercial ALI systems are a step forward, they lack the efficiency suitable for studying urban PM_{2.5}. In addition, new field-capable systems that are suited for all particle sizes are needed to study the entire toxic potential of ambient PM.

Our research group has previously developed an *in vitro* system named EAVES, which uses electrostatic precipitation to expose cells at the ALI to PM.¹⁹ A TSI 3100 electrostatic aerosol sampler was retrofitted to accommodate four co-exposed tissue inserts for up to one hour while housed in an incubator at 37°C.¹⁹ The EAVES efficiency is between 35-47% and was shown to be more sensitive than exposing cells under submerged culture conditions.^{19, 20} The proof of concept and advantages of a system like the EAVES have been shown^{19, 20, 48, 49} and disseminating this technology to other researchers can have a positive impact in future studies. Duplicating the EAVES, however, is not ideal since this system requires retrofitting a TSI 3100 electrostatic aerosol sampler (no longer commercially available) and must be housed in an incubator. Additionally, the 12 mm Millicell-CM membranes (EMD Millipore

Corporation) used with the EAVES require their height to be manually reduced from 10.5 mm to 5 mm using a micro-lathe.¹⁹ The membranes then undergo a wash process to be sterilized before being used for culturing cells. For these reasons, it was determined that a new system needed to be developed.

The focus of this chapter is to introduce the development of an improved *in vitro* system, named the Gillings Sampler. The following design goals were established prior to the design and development phase of the *in vitro* system: 1) maintain the features and principle of operation of the EAVES, 2) use commercially available components for ease of manufacturing and assembly, 3) incorporate a humidification and heating system to remove the need for a tissue culture incubator, 4) provide the flexibility to co-expose up to 9 tissue inserts without needing to modify them. Operational goals were also established and consist of the following: 1) deposit particles over the entire tissue insert cell growth area, 2) deposit particles across all tissue inserts with minimal variation from insert to insert, 3) do not induce toxicity to the cells from the use of the *in vitro* system, and 4) allow an exposure time of up to 4 hours. These design and operational goals are what our research group believe are essential components and characteristics of an ideal *in vitro* system. The Gillings Sampler was evaluated under controlled laboratory conditions to determine if all established design goals were accomplished. A detailed overview of the Gillings Sampler's operating performance and efficacy is described in the following sections.

Materials and Methods

Air Sampler Components and Operating Conditions

The Gillings Sampler is comprised of three sub-systems: Electrical Enclosure System (EES), Heated Humidification System (HHS), and Cell Exposure System (CES). The

principle mechanism to deposit particles directly onto cells using a two-stage electrostatic precipitator is described in Figure 2-1.

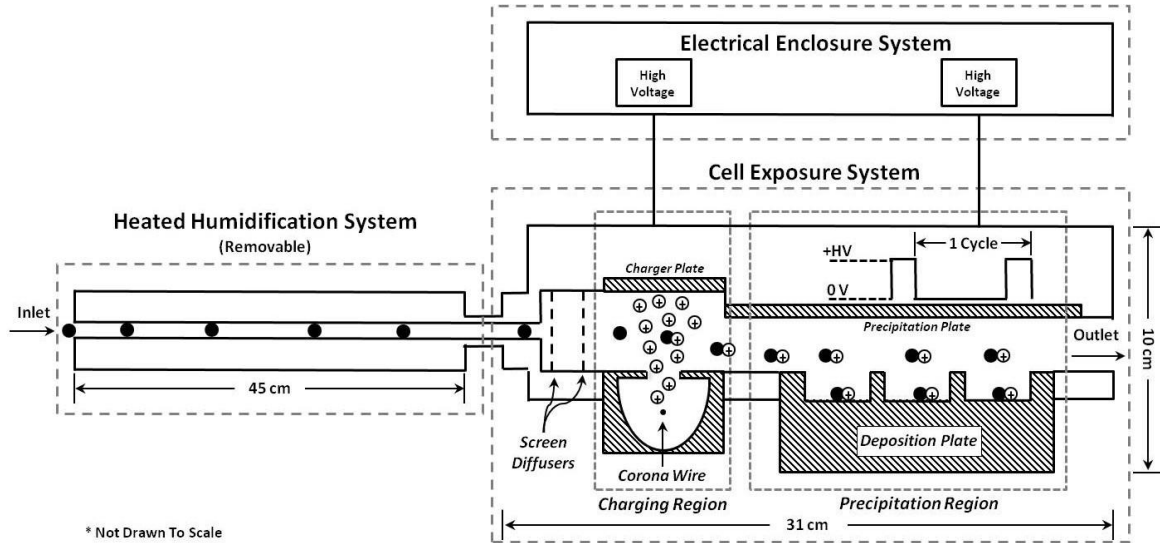


Figure 2-1: Side-view schematic of the Gillings Sampler. A vacuum pump on the sampler outlet pulls air through the device. Air first enters the Heated Humidification System where the air is warmed and humidified. The air then enters the Cell Exposure System where two perforated screens disperse the air into the charging region. In the charging region, a corona wire sitting below the flow path produces positive ions to electrically charge the incoming particles. The charged particles then enter the precipitation region where they are subjected to a positive electric field that forces the particles downwards onto the deposition plate. The particles deposit inside the wells of the deposition plate where cultured cells are exposed. The air then leaves via the outlet.

The EES is the source of power to both the CES and the HHS. All of the low and high voltage power supplies, as well as the temperature and humidity controllers, are safely housed in this compartment. The HHS was manufactured using commercially available components in the ESE Design Center located in the Gillings School of Global Public Health. This removable system is used to pre-heat and moisten the incoming airflow before it reaches the cells, as required by the sampling conditions. If one were conducting a field study where the climate is hot and humid, for instance, the use of the HHS may not be needed. In human airways, inspired air is rapidly warmed and moistened mainly in the nasal cavities and remainder of the upper airways. Inspired air is warmed from around 20°C at the portal of

entry to 31 °C in the pharynx and 35 °C in the trachea.⁵⁰ This system is, therefore, a critical component as it represents the pre-heating and humidification of inhaled air.

The CES was manufactured using commercially available components in the ESE Design Center. It is a modified, temperature-regulated (37 °C), two-stage electrostatic precipitator. An electrical current is applied to the corona wire to produce a corona discharge that produces high concentrations of unipolar ions used to charge the incoming particles in the sampled flow.^{22, 51} A high voltage is applied to the precipitation plate in a pulsed-precipitation pattern to generate an electric field, similar to that described by Liu and colleagues.⁵¹ One precipitation cycle in this 2-part, pulsed-precipitation pattern consists of having the electric field turned off for 4 seconds to allow the precipitation region to be filled with particles, followed by turning on the electric field for 1.5 seconds to force down the particles onto the collection area. The specified times in this cycle depend on the sample flow rate, electric field strength, and volume inside the CES. To help explain how this pulse-precipitation method to deposit particles works, a demonstration is shown in Figure 2-2. In the precipitation region, a 6-well or 9-well deposition plate allows 30 mm Millicell-CM membranes to be co-exposed. The multi-well deposition plates are composed of two parts; the compartmentalized well plate and a masking lid. The masking lid fits over the well plate and covers the cell culture media surrounding the inserts, minimizing evaporation and allowing for longer exposure times.

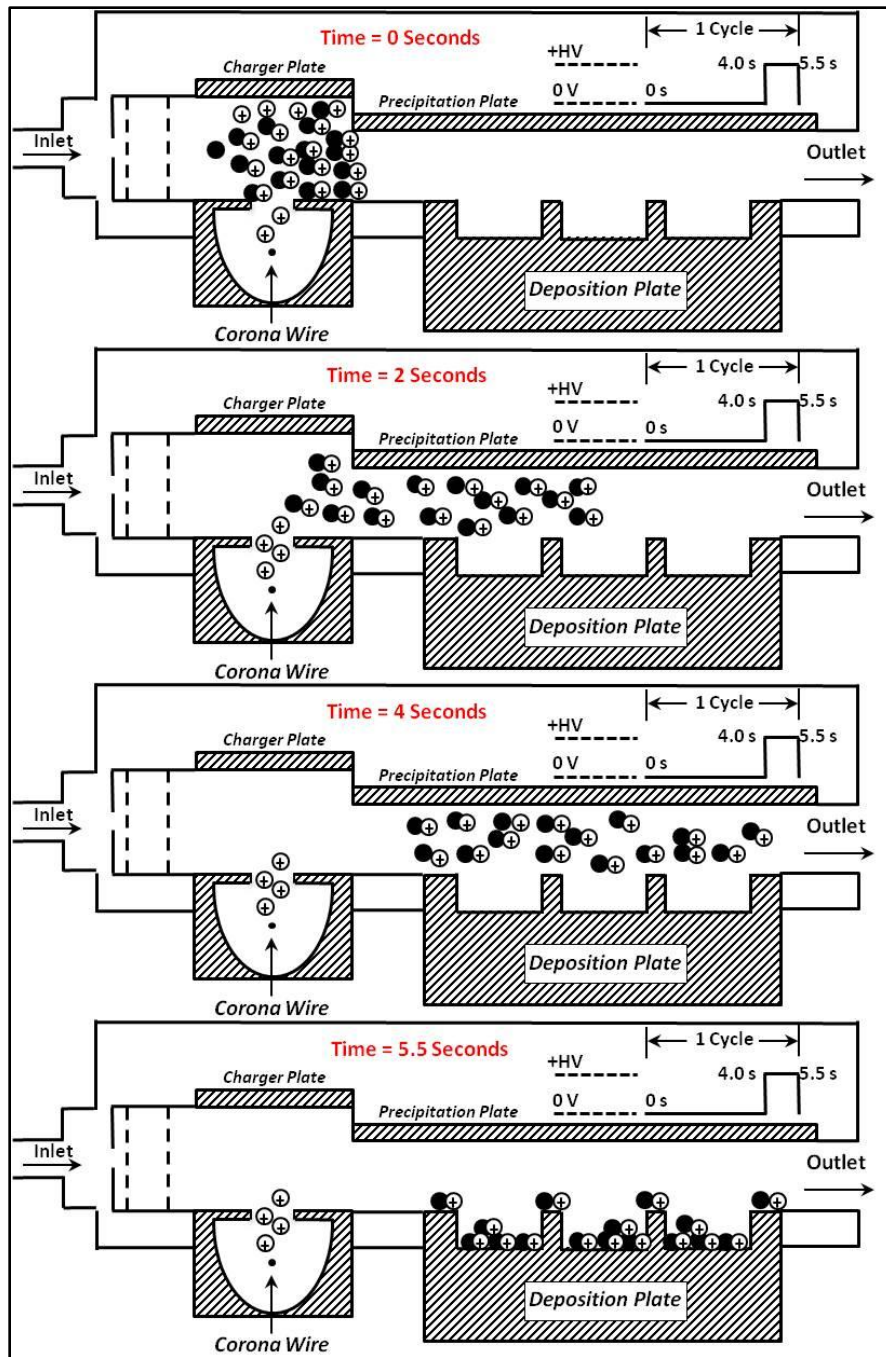


Figure 2-2: A demonstration of how one precipitation pattern occurs with an "air parcel" containing particles is shown here. One precipitation cycle in this 2-part, pulsed-precipitation pattern consists of having the electric field turned off for 4 seconds to allow the precipitation region to be filled with particles, followed by turning on the electric field for 1.5 seconds to force down the particles onto the collection area. At 0 seconds, all the particles are in the charging section, above the corona wire. At 2 seconds into the cycle, the charged particles are flowing over the deposition plate. At 4 seconds, the charged particles have "filled up" the volume over the deposition plate. At 5.5 seconds, the end of the cycle, all particles have been deposited on the deposition plate. Most particles have deposited inside the wells where cultured cells will sit and some particles will deposit on the masking lid.

Particle Deposition Efficiency and Imaging Analysis

Particle deposition efficiency was calculated using fluorescent 200 nm standard microspheres. The size of the microspheres was selected since it falls in the 50 - 500 nm size range of interest. Polystyrene latex (PSL) spheres were selected as test particles since they have been used as calibration standards in other applications. The PSL spheres, referred to as YG-PSL spheres, (0.20 μm , Yellow-Green Fluoresbrite Microspheres, Polysciences, Inc.) were nebulized using a glass micro spray nebulizer to a concentration of $\sim 1 \text{ mg/m}^3$. Prior to nebulization, 0.5 mL of the YG-PSL stock solution was diluted in 8 mL of HPLC-grade water. The nebulized aerosol flow passed through a charge neutralizer (model 3012, Kr-85, 2 mCi, 74 MBq, TSI, Inc.), then into a 20 L glass jar before sampling through the sampler, as previously described by de Bruijne.¹⁹ A 25 mm diameter foil substrate was placed over each Millicell-CM membrane to collect the YG-PSL spheres. The YG-PSL spheres were sampled and collected for 1,000 precipitation cycles (91.7 minutes). After collection, the foil substrates were placed inside glass tubes filled with 5 mL of ethyl acetate to dissolve the YG-PSL spheres and release the fluorescent dye. Variations of this method have been used previously by others to test the efficiency of their systems.^{19, 52, 53} Each sample was analyzed using a spectrofluorometer (FluoroLog, Horiba Scientific) at the peak excitation (440 nm) and emission (486 nm) wavelengths.

A scanning mobility particle sizer (SMPS) (model 3936L25, TSI, Inc.) with a sheath flow rate of 2.0 liters per minute (L/minin) and an aerosol sample flow rate of to 0.3 L/minin was used to measure the size distribution of the particles ranging from 19 to 882 nm in aerodynamic diameter. A Teflon membrane filter (47 mm diameter; Pall Corporation) was used to collect YG-PSL spheres at the same flow rate and duration as the Gillings Sampler to

determine the mass concentration in the air. The filter was weighed before and after to determine the total mass collected.

Three different imaging techniques were used to qualitatively assess the distribution of the deposited PSL spheres. These techniques also serve to demonstrate, as proof of principle, that the PSL spheres are in fact being collected on the membrane surface, ensuring that particles will be directly deposited on the cells during future exposures to PM. Each technique allows us to observe the deposition at different magnification levels.

An infrared imaging system (Odyssey Imaging System; LI-COR Biosciences) was used to observe the PSL sphere deposition over the entire membrane area. To conduct this technique, a different set of 200 nm PSL spheres, referred to as IR-PSL, (200 nm, Red Fluorophorex Fluorescent Microspheres, Phosphorex, Inc.) was used. These IR-PSL spheres were nebulized as described above and collected directly onto the membrane. Prior to nebulization, 0.75 mL of the IR-PSL stock solution was diluted in 7 mL of HPLC-grade water.

Episcopic fluorescence microscopy and transmission electron microscopy were used to observe the YG-PSL sphere deposition at greater magnifications. The YG-PSL spheres were collected directly on the membrane. Using an inverted light microscope configured for epifluorescence, the membrane was observed using an FITC filter block to reveal fluorescence of the YG-PSL spheres. On a separate membrane, a transmission electron microscope (TEM) grid was used to collect the YG-PSL spheres. The impacted particles were viewed directly on the grid in a Zeiss EM900 TEM at an accelerating voltage of 50 kilovolts (kV).

Cell Culture Conditions and Biological Analysis

The cell line A549 is a human pulmonary type II epithelial-like cell line derived from human alveolar cell carcinoma of the lung.⁵⁴ A549 cells were grown on collagen-coated Millicell-CM membranes in F12-K media with 10% fetal bovine serum (FBS) plus 0.01% penicillin/streptomycin. Cells were plated at a density of 7.5×10^5 cells per insert 28 hours prior to exposure and placed in commercial 6-well plates inside an incubator at 5% carbon dioxide (CO₂). The basolateral side received 1.2 mL of media, while 0.8 mL of media was added to the apical side. When the cells reached ~80% confluency, 4 hours prior to exposure, the FBS-containing media was replaced with serum-free media containing F12-K media and 1.5 micrograms (µg) per mL bovine serum albumin, plus 0.01% penicillin/streptomycin. Immediately before exposures, the membranes were transferred to the 9-well deposition plate and 2.8 mL of fresh serum-free media was added to the basolateral side only. After each exposure, the membranes were transferred to new commercially available 6-well tissue culture plates, along with 1.2 mL of serum-free media from the well that contained the membrane during exposure. Membranes were then placed into an incubator for an additional 9 hours to allow for the cells to produce and release biological markers of toxicity. A set of unexposed cells housed in an incubator were used as controls for each test presented in this study.

It is understood that an immortalized cell line may not accurately represent the biological response of primary passage, differentiated human airway epithelial cells. The goal of this work was to test the development of new technology. The A549 cells are reproducible, easy to culture on the Millicell-CM membranes, and provide a robust biological

signal in response to pollutant exposures. These cells were, therefore, ideally suited for this work as it allows for reliable replication of experiments.

For each cell exposure conducted, the basolateral supernatants for each membrane sample (n=6) were collected for toxicological analysis 9 hours post-exposure. Interleukin-8 (IL-8) and IL-6 protein, both markers of inflammation in the supernatant, were measured via enzyme-linked immunosorbent assay (ELISA; BD Biosciences) for the clean air exposures conducted. IL-8, among other cytokines, has been observed in humans when stressed by exposure to ozone and other air pollution mixtures in human clinical trials and measured in asthmatic and chronic obstructive pulmonary disease (COPD) patients,⁵⁵⁻⁵⁸ therefore it was selected as an appropriate endpoint for our study. Cytotoxicity was measured via levels of lactate dehydrogenase (LDH) in the collected basolateral supernatant using a coupled enzymatic assay (Takara Bio Inc.). These endpoints serve to demonstrate the efficacy of the Gillings Sampler; different endpoints for any *in vitro* model can be selected for any other research needs.

Data for LDH, IL-6 and IL-8 are presented as the mean \pm standard error from the mean and expressed as fold increase over control. Data were analyzed using an unpaired Student's t-test and differences were considered significant if $p \leq 0.05$.

A549 Cell Exposure Testing

To effectively evaluate the Gillings Sampler, a series of clean air cell exposures were conducted at various operating configurations. The laboratory is equipped with a clean air generator, which was the source of air for all negative control tests. No toxicity should be observed from any negative control exposures. In all tests, the exposures were conducted for

2,620 precipitation cycles (4 hours) at constant temperature (37°C), flow rate (2.2 L/min), and relative humidity (RH) above 75%, and at 5% CO₂ levels.

Results

Particle Deposition Efficiency

The YG-PSL sphere mass collected was quantified using a spectrofluorometer. The raw fluorescent readings obtained were converted into mass collected using standard curves generated by using the manufacturer's specified particle concentration in the YG-PSL stock solution (Figure 2-3). Using TEM, a diameter of 214 nm for the YG-PSL spheres was measured (Figure 2-4) and it was observed that multiplets (clusters of 2 or more spheres) were present. The SMPS was able to measure these multiplets (Figure 2-5). Formation of multiplets is a common problem that arises from atomizing these types of monodisperse aerosols.²² While the initial intent was to test the efficiency of 200 nm size particles, the resulting aerodynamic particle sizes ranged from 209 nm at the lower end to greater than 1000 nm at the higher end due to the multiplets formed. This wide range in particle sizes allowed us to demonstrate the ability of the sampler to collect both small and larger sized particles. It is important to note that the fluorescence method used to calculate the efficiency is not affected by the multiplets created since the spheres are internally dyed.

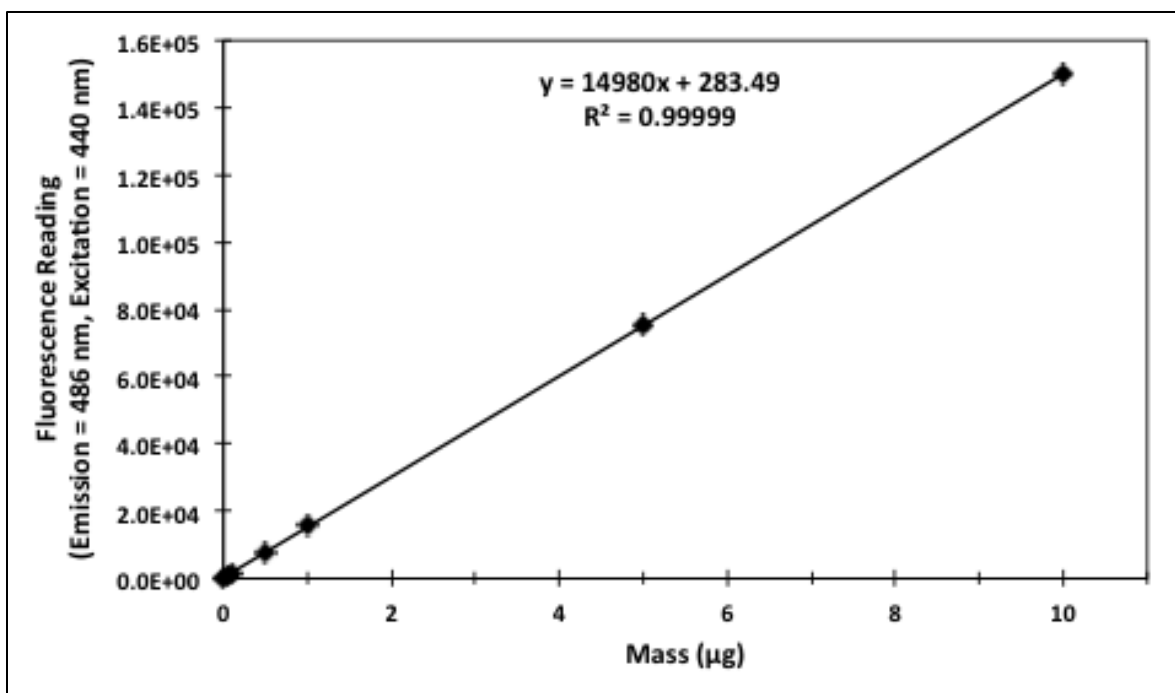


Figure 2-3: The standard curve was generated by making serial dilution standards from the YG-PSL sphere stock solution and obtaining their fluorescent output. This curve was then used to convert the raw fluorescence measurements obtained in the deposition efficiency tests into mass collected.

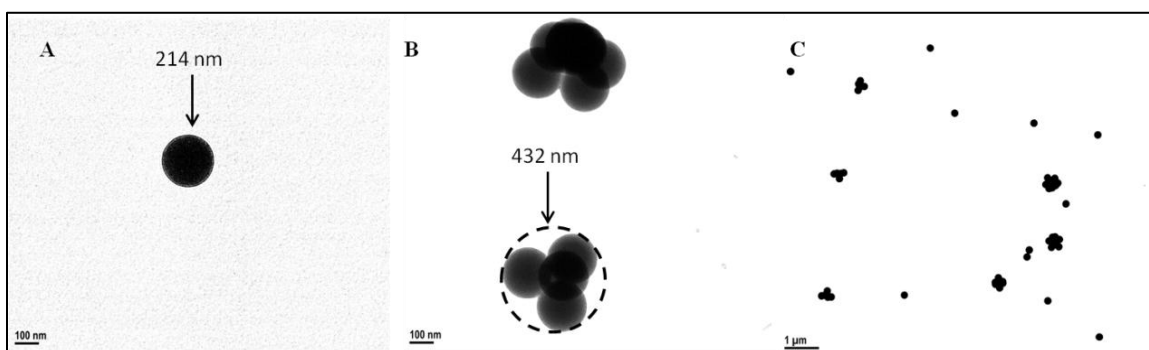


Figure 2-4: TEM micrographs of YG-PSL spheres collected on a TEM grid using the Gillings Sampler. Micrograph A shows the size of individual YG-PSL spheres was observed to be 214 nm, while micrographs B and C show various clusters of YG-PSL spheres.

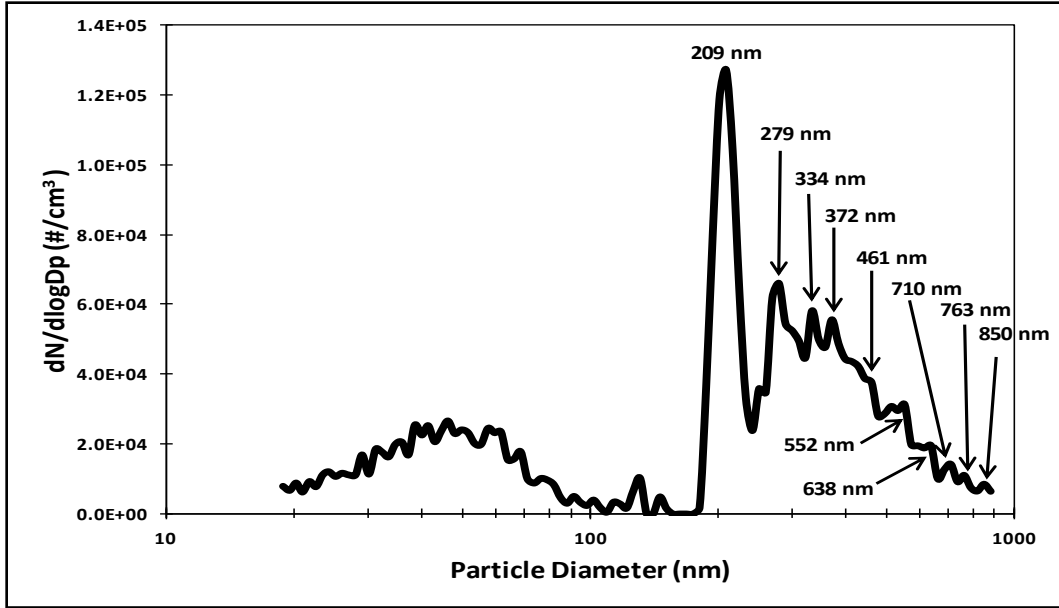


Figure 2-5: Number size distribution of the nebulized YG-PSL spheres obtained with the SMPS

Particle deposition efficiency (η) was calculated to be 45% for the 6-well deposition plate (coefficient of variability [CV] = 24.5%), and 38% (CV = 28.7%) for the 9-well deposition plate (Figure 2-6) using the equation below.

$$\eta = \frac{M_c}{M_t} = \frac{M_c}{C_p \times V_t} = \frac{M_c}{C_p \times A \times H \times n}$$

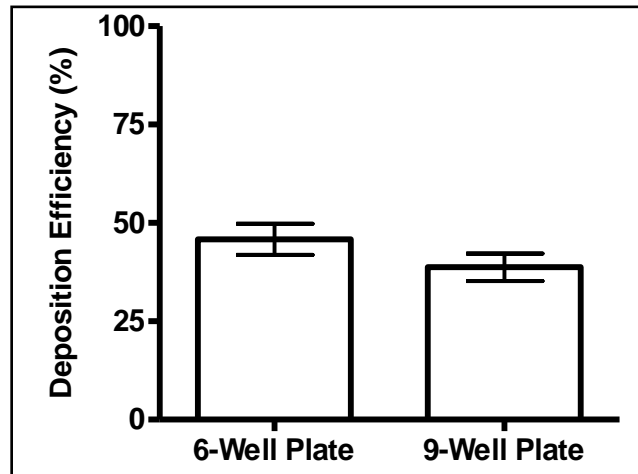


Figure 2-6: Calculated deposition efficiency using YG-PSL spheres with the 6-well and 9-well deposition plates. Statistical comparison via t-test indicates no statistical significant difference between the two deposition plates.

Here, efficiency is defined as the average mass collected (M_c) on a specified collection area over the total mass (M_t) in the volume sampled above that collection area. The collection area of interest is the Millicell-CM membrane growth area. I am only interested in how much PM is delivered to the membrane growth area. I assume the sampled air is uniformly distributed over the entire CES. To calculate the total particle mass in the volume sampled, the particle concentration (C_p) and total volume (V_t) must be known. The particle concentration (C_p) was determined by quantifying the mass collected with a Teflon filter over a specified period of time. Since the Gillings Sampler was operated with a pulsed deposition voltage, the volume of aerosol sampled is independent of the aerosol flow rate and depends only on the collection area (A) of the collecting surface, the distance (H) from the collection surface to the precipitation plate, and the number of precipitation cycles (n).^{51, 59}

An example of the efficiency calculation is provided next and an illustration can be seen in Figure 2-7. Various assumptions were made for the purpose of demonstrating how the efficiency equation is used for a particular collection area. We made the following assumptions: 1) the particle concentration (C_p) remains constant at 1 mg/m^3 and is uniformly distributed over the entire volume above the cell inserts, 2) the sampler has been operated for 1,000 cycles, and 3) the height (H) is 2 cm. The collection area (A) is 4.2 cm^2 , given by the cell growth area of the Millicell-CM insert.

For the sake of this example, I assume that we are collecting the YG-PSL spheres, as described in the methods section of Chapter 2. I also assume that our measured mass (quantified using a spectrofluorometer) is $3.78 \text{ } \mu\text{g}$. Now we have all the information needed to calculate deposition efficiency.

$$V = A \times H = 4.2 \text{ cm}^2 \times 2 \text{ cm} = 8.4 \text{ cm}^3$$

$$V_t = V \times n = 8.4 \text{ cm}^3 \times 1000 = 0.0084 \text{ m}^3$$

$$M_t = C_p \times V_t = 1 \text{ mg/m}^3 \times 0.0084 \text{ m}^3 = 0.0084 \text{ mg} = 8.4 \text{ }\mu\text{g}$$

$$\eta = \frac{M_c}{M_t} = \frac{3.78 \text{ }\mu\text{g}}{8.4 \text{ }\mu\text{g}} = 0.45 = 45\%$$

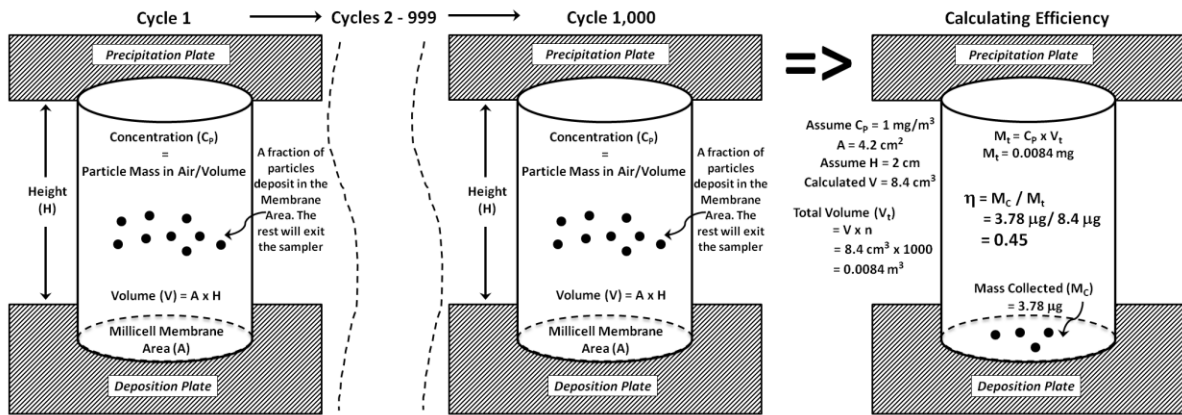


Figure 2-7: An illustration of 1000 deposition cycles to calculate the deposition efficiency on a Millicell-CM insert.

Qualitative Analysis of Particle Deposition

Three techniques were used to visually confirm the collection of the PSL spheres on the membranes at different magnification levels. First, IR-PSL spheres were collected directly onto the membranes and were observed using an infrared imaging system (Figure 2-8A & 2-8B). This technique allowed the entire 4.2 cm^2 surface area of the membrane to be visualized at once, and it can be seen that the IR-PSL spheres deposit over the entire surface. Episcopic fluorescence microscopy was then used to observe YG-PSL sphere deposition at 20 times magnification. Figure 2-8C shows the episcopic fluorescent image, and demonstrates randomly distributed deposition of the YG-PSL spheres. The YG-PSL spheres were also collected on a TEM grid that was placed on top of a membrane. An electron micrograph (Figure 2-8D) shows the randomly distributed deposition of the YG-PSL spheres.

This image shows the variation in size of the singlets versus the multiplets. After observing the images in Figure 2-8, it is clear that particle deposition does take place and is randomly distributed over the surface area of each Millicell-CM membrane.

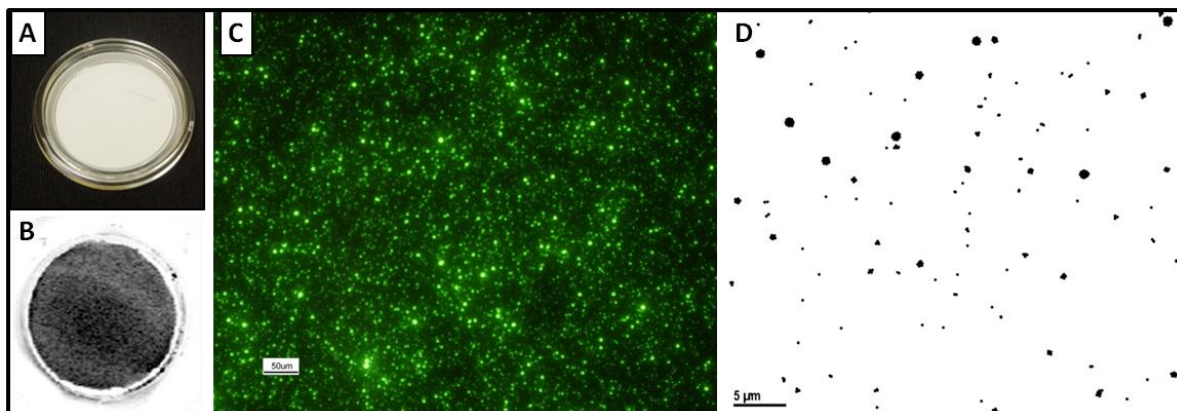


Figure 2-8: Infrared, episcopic fluorescence, and TEM images are observed here: A) View of a new Millicell-CM membrane without magnification. B) View of an infrared image of the IR-PSL spheres collected on a Millicell-CM membrane without magnification. The gray shades indicate fluorescence of the IR-PSL spheres. C) An episcopic fluorescence image of YG-PSL spheres collected on a Millicell-CM membrane at 20X magnification over a randomly selected area of the membrane. The top-right and top-left corners of this image lack brightness due to the microscope lighting itself, and not the lack of YG-PSL deposition in those areas. D) A TEM micrograph of YG-PSL spheres collected on TEM grid placed on top of Millicell-CM membrane over a randomly selected area of the TEM grid. The smallest dots are the single YG-PSL spheres, while the larger dots are the multiplets. The larger the dots, the larger the number particles present in the clusters.

Negative Control Exposures to Clean Air

Cells were first exposed to clean air while all high voltages remained turned off. This allowed us to investigate any potential problems with cell culture media evaporation that could lead to cell desiccation. No statistical difference in LDH, IL-6 and IL-8 levels between controls and exposures were observed. The exposure was repeated with the high voltages applied to the charging section of the CES only to investigate any potential toxicity from the O₃ produced during corona discharge. An average O₃ concentration of 69 parts per billion (ppb) was measured at the outlet of the sampler during the 4 hours the charging section was powered on (Figure 2-9). Again, no difference in LDH, IL-6 and IL-8 levels was observed.

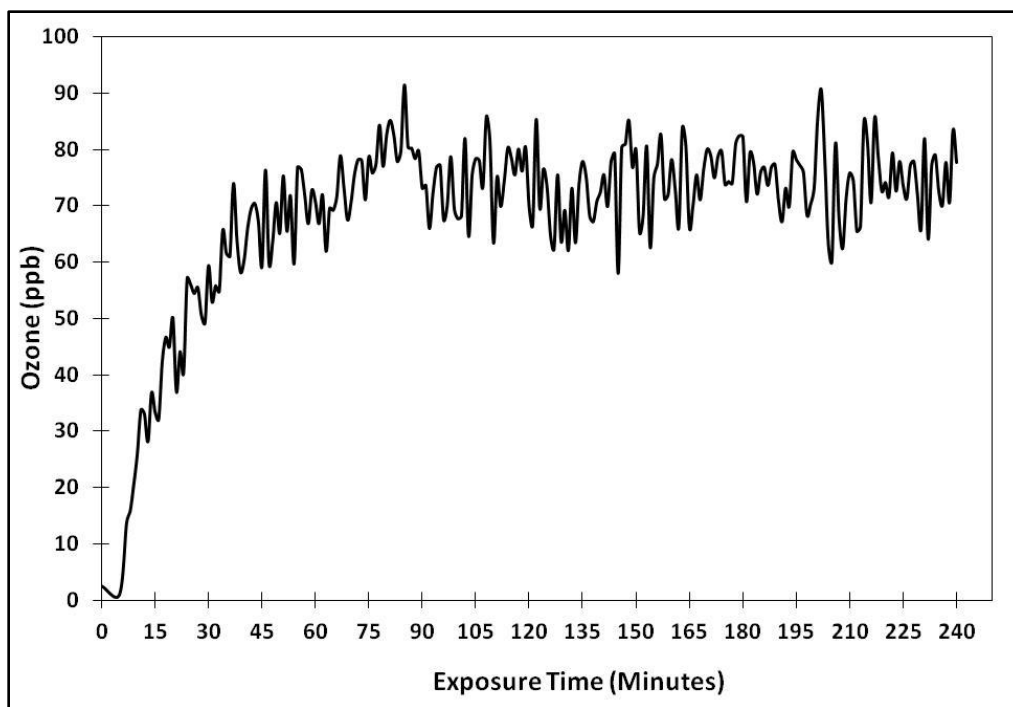


Figure 2-9: Ozone measured at the outlet of the Gillings Sampler during a 4-hour clean air exposure where the charging section was powered on only. An average of 69 ppb of ozone was generated by the corona wire.

The exposure was repeated, but this time only a high voltage was applied to the precipitation plate to address potential toxicity interference from the electric field. No difference in LDH, IL-6 and IL-8 levels was observed. From these data, it was determined that the individual components and parameters of the Gillings Sampler do not induce any elevated levels of cytotoxicity and inflammation, as measured by LDH, IL-6 and IL-8. The exposure was repeated a final time with all high voltages turned on to verify that, when all components are working together, there are no potential LDH, IL-6 and IL-8 responses resulting from the Gillings Sampler itself. These results validate that the Gillings Sampler can be operated for up to 4 hours with all the high voltages turned on without inducing adverse effects on the cells for these measured endpoints (Figures 2-10 to 2-12).

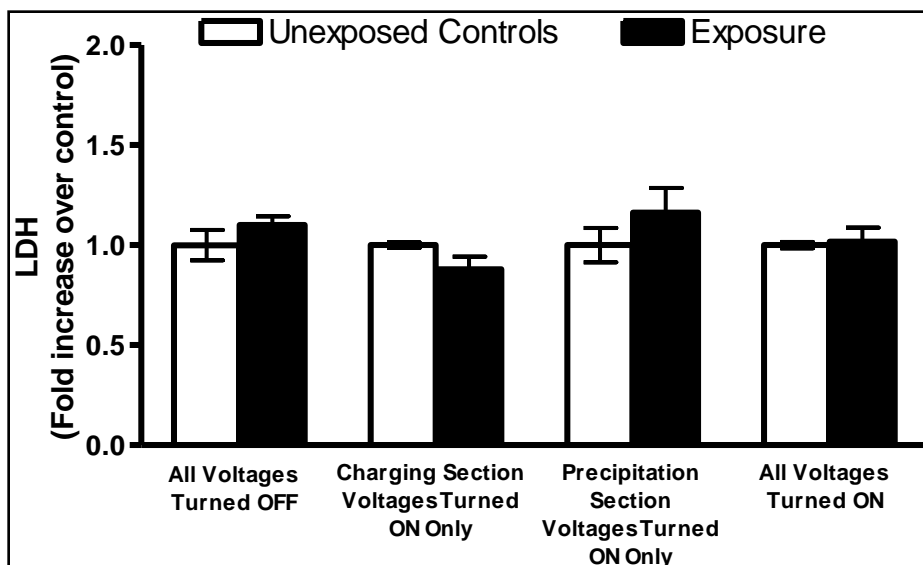


Figure 2-10: Fold increase in cytotoxicity, as measured by LDH, from 4-hour long (2,620 cycles) exposures to clean air using the Gillings Sampler at various operational conditions. No statistical difference observed when comparing exposed cells to unexposed controls under any conditions.

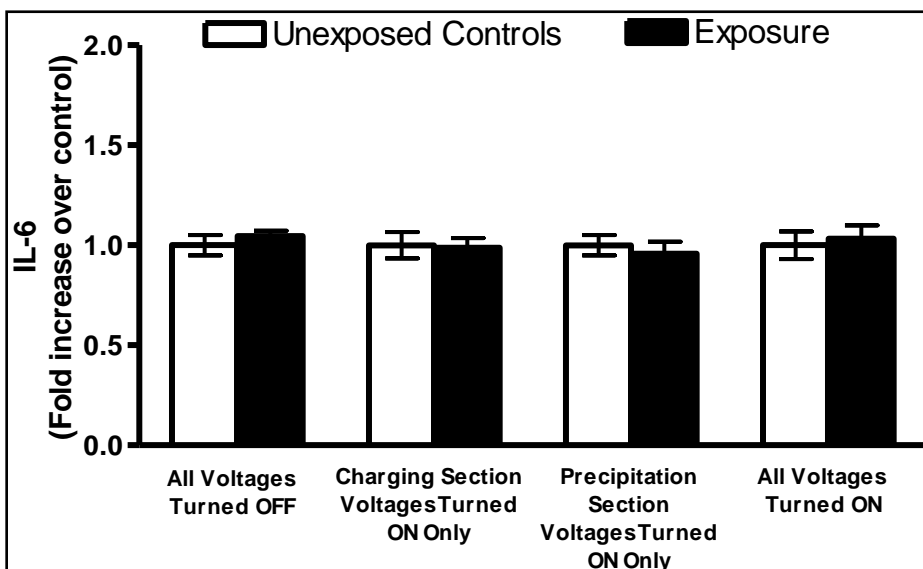


Figure 2-11: Fold increase in inflammation, as measured by IL-6, from 4-hour long (2,620 cycles) exposures to clean air using the Gillings Sampler at various operational conditions. No statistical difference observed when comparing exposed cells to unexposed controls under any conditions.

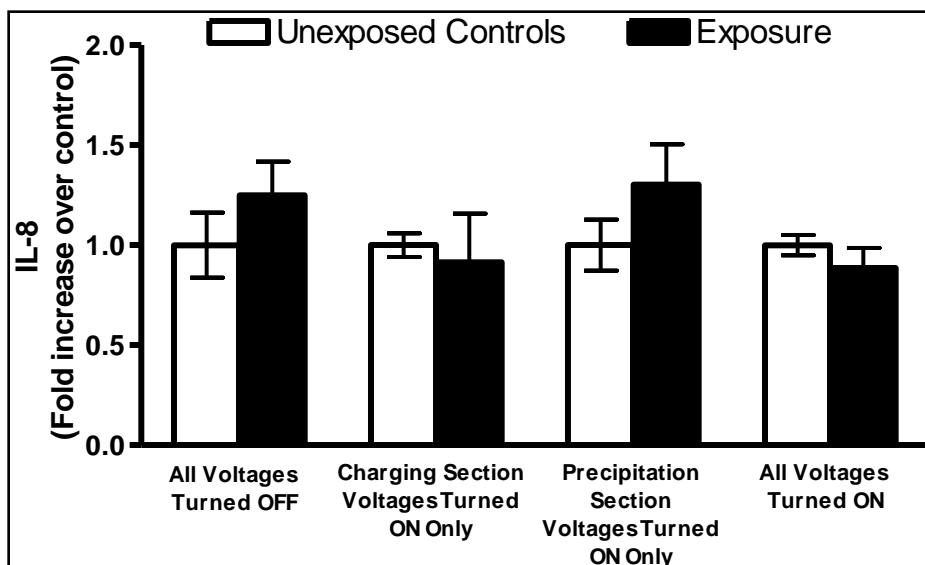


Figure 2-12: Fold increase in inflammation, as measured by IL-8, from 4-hour long (2,620 cycles) exposures to clean air using the Gillings Sampler at various operational conditions. No statistical difference observed when comparing exposed cells to unexposed controls under any conditions.

Discussion

Exposing cells to PM at ALI conditions better emulates exposure in humans compared to cell exposures under submerged conditions and has been shown to be more sensitive.^{19, 20} Exposing cells in submerged conditions, however, is still widely accepted due to the ease of PM collection and resuspension procedures. Understanding the advantages of exposing cells at ALI has encouraged our research group to develop an instrument that is easy to manufacture and can be shared with other researchers. A list of design and operational goals believed to be essential components and characteristics of an ideal *in vitro* system were outlined prior to the design and development phase of the Gillings Sampler. This new system was then evaluated under controlled laboratory conditions to determine if the established goals were met.

The Gillings Sampler maintained the features and principle of operation of the EAVES, and was manufactured and assembled using commercially available components, such as

power supplies, heaters, and controllers. The use of heaters and temperature controllers allows the temperature throughout the entire system to be maintained at 37°C, while the use of the HHS allows the sampler to be operated at optimal RH conditions. The temperature and humidity regulation system implemented in the Gillings Sampler introduces a portability feature that allows for potential usage in a wide range of settings. In an effort to provide the flexibility to co-expose multiple commercially available tissue inserts, interchangeable deposition plates were developed. These deposition plates can be customized to fit multiple configurations without needing to manually modify each insert. These unique deposition plates provide researchers the flexibility to conduct time-series studies, co-expose multiple cell types, or simply increase their statistical power with a higher number of samples. Here, 6-well and 9-well deposition plates were manufactured to accommodate the 30 mm Millicell-CM membranes, which are already 5 mm in height, and do not need to be modified.

One of the biggest concerns in these types of exposure systems is the distribution of particle deposition within each membrane insert. A difficult task is to ensure that cells within each membrane are uniformly exposed to the particles. It is not ideal, for example, if particle deposition is localized, for example, in the center or at the edges of the membrane. The infrared image obtained using the IR-PSL was crucial to this work as it provided visualization of the particle deposition distribution over the entire area. From this observation, it was determined that the Gillings Sampler adequately deposits particles across the entire 4.2 cm² membrane area.

Another concern when using these types of exposure systems is ensuring minimal variation in particle deposition from insert to insert so the dose of PM delivered to each tissue insert is similar across all co-exposed inserts. Results from the YG-PSL spheres showed that

there exists some variation in mass deposition from insert to insert as observed by the coefficient of variability between 24-29% calculated. This suggests that the exposure dose, when conducting future experiments, will not be identical in each cell culture insert. With the current data available, it cannot be determined to what extent the variation in dose from insert to insert will affect the toxicological results of the co-exposed samples. The resulting biological response can vary depending on cell type and type of PM sampled. One outcome could be that the variation in dose across all co-exposed samples is insignificant when analyzing the toxicological results or, on the other extreme, the variation in dose can significantly affect the overall toxicological results. This will be further investigated in the next chapters where the sampler will be evaluated under various test atmospheres.

Testing individual components of the Gillings Sampler demonstrated that the instrument itself does not induce toxicity, based on the three biological endpoints measured. Additionally, the Gillings Sampler was operated successfully for up to 4 hours. The two main concerns that could have limited the maximum exposure time were media evaporation and the O₃ generated by the corona wire. The plate design has a masking lid fitted over the cell culture media surrounding the inserts. This design significantly decreases evaporation, thereby allowing for longer exposure times. The 69 ppb of ozone produced by the corona wire proved to be insignificant as it did not increase the cytotoxicity and inflammation expression levels measured.

The Gillings Sampler was successful in meeting all established design and operational goals. It is acknowledged that several improvements can still be made in two major areas, deposition efficiency and variability of deposition from insert to insert. Increasing the deposition efficiency can be achieved by improving electrical charging of the incoming

particles. Currently, two diffuser screens are placed in the flow path to disperse the incoming aerosol over the entire volume inside the CES. Visual inspection of the deposition inside the entire CES indicates that the diffuser screens are not dispersing the flow as uniformly as expected. Redesigning the inlet head of the sampler can help with better flow dispersion resulting in less insert to insert variation.

The Gillings Sampler has the potential to be a very useful device for future *in vitro* exposure studies. The next steps are to further evaluate this new system under controlled laboratory exposures to determine the reproducibility and sensitivity of the sampler. The Gillings Sampler also needs further evaluation under various testing conditions to determine its feasibility for conducting future exposure studies. Testing with both immortalized cell lines and primary cell cultures would be ideal to better understand the limitations of this instrument.

CHAPTER 3: A POSITIVE AEROSOL CONTROL METHOD FOR QUALITY ASSURANCE TESTING OF IN VITRO EXPOSURE SYSTEMS

Introduction

Human exposure to airborne PM has been associated with increased morbidity and mortality.⁴³⁻⁴⁶ Inhalation exposure to airborne PM can take place indoors (e.g. residential and occupation settings) and outdoors (e.g. stationary and mobile sources). Animal inhalation exposure studies have been conducted in an effort to assess the toxic effects of inhaled aerosols and have been considered the “gold standard.”^{10, 18} The use of animal research in the field of inhalation toxicology can be ideal to observe changes in the living model organism, but due to animal testing protocols and guidelines imposed by the Institutional Animal Care and Use Committee (IACUC) studies are limited to controlled laboratory conditions. In addition to these logistical issues, ethical reasons have caused the European Guideline Registration, Evaluation and Authorization of Chemicals (REACH) to demand the reduction and replacement of animal testing with alternate methods.^{18, 60} Additionally, the Health Effects Institute (HEI) strategic plan aims to develop and apply next-generation multi-pollutant approaches to understanding exposure to and health effects of air pollutants.³ For these reasons there is a need to develop alternative *in vitro* methods and exposure systems. The development of new *in vitro* exposure systems could permit future cell exposure studies outside of the laboratory and in specific micro-environments (e.g. downwind from a power plant or next to a major highway). These alternative methods and exposure systems can

provide new insights into the pollutant-cell interactions that lead to the observed adverse health effects in humans,⁹ but they must first be validated and standardized.

The standardized method for traditional *in vitro* exposures studies relies on submerged culture conditions where the airborne pollutant is added to a culture medium and then directly added to cells.^{9, 10, 17, 18} In this exposure method a particle dose is delivered to the cells in a liquid suspension altering the particles' physical and chemical characteristics.^{19, 20} This method also assumes that all particles deposit over the cells' surface, but the number or mass of particles that actually interact with the cells cannot be determined.¹⁰ The major challenge in developing an alternative to this method is achieving a direct air-to-cell inhalation exposure. In the last 15 years alternative exposure systems through the use of new *in vitro* technology have been developed where cells are exposed at an ALI. These exposure systems allow the apical surface of the cells to be exposed to the air while the basolateral surface is nutritionally supported with culture media through a porous membrane.^{18, 47}

Various ALI exposure systems have been developed both in-house and commercially (Table 1).^{19, 32, 36, 37, 60-64} Each of the exposure systems shown in Table 1 uses different mechanisms to deposit particles, which include diffusion, sedimentation, cloud settling, and electrostatic precipitation. When developing this new technology, researchers ensured that basic conditions such as direct pollutant-cell interaction, tissue culture environments, and uniform exposures to pollutants were met.^{35, 60} Using various test atmospheres, the ALI exposure systems were shown to be more sensitive than the traditional submerged culture conditions.^{20, 37, 65} These test atmospheres varied and included photochemically-aged diesel exhaust, concentrated ambient coarse PM, and cookstove emissions. While all exposure systems demonstrated basic deposition and showed a positive biological response after

exposure, no standardized testing protocol was established. The lack of standardized testing for ALI exposure systems and the limited availability of the in-house system to be shared with other research groups makes it difficult to fully compare the various systems to each other.

Table 3-1: Comparison of Positive Controls used for Testing Air-Liquid Interface (ALI) Exposure Systems

ALI System	Deposition Mechanism	In Vitro Model	Positive Particle Control	Negative Control	Reference
Cultex CG	Diffusion and Sedimentation	HFBE21	Titanium Dioxide; Diesel Soot	None	Aufderheide 2000
Cultex RFS	Diffusion and Sedimentation	16HBE14o-	Cigarette Smoke (K3R4F and K1R5F)	Clean Air	Aufderheide 2011
ALICE	Cloud Settling	A549	Zinc Oxide	10mM NaCl and 10mM citrate Solutions	Lenz 2009
NACIVT	Electrostatic Precipitation	BEAS-2B; Porcine Lung Macrophages	None	Polystyrene Latex Spheres	Savi 2008
EAVES	Electrostatic Precipitation	A549	Diesel Exhaust	Clean Air and Polystyrene Latex Spheres	de Bruijne 2009
Modified EAVES	Electrostatic Precipitation	Normal Human Bronchial Epithelial (NHBE)	Concentrated Coarse Ambient PM	Clean Air	Volckens 2009
Whole-Smoke Perspex Chambers (BAT)	Electrostatic Precipitation	NCI-H292	Cigarette Smoke (A, B, and 2R4F)	Clean Air	Phillips 2005
VitroCell	Electrostatic Precipitation	A549	None - VOCs only	Clean Air	Anderson 2010
EPDExS	Electrostatic Precipitation	Murine alveolar epithelial cells (C10)	1,4-naphthoquinone	Titanium Dioxide and Polystyrene Latex Spheres	Stevens 2008

One method of evaluating the ALI exposure systems is to compare their deposition efficiencies. Not all exposure systems, however, used the same efficiency testing method making direct comparisons difficult. For example, the EAVES and modified-EAVES systems deposited fluorescent PSL spheres or ammonium fluorescein particles directly onto

porous membranes and measured their fluorescence intensities, while the ALICE system uses quartz crystal microbalance to determine mass deposition. In addition to deposition testing, all ALI exposure systems were evaluated with a positive control exposure. Replicating a positive control can be problematic as detailed protocols might not always be described fully or the source of particles, such as combustion sources, makes it difficult to reproduce. For example, reproducing diesel exhaust emissions from an engine is challenging since the chemical and physical composition of the diesel exhaust can change due to the type of engine used, operating mode (idle vs. throttle), and source of diesel fuel. Comparison of positive control results from ALI exposure systems is further hampered by the varying *in vitro* models that were used (i.e. immortalized cell lines and primary cells), the positive control tests conducted, and different doses of particles delivered to the cells. For these reasons attempting to compare the systems based on their toxicological results is highly problematic. A positive aerosol control method that can be reproduced by any research group is needed to adequately compare the various exposure systems that have been developed.

The aerosol used with a new positive aerosol control method should be (a) easy to generate, (b) reproducible in particle size, composition, and concentration (c) maintained at a constant concentration during the exposure time, and (d) toxic to the cells. I developed a positive aerosol control method that meets these criteria. The study presented here will describe a newly developed positive aerosol control method that has been tested using the Gillings Sampler and can be adapted for testing other ALI *in vitro* exposure systems. Three important factors that varied when the previously developed ALI *in vitro* systems underwent testing were the cell type, the aerosol source, and the dose delivered to the cells. These

variables have been fixed in this study to demonstrate the reproducibility of the presented method for conducting controlled exposures in ALI *in vitro* exposure systems.

Materials and Methods

Toxic Mineral Oil Aerosol Generation and Characterization

In a previous study by our research group, a mineral oil aerosol (MOA) was generated to serve as a surrogate for organic-containing ambient PM.⁴⁸ In this study, Ebersviller and colleagues nebulized mineral oil into a 120m³ smog chamber using a Collison nebulizer. This study showed that the MOA elicits no acute biological effects on A549 human lung epithelial cells. Later, p-tolualdehyde (TOLALD) was introduced into the chamber and allowed to mix with the MOA. The TOLALD partitioned on the MOA causing it to become toxic. When cells were exposed to a dose of 4.7–7.0 ng/cm² of the toxic MOA, a 2.6 and 3.9 fold increases in inflammation and cytotoxicity levels were observed when compared to controls. This study showed that the MOA acted as a delivery mechanism to deposit TOLALD on the cells. More importantly, this simple mix consisted of one toxic component that is widely available. I modified the existing method to generate a toxic MOA by eliminating the need to use a smog chamber, making it easier for other researchers to use in a laboratory as a positive aerosol control for quality assurance testing of any ALI *in vitro* exposure system.

A toxic positive aerosol control was generated by starting with 100 mL of fresh, steri-filtered mineral oil (pharmaceutical grade, 100%). Each batch of mineral oil was steri-filtered in the laboratory, as described by Ebersviller and colleagues,⁴⁸ one day before to remove any particulate or biological contaminants. The steri-filtered mineral oil was kept sealed and stored overnight in a sterile laboratory. The mineral oil was then ready to be mixed with a toxic chemical. TOLALD is a semi-volatile species likely to be in both the gas and particle

phases in the ambient environment.⁴⁸ It has also been shown to be a major component in diesel exhaust.⁶⁶ For these reasons and due to the successful results presented by Ebersviller and colleagues⁴⁸, TOLALD was selected as an appropriate compound. To generate a toxic mineral oil, 25 μL of TOLALD was injected directly into the 100 mL of mineral oil and mixed well. The mixed mineral oil containing TOLALD was then nebulized using a Collison nebulizer,⁶⁷ generating a toxic MOA. A schematic of the experimental setup is shown in Figure 3-1.

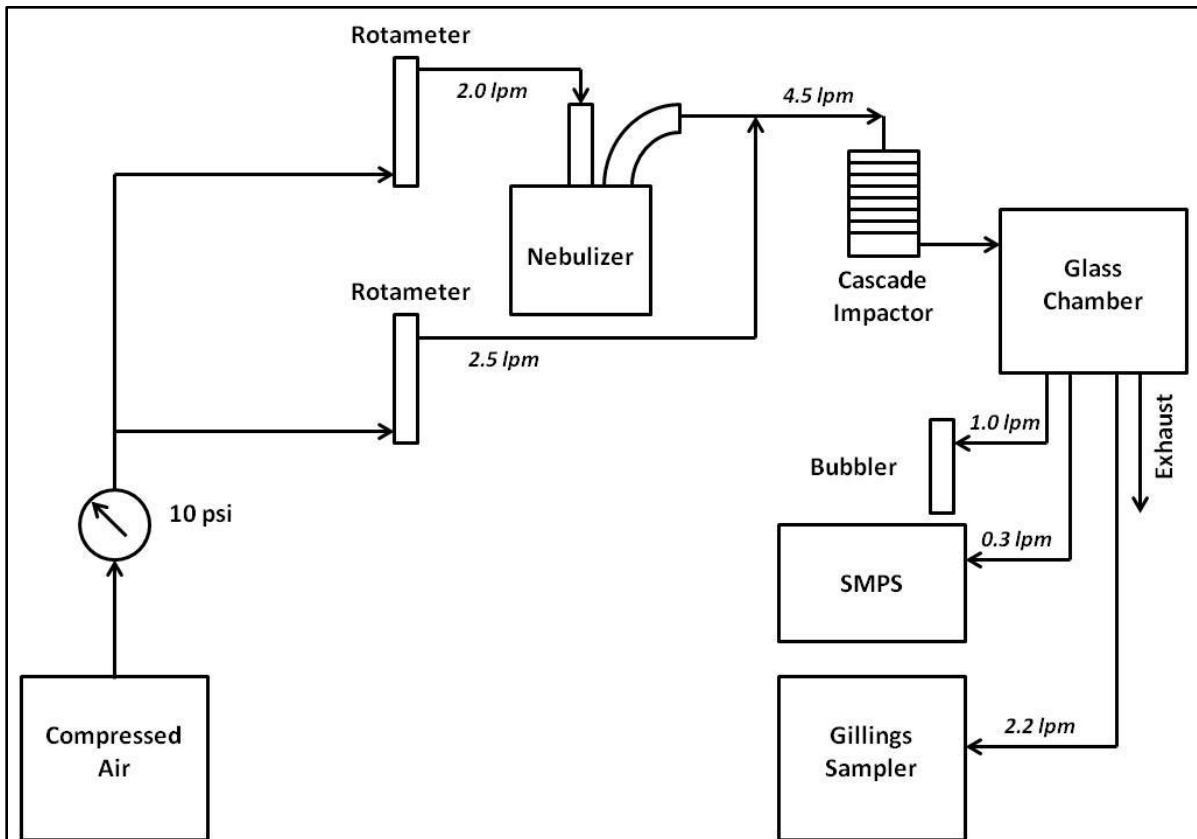


Figure 3-1: A schematic of the experimental set up used for mineral oil aerosol exposures. A clean air generator serves as the source of air. The mineral oil (with and without TOLALD) is first nebulized using a Collison nebulizer. Clean air is added to dilute the aerosol output which then enters a personal cascade impactor. The mineral oil aerosol is then introduced into a 3.8-liter glass chamber. The air sampled by the Gillings Sampler, the SMPS, and the midjet impinger is drawn from the glass chamber.

A scanning mobility particle sizer (SMPS) was used to measure the size distribution of the aerosol. A midjet impinger, used as a bubbler, was filled with 10 mL of o-(2,3,4,5,6-pentafluorobenzyl) hydroxylamine chloride (PFBHA) solution and sampled the mineral oil aerosol at 1 L/min for 2 hours during the cell exposure time. Analysis of the carbonyl content of these samples was conducted using the previously described protocol.^{20, 48} The PFBHA derivatives were analyzed by gas chromatography/mass spectrometry (GC-MS) on a Varian 3800 GC/Saturn 2200 Ion Trap MS.

Cell Culture

The A549 cell line is a human pulmonary type II epithelial-like cell line derived from human alveolar cell carcinoma of the lung.⁵⁴ While an immortalized cell line may not be a perfect representative of the biological response of primary cells, the A549 cells are reproducible, easy to culture on the Millicell-CM membranes, and provide a robust biological signal in response to pollutant exposures. These cells were, therefore, ideally suited for this work as it allows for reliable replication of experiments. Follow up studies testing the toxic MOA can be conducted using models of primary cells.

A549 cells were grown on collagen-coated Millicell-CM membranes in F12-K media with 10% fetal bovine serum (FBS) plus 0.01% penicillin/streptomycin as described in Chapter 1. For this study, the recently developed Gillings Sampler was used as the exposure system. In brief, the Gillings Sampler uses electrostatics to deposit the incoming aerosol onto cells at the ALI. The cells are located in the precipitation region, where they sit in a 6-well deposition plate. Cells were plated at a density of 8.5×10^5 cells per insert 28 hours prior to exposure and placed in commercial 6-well plates inside an incubator at 5% CO₂. When the cells reached ~80% confluency, 4 hours prior to exposure, the FBS-containing media was

replaced with serum-free media containing F12-K media, 1.5 µg/mL bovine serum albumin, plus 0.01% penicillin/streptomycin. Immediately before exposures, the membranes were transferred to the 6-well deposition plate.

Cell Exposure and Toxicity Analysis

A549 cells were first exposed to fresh, steri-filtered mineral oil containing no TOLALD. This sham exposure served to assess if mineral oil itself induces any acute biological effects. Based on the study by Ebersviller and colleagues,⁴⁸ it is expected that mineral oil elicits no acute biological effects from A549 cells. An exposure to the toxic MOA was then conducted using the Gillings Sampler. In total, three replicate exposures to the toxic MOA were conducted to test the reproducibility of the aerosol generation, aerosol size, TOLALD concentration, and measured toxicity. These exposures were conducted for 1,310 precipitation cycles (2 hours) at constant temperature (37°C), flow rate (2.2 L/minin), and relative humidity (RH) above 70%, and at 5% CO₂. After each exposure, the membranes were transferred to new commercially available 6-well tissue culture plates with fresh serum-free media in the basolateral side only. Membranes were then placed into an incubator for an additional 9 hours to allow for the cells to produce and release biological markers of toxicity. A set of unexposed cells housed in an incubator were used as controls for each test presented in this study.

For each cell exposure conducted, the basolateral supernatants and total RNA were collected for each membrane sample (n=6) for toxicological analysis 9 hours post-exposure. Total RNA was isolated from cells using Trizol (Invitrogen). IL-8 mRNA, a marker of inflammation, was measured with quantitative real-time reverse-transcription polymerase chain reaction (qRT-PCR) and normalized against β-actin mRNA levels. For cytotoxicity

analysis, levels of lactate dehydrogenase (LDH) were measured in the collected basolateral supernatant using a coupled enzymatic assay (Takara Bio Inc.). IL-8 and LDH have been shown in previous studies^{19, 20, 48, 68-70} by our research group to be appropriate endpoints of inflammation and cytotoxicity therefore they were selected as appropriate endpoints for this study. These endpoints serve to demonstrate the efficacy of this method.

Data for LDH and IL-8 are presented as the mean \pm standard error from the mean and expressed as fold increase over control. Data were analyzed using an unpaired Student's t-test and ANOVA where differences were considered significant if $p \leq 0.05$.

Results

Generating a Reproducible Toxic Aerosol

Using the experimental setup described in Figure 3-1, an MOA was generated (with and without the addition of TOLALD) to expose the lung cells to a reproducible aerosol. Mineral oil aerosolized with a Collison nebulizer produces a wide range of particle sizes. An eight-stage Marple Personal Cascade Impactor (New Start Environmental, LLC) was used in this setup to remove larger size particles (Figure 3-2). A count median diameter (CMD) between 217-237 nm was observed for all experiments. The personal cascade impactor can be replaced with any other size selective particle inlets as desired by the intended user. An aerosol concentration between 1.3-1.6 mg/m³, as measured by the SMPS and assuming a density of 0.85 g/cm³ for the mineral oil, was maintained throughout the exposure duration in all experiments. Figure 3-3 demonstrates that aerosol size and concentration is repeatable across all experiments.

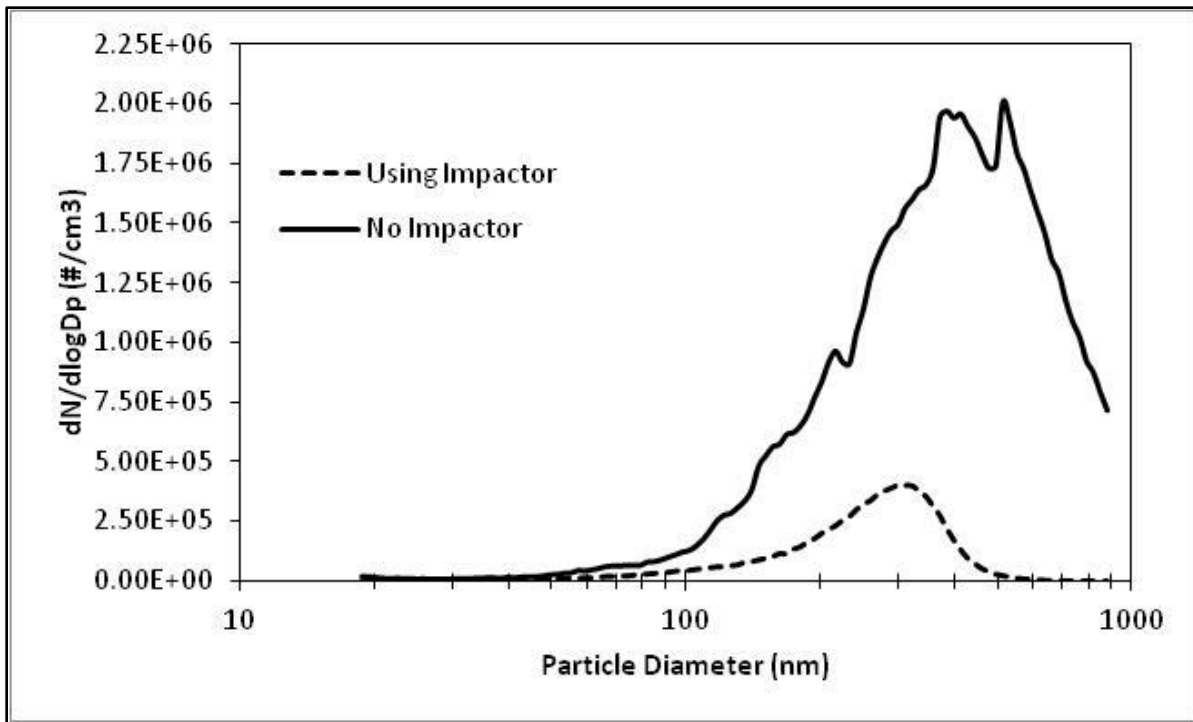


Figure 3-2: Number size distribution of the mineral oil aerosol was measured with and without a personal cascade impactor as a size selective inlet in the experimental setup.

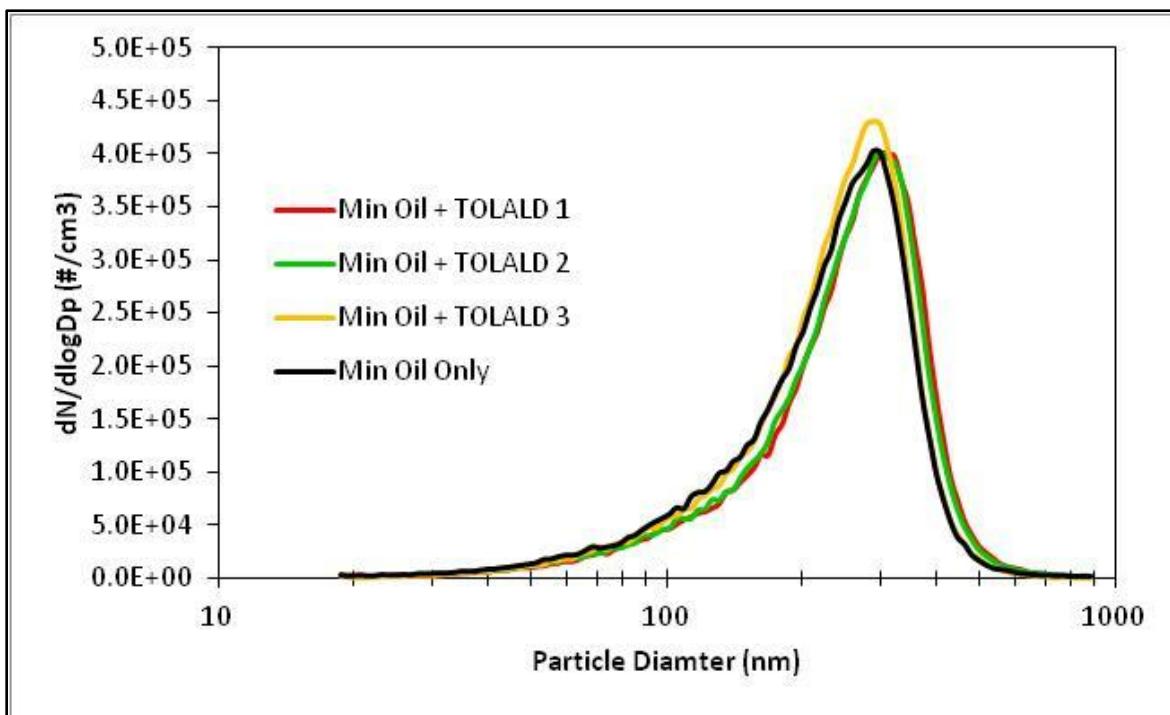


Figure 3-3: Number size distribution of the mineral oil aerosol for all experiments was measured with an SMPS for all experiments conducted. Repeatable size and concentrations were achieved.

The carbonyl content in the MOA was measured after collecting the aerosol sample in a PFBHA solution. Figure 3-4 shows the 3 chromatographs for each experiment containing TOLALD. As expected, only the TOLALD and the unreacted PFBHA are detected by GC-MS. By comparing the detected TOLALD to an internal standard, an average of dose of 8 ng of TOLALD was calculated to be delivered to each Millicell-CM insert based on the measured SMPS concentrations and efficiency calculated in Chapter 2

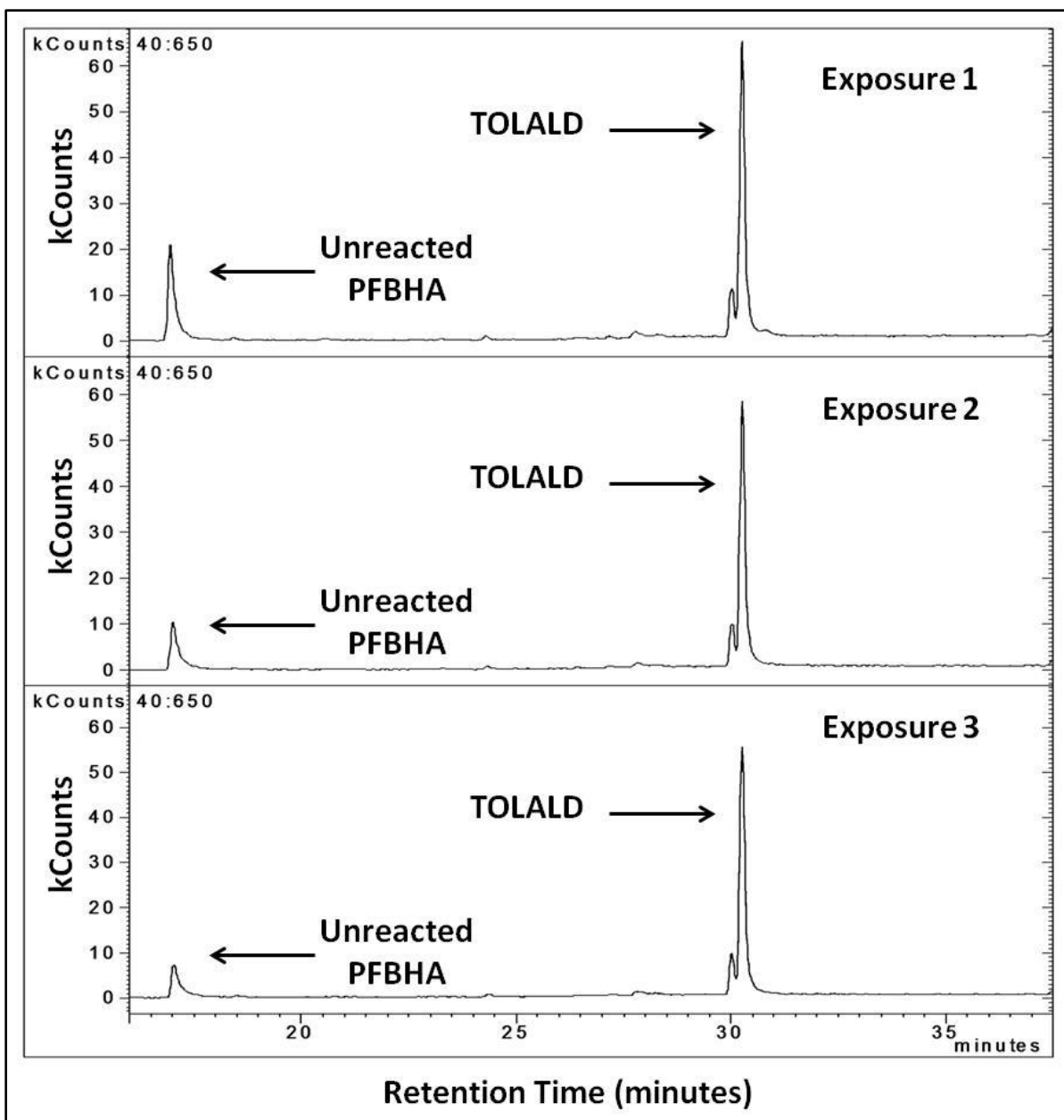


Figure 3-4: GC-MS chromatograph from all three experiments containing TOLALD. The unreacted PFBHA is observed at retention time of 17 minutes. The TOLALD peak is detected at the retention time of about 30.5 minutes.

Exposure to TOLALD Induces Reproducible Toxicity

The goal of the first experiment was to confirm that exposure to just the mineral oil itself does not induce any acute biological effects. To do this, cells were initially exposed to the MOA without the addition of TOLALD. Analysis of the LDH levels was conducted in

the basolateral media for both the unexposed cells and cells exposed to the mineral oil. The results from this analysis demonstrate that there is no statistical significant difference in the LDH levels observed from the unexposed and exposed cells. Using qRT-PCR, IL-8 mRNA levels were analyzed for the unexposed and exposed cells. Results from this analysis show small, but statistically significant increase in the exposed cells (Figure 3-5).

Since mineral oil alone did not induce drastic changes in LDH and IL-8 mRNA level, a cell exposure was then conducted using the MOA containing TOLALD. Again, their LDH and IL-8 mRNA levels were analyzed and the results are shown in Figure 3-5. As can be seen, the MOA becomes more toxic to the cells as a 3 and 4 fold increase over control is observed in the LDH and IL-8 mRNA levels.

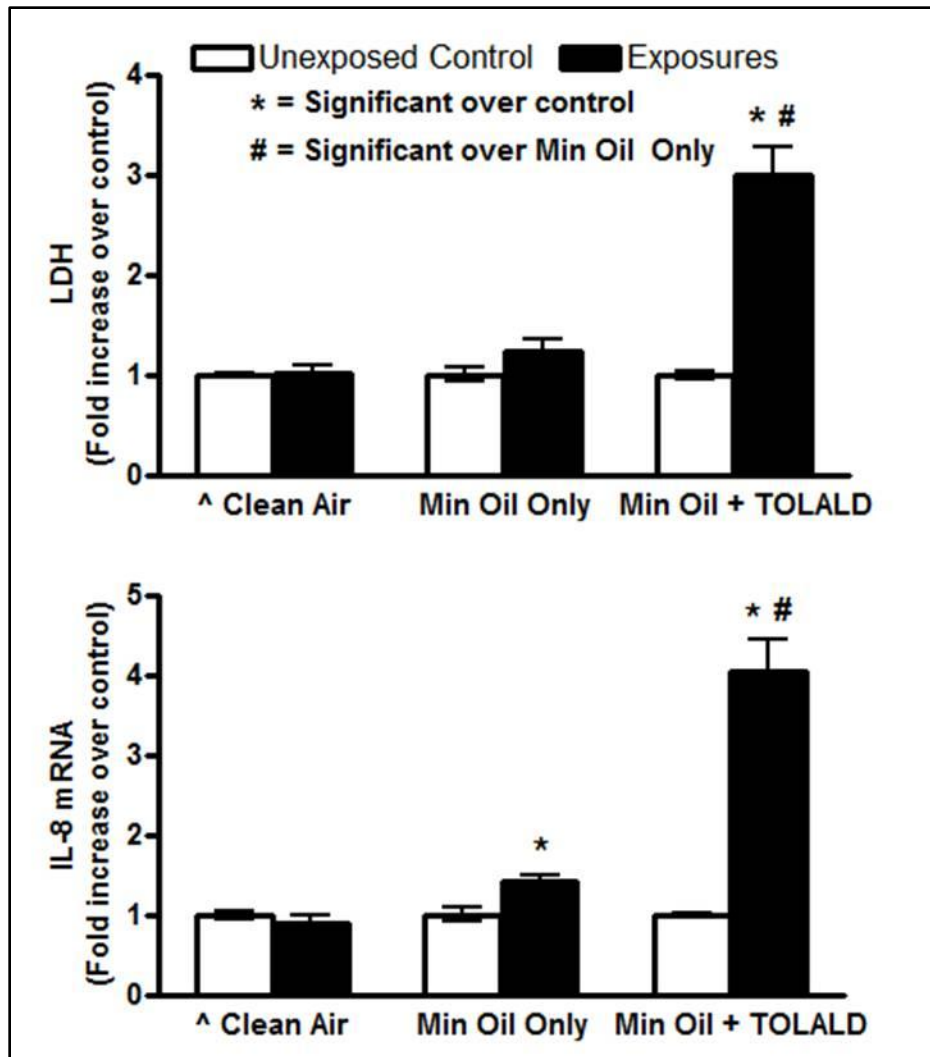


Figure 3-5: Fold increase in LDH and IL8 mRNA levels of exposures to mineral oil only and mineral oil with TOLALD compared to their respective controls. The asterisk symbol (*) indicates a statistically significant difference (t-test; $p < 0.05$) over unexposed controls. The pound sign (#) indicates a statistically significant difference (t-test; $p < 0.05$) between the mineral oil only exposure and the mineral oil with TOLALD exposure. The caret symbol (^) indicates results obtained from the clean air exposures presented in Chapter 2.

Images of unexposed and exposed cells at 9-hours post exposure, before sample collection, were captured (Figure 3-6) with a camera mounted on an inverse microscope (Olympus IX71). Changes in cell morphology can be observed after cells have been exposed to the toxic MOA. The cells that were exposed to the toxic MOA show a more circular shape, which is an indication of cytotoxicity. While these images were not originally intended to be

used for publication, they do provide a good visual of the changes in cell morphology that occurred after exposure.

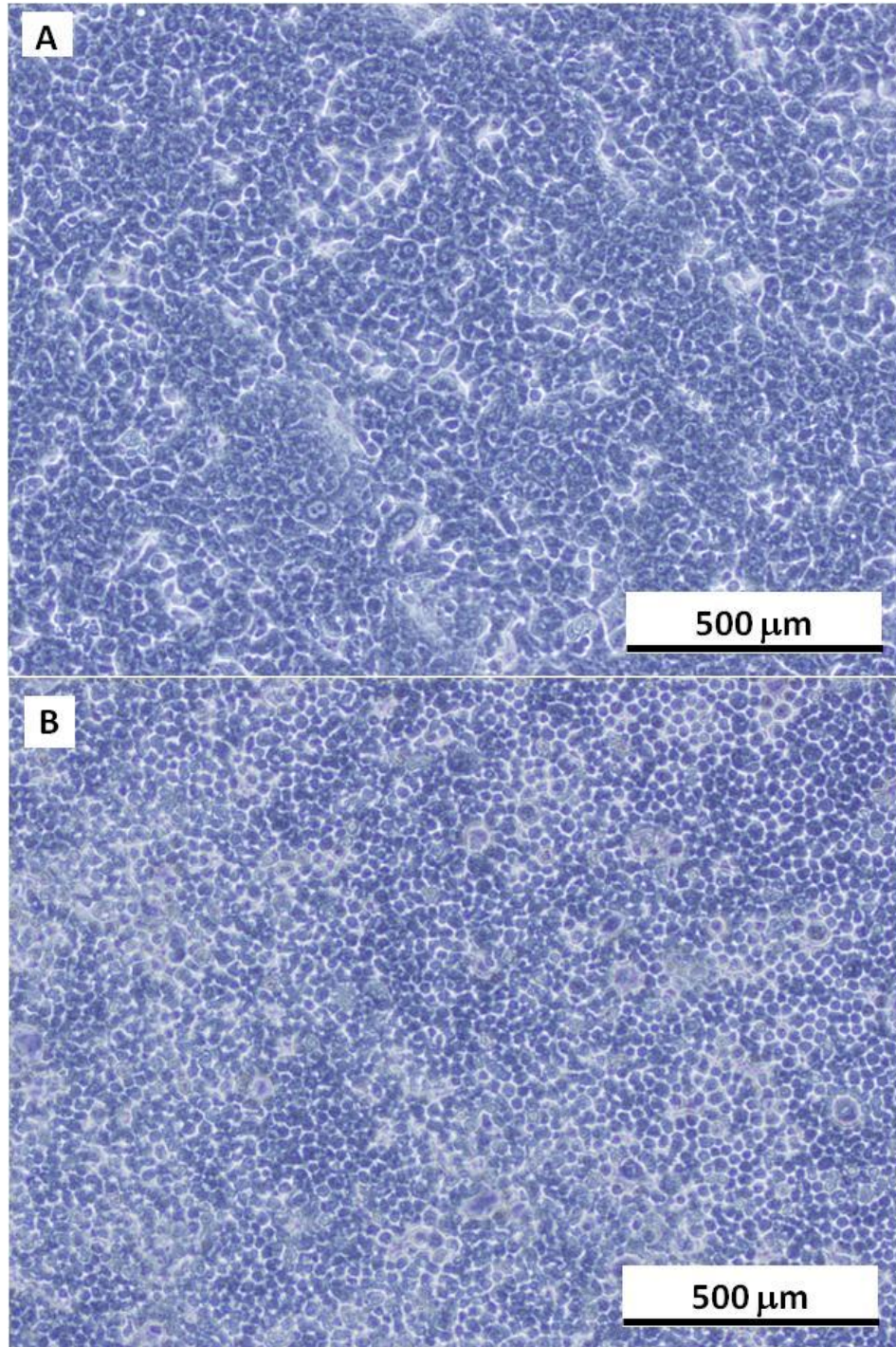


Figure 3-6: Images captured with a 10X objective lens of cells at 9-hours post-exposure for (A) unexposed controls and (B) exposed cells to the mineral oil aerosol containing TOLALD. Changes in the cell morphology are observed after cells have been exposed to the toxic mineral oil aerosol.

Since positive results were obtained from exposing cells to the toxic MOA containing TOLALD, repeat exposures were then conducted to determine if reproducible biological results could be obtained. A total of 3 exposures to the MOA containing TOLALD were conducted. The LDH and IL-8 mRNA expression levels were analyzed and compared to each exposure to determine their reproducibility. As stated above, an average of dose 8 ng of TOLALD (or 1.9 ng/cm²) was delivered to each membrane containing cells. Normalizing their LDH and IL-8 mRNA expression levels to the TOLALD dose delivered, we can observe the fold increase associated with each biological endpoint. On average, a 1.4 fold increase in LDH levels over unexposed controls is measured per 1 ng/cm² dose of TOLALD delivered to the cells (Figure 3-7). Similarly, on average, a 2 fold increase in IL-8 mRNA levels over unexposed controls is measured per 1 ng/cm² dose of TOLALD (Figure 3-8). In each of the two endpoints measured, there is no statistical difference in fold increase per 1 ng/cm² dose of TOLALD from exposure to exposure. These results confirm our hypothesis that we can accurately reproduce a biological response when using a controlled and reproducible aerosol source.

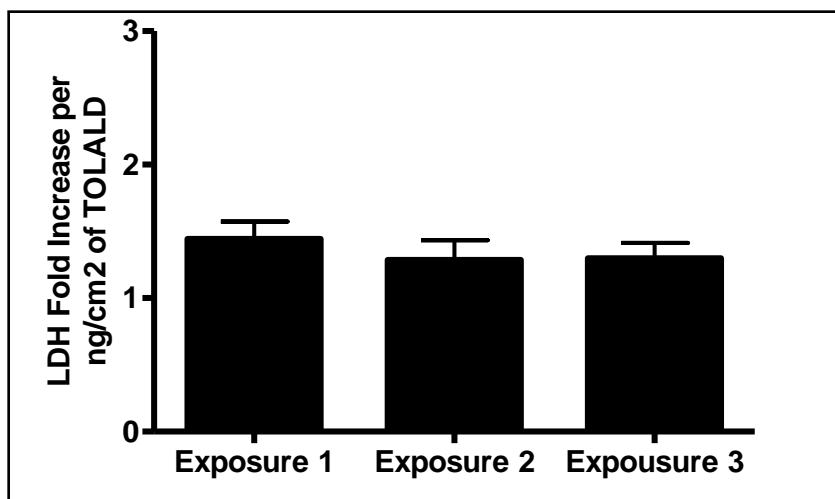


Figure 3-7: Fold increase in LDH levels of exposures mineral oil with TOLALD compared to their respective controls for every ng/cm² of TOLALD dose delivered to the cells. ANOVA analysis indicates no statistical difference in replicate exposures.

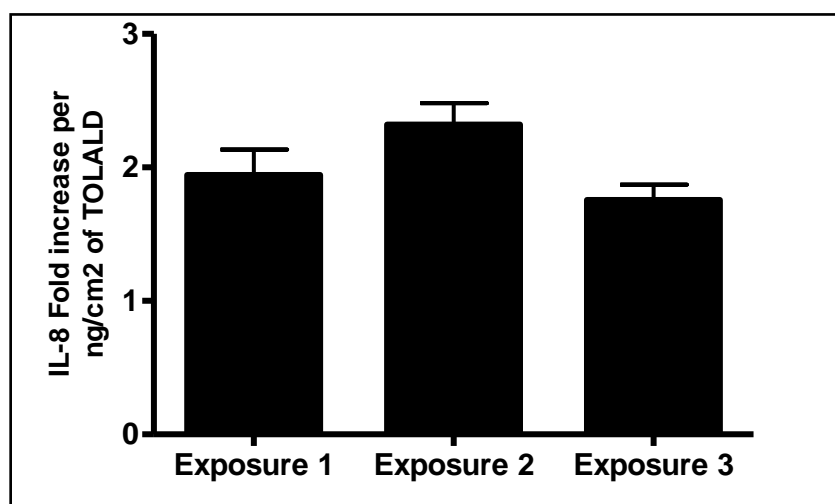


Figure 3-8: Fold increase in IL8 mRNA levels of exposures mineral oil with TOLALD compared to their respective controls for every ng/cm² of TOLALD dose delivered to the cells. ANOVA analysis indicates no statistical difference in replicate exposures.

In Chapter 2, IL-8 protein was measured in the supernatant via enzyme-linked immunosorbent assay (ELISA). Previous studies, however, have shown that the carbonaceous particles and engineered nanomaterials can interfere with the ELISA assay⁷¹⁻⁷³ whereby cytokines bind to the particles and can no longer be detected in the supernatant. Therefore, quantitative real-time reverse-transcription polymerase chain reaction (qRT-PCR)

is the preferred analysis tool for these types of exposures. After conducting exposures to the mineral oil aerosol (MOA), IL-8 protein results indicate that ELISA interference also occurs with this aerosol (Figures 3-9). Measurement of IL-8 protein via ELISA was not possible since the cytokines seem to also bind to the deposited MOA. To my knowledge, this has not been previously shown.

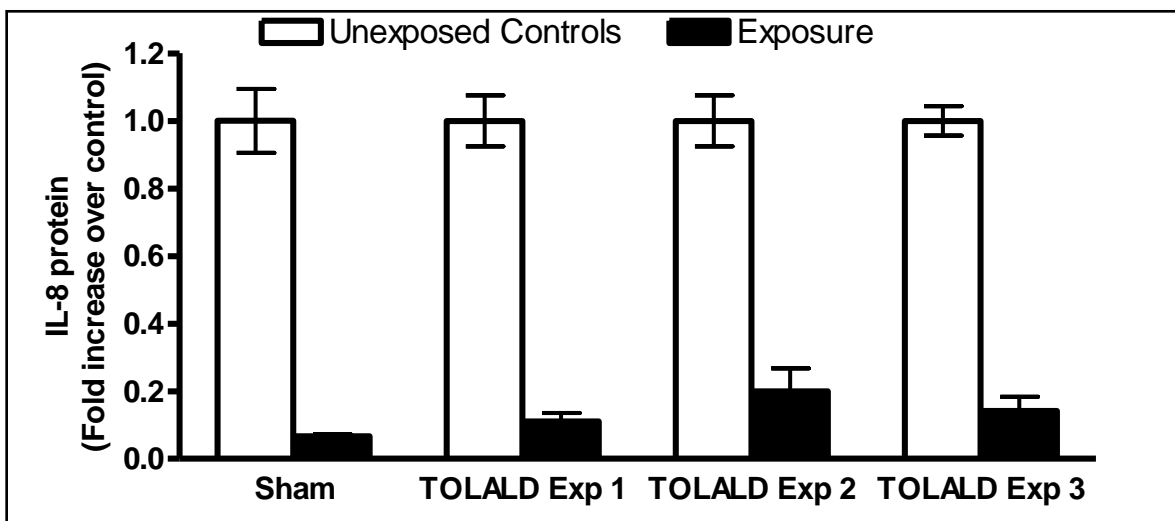


Figure 3-9: IL-8 protein in the supernatant was measured via ELISA in all cell exposures conducted to the mineral oil aerosol. Results show that IL-8 protein levels are suppressed after exposure, however these results show interference with the biochemistry of the assay. After conducting qRT-PCR (results shown in Figures 3-5, 3-7, and 3-8), it was observed that IL-8 mRNA levels increased. This indicates that ELISA interference is occurring.

A Cocktail Mineral Oil Aerosol as a Synthetic Complex Mixture

In an effort to further explore other applications of the toxic MOA, a separate batch of mineral oil was injected with a "cocktail" of 25 μ L each of TOLALD, acetone, acrolein, and methacrolein. These chemicals are all major components of diesel exhaust.⁶⁶ This mineral oil with the addition of the "cocktail" was nebulized as described previously. No cell exposures were conducted with this "cocktail" MOA, but PFBHA samples were collected for GC-MS analysis. A chromatograph from the collected sample is shown in Figure 3-10. As can be seen, each of the four components in the "cocktail" mix was clearly identified. These results

demonstrate that other toxic VOCs have the potential to be used in placed of TOLALD. In the study by Ebersviller and colleagues⁴⁸ described in the methods section of this chapter, acrolein was a second VOC tested and provided similar results to TOLALD. For this reason, it is believed acrolein, among other VOCs, can be used in this toxic mineral oil aerosol exposure method. Also, having the ability to inject various compounds of interest, one can generate a synthetic aerosol that can be representative of a more complex source, as presented here with major components of diesel exhaust.

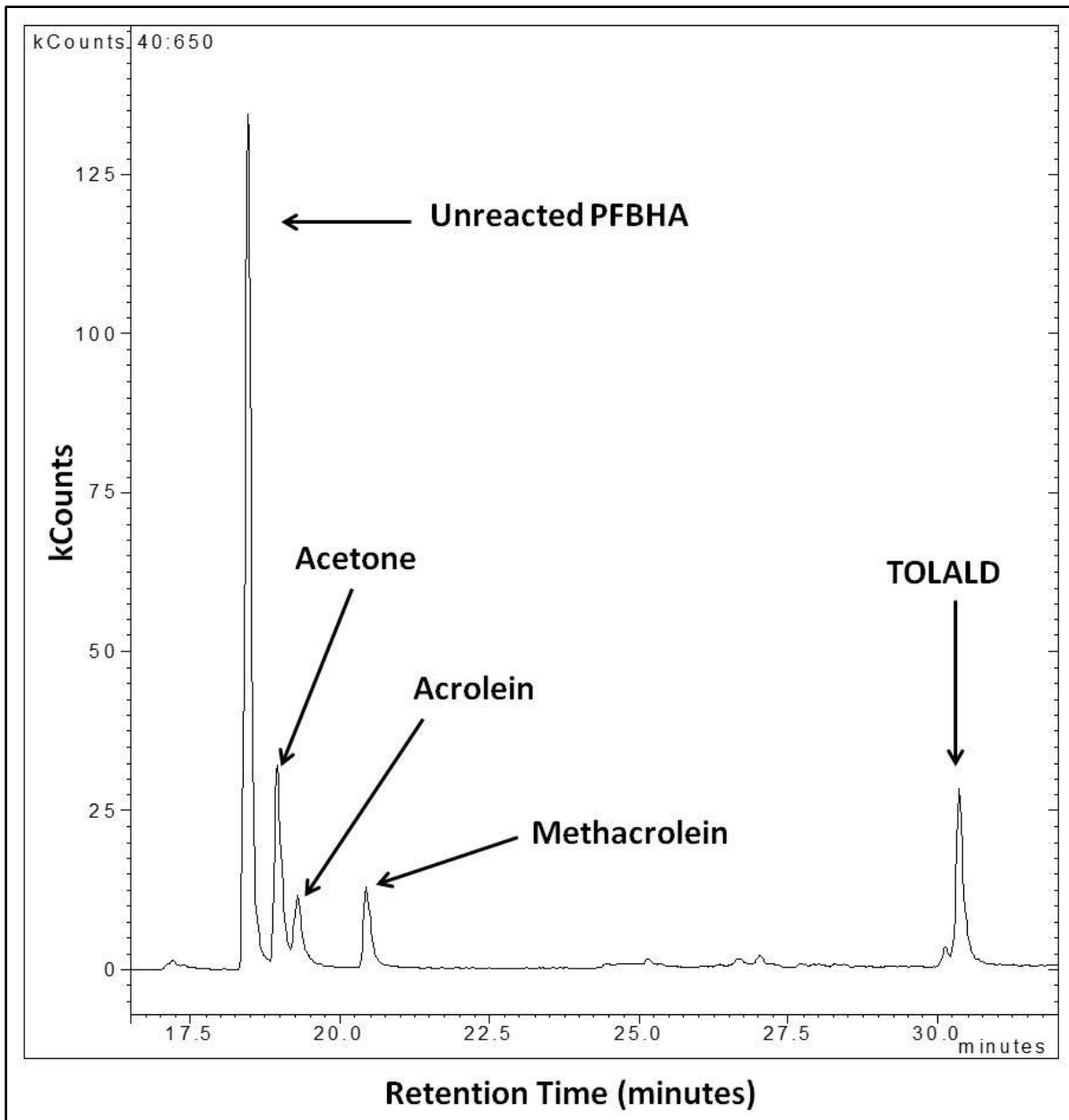


Figure 3-10: GC-MS chromatograph from the "cocktail" mineral oil aerosol containing acetone, acrolein, methacrolein, and TOLALD.

Discussion

There is a lack of standardized testing to determine the efficacy of exposing cells to airborne PM using ALI exposure systems that have been introduced in recent years. To quantify efficacy we sought to develop a positive particle control testing method that can be used to facilitate comparison of the various exposure systems. We identified three important

variables that once fixed can allow easier comparison of *in vitro* exposure systems. These variables are the cell type, the aerosol source, and the dose delivered to the cells. The cell type chosen for this method was the A549 cell line as it is widely available and it is known to provide reproducible and robust biological signals in response to pollutant exposures. We generated our own aerosol that is (a) easy to generate, (b) reproducible in particle size, composition, and concentration (c) maintained at a constant concentration during the exposure time, and (d) is toxic to cells. Our experimental setup consisted of compressed air, rotameters to control air flow, a Collison nebulizer, a 3.8-liter glass chamber, and a personal cascaded impactor used as size selective particle inlet. All of the materials described in this study are widely available and the experimental setup can be easily put together in any laboratory.

I sought to generate a toxic aerosol source that could elicit an acute biological effect from the cells upon exposure. Mineral oil was selected as a source that could be nebulized with a Collison nebulizer to generate an MOA. By injecting TOLALD, a toxic VOC, directly into the mineral oil we were able to control the toxicity of the aerosol. The A549 cells were then exposed to the toxic MOA and their biological response via LDH and IL-8 mRNA were analyzed. We showed that the MOA with the addition of TOLALD was in fact toxic to cells and clearly demonstrated that when using this method we can elicit a reproducible biological effect. The simplicity of the method makes it a reliable option that can aid in the standardization of testing ALI exposure systems since it is only one toxic compound that is responsible for the induced toxicity observed. In this study, 25 μL of TOLALD were injected into 100 mL of steri-filtered mineral oil. Increasing the volume of TOLALD injected into the

mineral oil should result in a more toxic MOA that yields higher fold increases over unexposed controls.

While this new positive aerosol control method can be used as a standardized method for comparing the efficacy of various ALI exposure systems, it can also serve as a quality assurance test for each ALI exposure system. By conducting this reproducible positive aerosol control test on a regular basis, as a quality assurance or "calibration" test, researchers can assure themselves that their ALI exposure system is operating at optimal conditions. For example, the Gillings Sampler uses electrostatics as its principle of operation to deposit the particles in the air onto the cells. Any malfunction in the electronics that might not be easily detected can diminish the performance of the sampler. By conducting a quality assurance test before a study is conducted or, for example, once a month, researchers can determine if their ALI exposure system is performing adequately based on the biological response measured. Any changes in observed toxicity can indicate a possible malfunction in the ALI exposure system and further troubleshooting might be required.

In addition, injecting multiple compounds into the mineral oil can be done to generate a synthetic aerosol that can be representative of a more complex pollutant source. Exposures to this synthetic complex aerosol can be conducted and compared to the actual complex pollutant source to observe any difference in toxicity. If exposure to the synthetic aerosol results in similar biological response, then this could suggest that the major components of the complex pollutant source are responsible for the observed toxicity. Additionally, those major components can be further studied individually to observe the toxicity that each component contributes and if the toxicity of the individual components is additive or not when compared to the complex synthetic mixture.

Further testing of this method can be conducted to answer more questions and help refine this new method. Testing the stability of the spiked mineral oil, as a function of time (days to weeks) and temperature (stored at room temperature versus 4°C) will provide better insights into whether the spiked MOA needs to be made fresh immediately prior to being used or if it can be made days or weeks in advance without losing the VOC contents due to offgassing. It would be also be important to test other cell lines to determine if we can also obtain reproducible biological results and determine if they are more or less sensitive than A549 cells. While this is an initial attempt to develop a positive aerosol control, I have demonstrated a promising method that, once refined, can serve as both a standardized test and a quality assurance test for ALI exposure systems.

CHAPTER 4: PERFORMANCE TESTING OF THE GILLINGS SAMPLER UNDER VARIOUS TEST ATMOSPHERE

Introduction

In the initial testing phase, the Gillings Sampler was evaluated under controlled and pristine experimental conditions. In chapters 2 and 3, the Gillings Sampler underwent experimental testing under controlled conditions using clean air as a negative control test or a one-component toxic aerosol as a positive control test. In all of the exposure tests the A549 cell line was used. The results obtained from these past negative and positive control test indicate that the Gillings Sampler is operating exactly as expected. Negative control tests confirmed that the use of the instrument does not induce any toxicity on the cells and therefore can be used under the tested conditions. Positive control testing showed that a toxic pollutant can induce elevated levels of toxicity as a result of exposure in a reproducible manner. These results indicate that the Gillings Sampler can be a promising research tool; however, more testing is needed before this instrument can be validated as a research tool.

To fully evaluate the Gillings Sampler it must undergo an extensive testing program that will test the sampler's performance under realistic conditions used by researchers to satisfy a wide range of airborne pollutant studies. For this reason, the sampler should be evaluated under realistic conditions before disseminating the technology to others. As a starting point, I have developed a condensed testing program that spans several areas of interest in the field of inhalation toxicology. The objective of this condensed testing program was to test the performance of the Gillings Sampler under various test atmospheres that were

generated in the laboratory using smog chambers and bench top reactors. The test atmospheres in this study were selected since they have been previously studied and are known to induce toxicity on the cells. The goal of these toxicological analyses is to quantify the biological response from the cells as output measurement. It is beyond the scope of the data available to identify specific component(s) in the test atmosphere that lead to the activation of signaling pathways or identifying the signaling pathways that were activated as a result of exposure.

The first test atmosphere simulated an urban-like ambient environment using diesel exhaust as the main source of particulate matter (PM). Our research group has extensive experience studying the toxicity of newly emitted and photochemically-aged diesel exhaust with the EAVES.^{19, 20, 49} These studies have shown the EAVES is much more sensitive than the particle resuspension method and have demonstrated that the photochemically-aged diesel exhaust is much more toxic than the freshly emitted exhaust. For this reason, exposures conducted with the Gillings Sampler will consist in exposing the cells to a photochemically-aged diesel exhaust environment.

A second test atmosphere that simulated a residential-like environment where a liquid-fuel lantern was ignited to emit combustion pollutants was selected. In developing countries, indoor PM typically comes from cook stoves and fuel-based lighting, but fuel-based lighting has received minimal attention.⁷⁴ In a study by Schare and Smith, a simulated village house with a volume of 16.9 m³ was used to measure total suspended particulate matter (TSP) concentrations from a single wick fuel-based lamp. Here, indoor steady state TSP concentrations of 3.4 ± 0.9 mg/m³ were measured.⁷⁵ Positive associations between allergic

skin sensitization and allergic symptoms with the use of kerosene lamps have been identified.⁷⁶

A third test atmosphere containing secondary organic aerosols (SOA) was selected to represent the PM found both indoors and in the ambient environment that is composed of compounds formed from the chemical transformation of organic species. Terpenes are naturally occurring, unsaturated volatile organic compounds emitted by vegetation and trees.⁷⁷ These terpenes can be found in indoor settings since they are emitted by wood products, used as solvents, and odorants in cleaning products and air fresheners.⁷⁷⁻⁷⁹ The most widely used terpene is limonene, which has a citrus scent.⁷⁷ Ozone (O₃) is also present indoors and can react with these terpenes, producing secondary products and these secondary pollutants may be responsible for some of the health effects associated with indoor air exposures.⁷⁷⁻⁷⁹

The last test atmosphere to be used for testing of the Gillings Sampler is composed of O₃ only. O₃ is one of the six criteria pollutants and the National Ambient Air Quality Standard has been set to 75 ppb for a daily 8-hr average. Previous studies have shown that O₃ exposures have an adverse effect on humans,^{80, 81} animals,^{82, 83} and cell cultures.^{54, 84} This test aims to explore a toxic test atmosphere without the presence of PM.

While it is impossible to test *all* potential uses of the Gillings Sampler, the selected test atmospheres represent possible areas of interests that could be further explored in future studies.

Materials and Methods

Generation of Test Atmospheres

Photochemically-aged Diesel Exhaust with Synthetic Urban Mixture

The 120 m³ (triangular-cross-section; 7.4 m by 6.0 m by 5.4 m high) Gillings Outdoor Irradiation Chamber enclosed in Teflon film walls was used to generate an urban-like atmosphere and conduct cell exposures to the test atmosphere using the Gillings Sampler. This outdoor chamber is located on the roof of the Gillings School of Global Public Health at UNC-Chapel Hill. Directly below the chamber, on the top floor of the building, resides an analytical and toxicological laboratory with direct access to the chamber via parallel thermally-insulated sample lines through the roof. These sample lines are connected to the analytical instruments and *in vitro* exposure systems, preserving both gases and particles together as they exist inside the rooftop chamber. Access to the roof is available for filter collection and for difficult-to-sample species (such as carbonyls) immediately underneath the chamber floor.

A commercially available diesel generator was used as the source of diesel exhaust (DE). On the morning of the exposure, the chamber was humidified naturally by pre-flushing with HEPA-filtered ambient air. The exhaust of the diesel generator was injected directly into the smog chamber at 0700 hours via a stainless steel exhaust-transfer manifold that is connected directly to the rooftop chamber (Figure 4-1). This manifold runs adjacent to the building, down to the parking lot where the diesel generator is operated. DE was injected into the chamber until the particle concentration reached ~1 mg/m³. This target particle concentration was selected to mimic previous photochemically-aged DE exposure studies conducted by our research group.^{19, 20, 48, 49} Immediately after DE injection, a Synthetic Urban

Mix⁸⁵ and NO_x [nitric oxide (NO) and nitrogen dioxide (NO₂)] were added to the chamber for the test atmosphere to simulate an urban-like environment. The synthetic particle-free urban mixture contains 55 different hydrocarbons at specific ratios that represent chemicals present in urban atmospheres.⁷⁰ The DE and Synthetic Urban Mix were mixed inside the chamber throughout the day allowing for photochemical aging to occur producing O₃ and other secondary products.

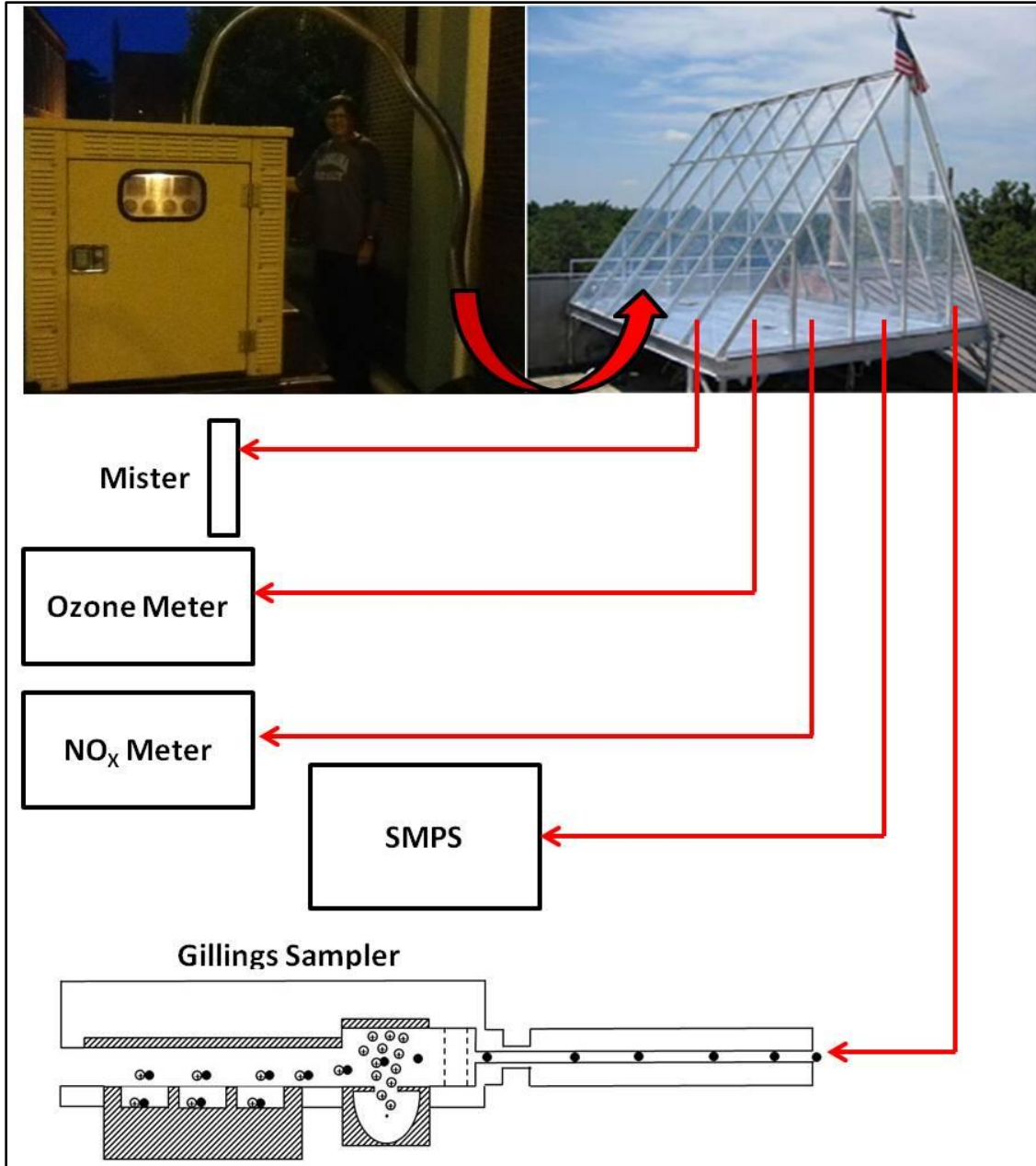


Figure 4-1: Injection of diesel exhaust into the rooftop chamber and sampling of the chamber contents in the laboratory.

The chemical and physical monitoring of the rooftop chamber is described extensively by Ebersviller and colleagues⁴⁹ and will only be briefly summarized. Ozone was measured with a Teledyne model 9811 ozone monitor (Teledyne Monitor Labs), while NO_x was measured with a Teledyne model 9841 NO_x analyzer (Teledyne Monitor Labs). Ozone and

NO_x chamber data were recorded with one-minute resolution using a data acquisition system connected to a computer. The O₃ and NO_x meters were calibrated by gas-phase titration using a NIST standard NO tank and stable O₃ source. To measure the carbonyl content in the rooftop chamber test atmosphere we used modified mister samplers similar to those described by Seaman and colleagues.⁸⁶ The sampled carbonyls were detected using the PFBHA method⁸⁶⁻⁸⁹ and the PFBHA derivatives were analyzed by GC-MS on a Varian 3800 GC/ Saturn 2200 Ion Trap MS. Total particle concentration was measured by sampling the chamber contents through a pre-weighed Teflon membrane filter (2.0 μm pore size, 47 mm diameter; Pall Corporation) at 24.6 L/min for 1 hour halfway through the cell exposure period. An SMPS was used to measure the size distribution of the DE particulates during the exposure period.

Freshly Generated Kerosene Soot

A 22 m³ (3.0 m X 3.0 m X 2.45 m) indoor environmental chamber enclosed in Teflon film walls was used to generate a residential-like atmosphere after a combustion source has been ignited. Cell exposures were conducted to the test atmosphere using the Gillings Sampler. A double wick Aladdin® kerosene lamp with standard K-1 kerosene fuel was used as the source of kerosene soot. Kerosene soot was introduced into the indoor chamber located in our laboratory until the desired concentrations were achieved (2-20 minutes of burning). The target particle concentrations for these exposures were 0.5, 1.5, and 5 mg/m³ to observe the sensitivity of the sampler with changes in particle concentrations.

Monitoring of the indoor chamber contents, which included NO_x, particle size and particle concentration was conducted as described above. Monitoring of the carbonyl content was conducted by using a bubbler filled with 10mL of the PFBHA solution and sampling the

kerosene soot at ~1 L/min for 2 hours during the cell exposure time. Analysis of the carbonyl content of these samples was conducted using the described protocol above. In addition, carbon monoxide (CO) concentrations were measured using a Model 48 gas filter correlation analyzer with an EPA approved method (Thermo Environmental Instruments Inc.).

Secondary Organic Aerosols as a Product of Ozone-Limonene Reaction

To generate a test atmosphere containing secondary organic aerosols (SOA) we used the experimental setup shown in Figure 4-2. First, a stable source of O₃ was generated by passing compressed air through an ultraviolet (UV) light at 4 L/min. O₃ was generated and the air flow then mixed with an incoming source of humid air before entering the 20-Liter glass reactor. A total of 5 mL of R-(+)-Limonene (97% purity; Sigma-Aldrich) was added to the 20-liter glass reactor. O₃ passed through the glass reactor where it mixed with the limonene, which then produced SOA as a result of this reaction. To facilitate sampling of this test atmosphere by the various instruments, the air containing the newly generated SOA was passed into a 3-liter glass reactor containing several sampling ports. Monitoring of the aerosol size distribution was conducted with the SMPS while the concentration of ozone before reacting with limonene was measured using the ozone meter described above. Monitoring of the carbonyl content was exactly as described above for the kerosene soot.

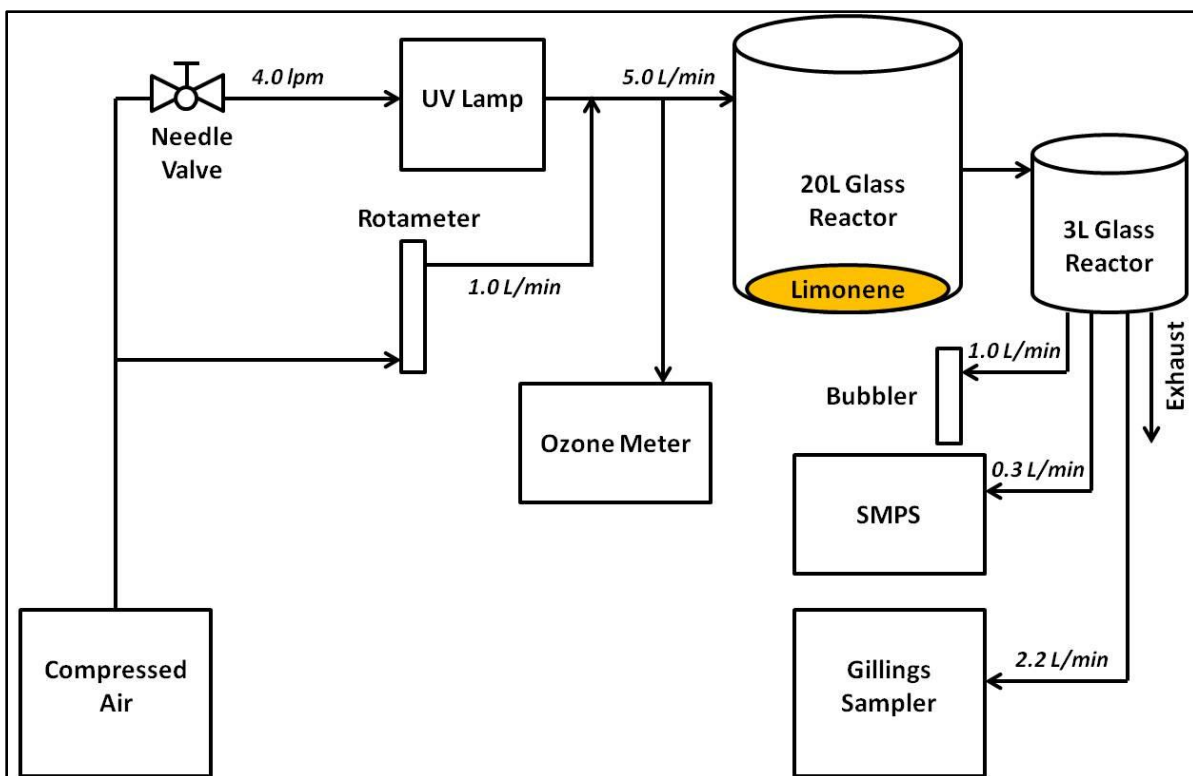


Figure 4-2: Schematic of experimental setup for generating secondary organic aerosols as a result of reacting ozone with limonene.

Ozone

The Gillings Outdoor Irradiation Chamber was used to generate an O₃-only test atmosphere. O₃ was generated from oxidized air using an O₃ generator (model OL80A; Ozone Services, Yanco Industries) and injected directly into the chamber. A target concentration of 400 ppb of O₃ was used for this test atmosphere as it has been used previously by our research group. The objective of this exposure was to determine if gaseous pollutants alone can induce toxicity when using the Gillings Sampler. Findings from previous studies using the EAVES showed that in this type of exposure system the exposed cells only respond to the PM deposits and not the gases.^{19, 20, 48, 49} A set of cells was exposed to O₃ using the Gillings Sampler and another set was co-exposed using the Gas In-Vitro Exposure System (GIVES). The GIVES is an 8-liter, cylindrical modular cell-exposure chamber

(Billups-Rothenber, MIC-101TM) previously described in detail by Ebersviller and colleagues.⁴⁸ In brief, air enters the GIVES from below a mesh floor where the cells are exposed at an air-liquid interface. The air randomly circulates over the cells and eventually exits the exposure chamber. Since the GIVES has been used solely as a gas exposure chamber in our research group, it was used as a bench mark to determine how the Gillings Sampler compares. Co-exposing cells with these two systems provide a clear comparison of a true gas exposure chamber and the Gillings Sampler. Monitoring of O₃ was conducted once a minute as described above.

Human and Mouse Cell Cultures

The human type-II alveolar epithelial cell line, A549, was used in all test atmospheres presented here since they have been used previously in the Gillings Sampler (Chapters 2 and 3). These cells were cultured on collagen-coated Millicell-CM membranes at a density of 8.5×10^5 cells per insert 28 hours prior to exposure and placed in commercial 6-well plates inside an incubator at 5% CO₂. Four hours prior to exposure, the FBS-containing media was replaced with serum-free media as previously described (Chapters 3).

For the photochemically-aged diesel exhaust test atmosphere only, various cell types were used simultaneously in the Gillings Sampler while conducting these exposures. In an effort to observe if other cell types can be used in this exposure system and to compare how the biological response differs in different human-derived and mouse-derived cell cultures, 3 other cell types were used. The EpiAirway cells are 3-D human-derived tracheal/broncheal epithelial cells purchased from the MatTek Corporation. The mouse cells used were fully differentiated tracheal epithelial cells with visible cilia isolated from C57BL/6J and BALB/cJ mice. Mice were purchased from Jackson Laboratories (Bar Harbor, ME). All experimental

procedures were approved by the University of North Carolina Institutional Animal Care and Use Committee. Murine tracheal epithelial cell (MTEC) isolation and culture was performed as described by You and colleagues.⁹⁰ MTEC were expanded to passage one in Ham's F-12 medium (Invitrogen) before use.

Cell Exposure and Toxicity Analysis

In all exposures to the test atmospheres, cells were exposed for either 1,310 precipitation cycles (2 hours) or 2,620 precipitation cycles (4 hours), while maintained at 37°C, RH above 70% and at 5% CO₂ levels. After each exposure, the membranes were transferred to new commercially available 6-well tissue culture plates with fresh serum-free media in the basolateral side only. Membranes were incubated for an additional 9 hours to allow for the cells to produce and release biological markers of toxicity.

For each cell exposure conducted, the basolateral supernatants and total RNA were collected for toxicological analysis 9 hours post-exposure. Total RNA was isolated from cells using Trizol (Invitrogen). The following markers of inflammation were analyzed with either ELISA or qRT-PCR normalized against β -actin mRNA levels as described in Chapters 2 and 3; Interleukin-6 (IL-6), Interleukin-8 (IL-8), and cyclooxygenase-2 (COX-2). For cytotoxicity analysis, levels of lactate dehydrogenase (LDH) were measured in the collected basolateral supernatant. Heme oxygenase-1 (HO-1) mRNA levels will be used to determine oxidative stress after exposure. Not all of these endpoints were used for each exposure. Refer to Table 4-1 in for a summary of the endpoints used for each test atmosphere exposure.

Data presented as the mean \pm standard error from the mean and expressed as fold increase over control. Data were analyzed using an unpaired Student's t-test where differences were considered significant if $p \leq 0.05$.

Table 4-1: Exposure times, cell types used and biological endpoints measured for the exposures conducted

	Diesel Exhaust	Kerosene Soot	SOA	Ozone
Deposition Cycles	2620	1310	1310	2620
Exposure Time (Hours)	4	2	2	4
Cell Type	A549 (n=1), EpiAirway (N=3), C57BL/6J (n=2), BALB/cJ (n=3)	A549 (n=6)	A549 (n=6)	A549 (n=6)
Endpoints	LDH, IL-6 mRNA, IL-8 mRNA, HO-1 mRNA	IL-6 mRNA, IL-8 mRNA, COX-2 mRNA	LDH, IL-6 mRNA, IL-8 mRNA	LDH, IL-8 protein

Results and Discussion

Photochemically-aged Diesel Exhaust Induces Varying Toxicity Depending on In Vitro Model

Diesel exhaust was injected into the rooftop chamber at 0700 hours and allowed to photochemically age to generate an urban-like atmosphere. Two different human cell types (A549 and EpiAirway) and two different mouse strains (C57BL/6J and BALB/cJ) were exposed simultaneously in the Gillings Sampler to the aged diesel exhaust for 4 hours starting 1500 hours. An average DE particle concentration inside the rooftop chamber was calculated to be $426 \mu\text{g}/\text{m}^3$ and an average of 146 ppb of ozone was measured during the exposure period. The decrease in particle concentration throughout the day from $\sim 1 \text{ mg}/\text{m}^3$ to $426 \mu\text{g}/\text{m}^3$ is attributed to particle loss to the chamber walls, particle removal from filters and misters for analysis, and leaks in the chamber. Based on the particle concentrations measured in the chamber during the exposure period, an estimated particle dose of $0.41 \pm 0.1 \mu\text{g}/\text{cm}^2$

was delivered to the cells. The number size distribution of the DE particulates present in this test atmosphere during the exposure can be seen in Figure 4-3, while chromatographs of the measured carbonyls are shown in Figure 4- 4.

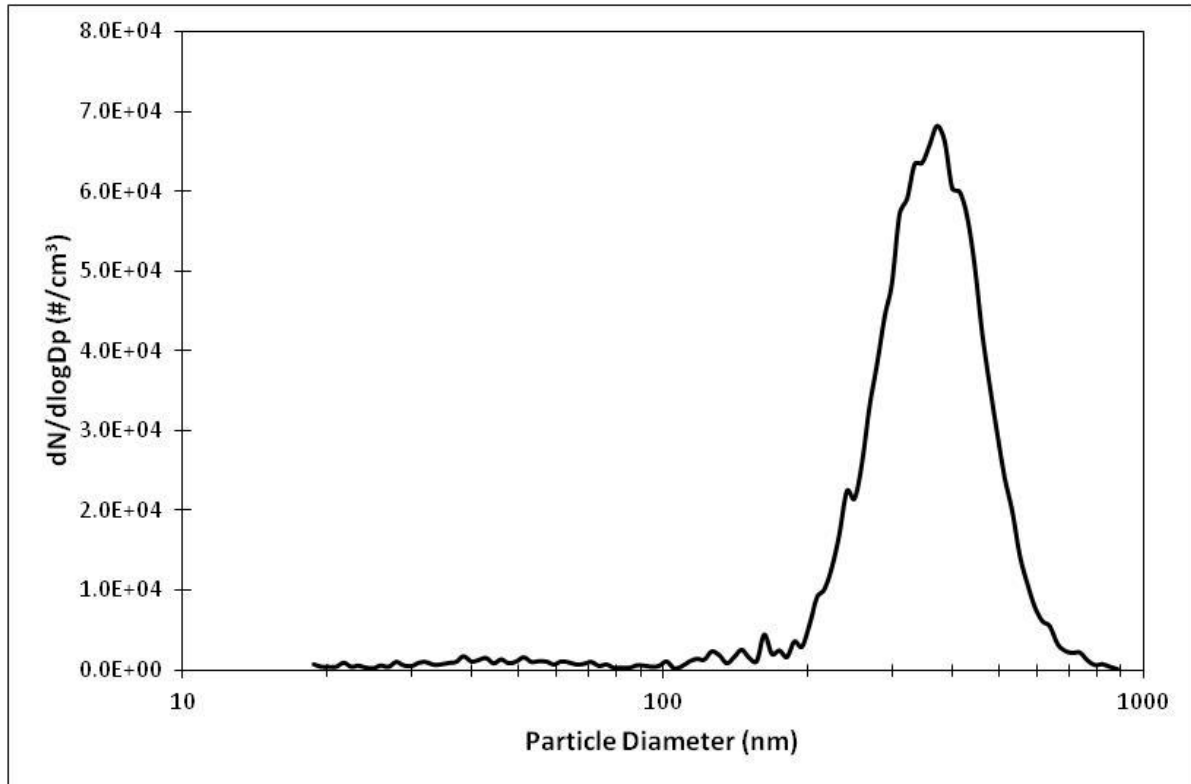


Figure 4-3: Number size distribution of diesel exhaust particles sampled from the UNC rooftop chamber while cell exposures were being conducted with the Gillings Sampler.

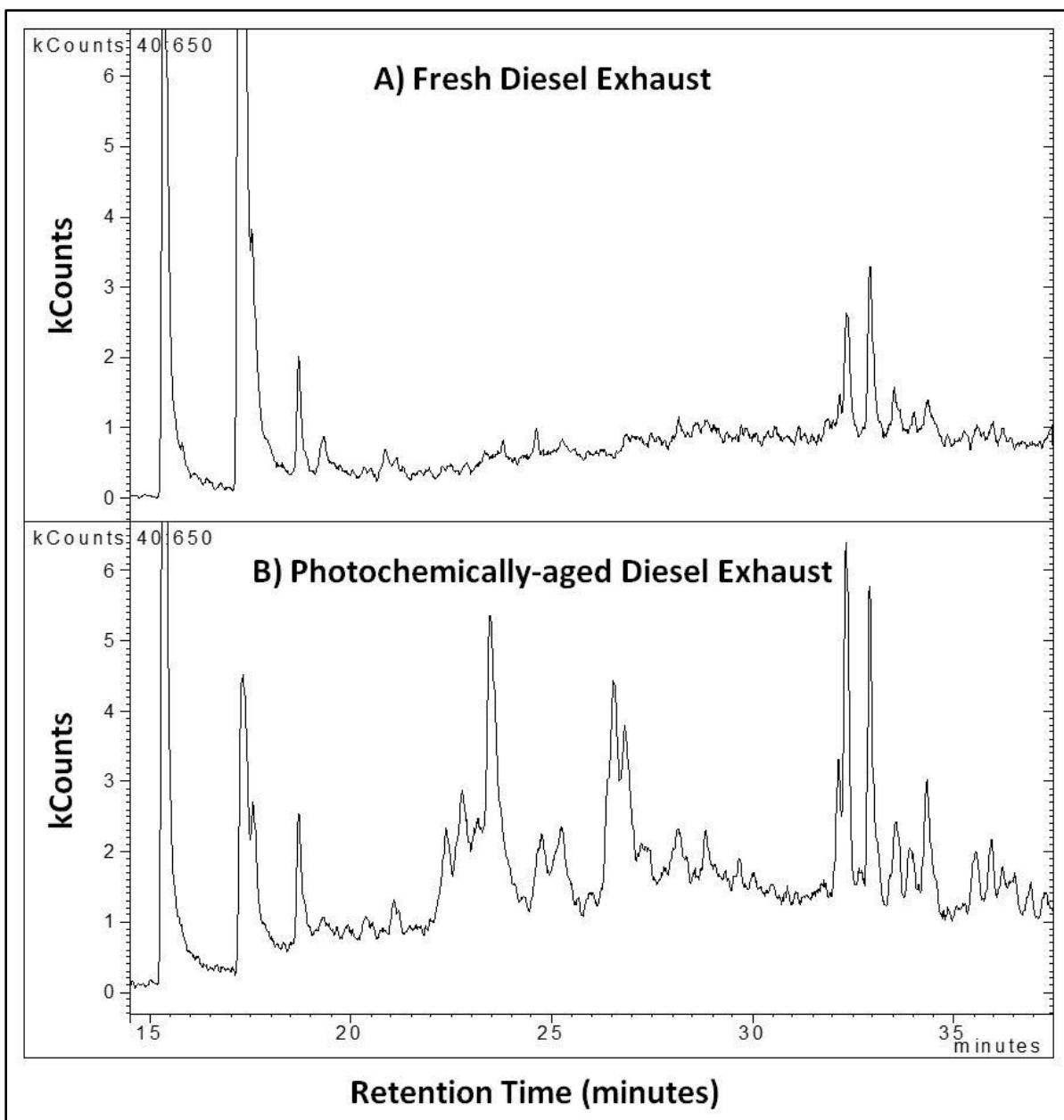


Figure 4-4: GC/MS chromatograph of the measured carbonyls of the diesel exhaust in the morning (Fresh) and evening (Photochemically-aged) inside the UNC rooftop chamber while cell exposures were being conducted with the Gillings Sampler.

An electron micrograph of diesel particulates was captured using a transmission electron microscope (TEM) grid (Standard Copper with Carbon Film, 400 Mesh, Electron Microscopy Sciences) placed over the deposition plate inside the Gillings Sampler during the

diesel exhaust exposures. The collected particles were viewed directly on the TEM grid in a Zeiss EM900 TEM at an accelerating voltage of 50 kV (Figure 4-5).

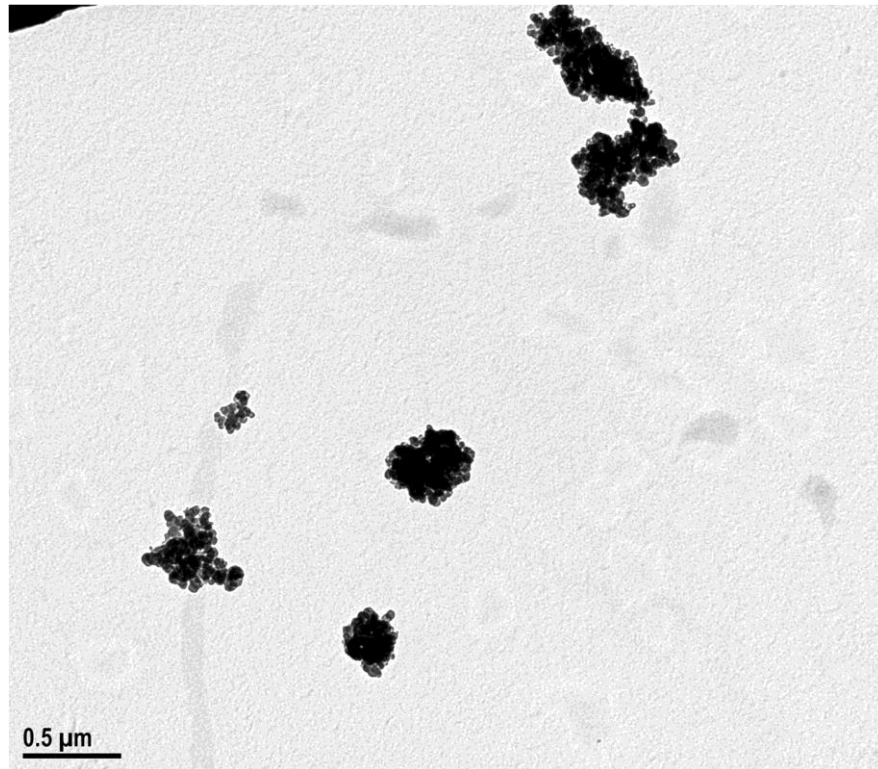


Figure 4-5: TEM micrograph of photochemically-aged diesel exhaust particles collected on a TEM grid placed on the deposition plate inside the Gillings Sampler during cell exposure.

Toxicological analysis of cytotoxicity, inflammation, and oxidative stress was conducted on the biological samples collected at 9 hour post-exposure (Figure 4-6). Results indicate that the type and magnitude of responses varies from cell type to cell type. For example, the A549 cells show increases in LDH, IL-6 mRNA, and IL-8 mRNA levels, while the EpiAirway cells show no difference from exposed cells compared to controls. The trends observed in both mouse cell strains were similar for the IL-6 and HO-1 endpoints as they increase after being exposed to diesel exhaust. The LDH levels increased in BALB/6J derived cells after exposure, but decreased in C57BL cells.

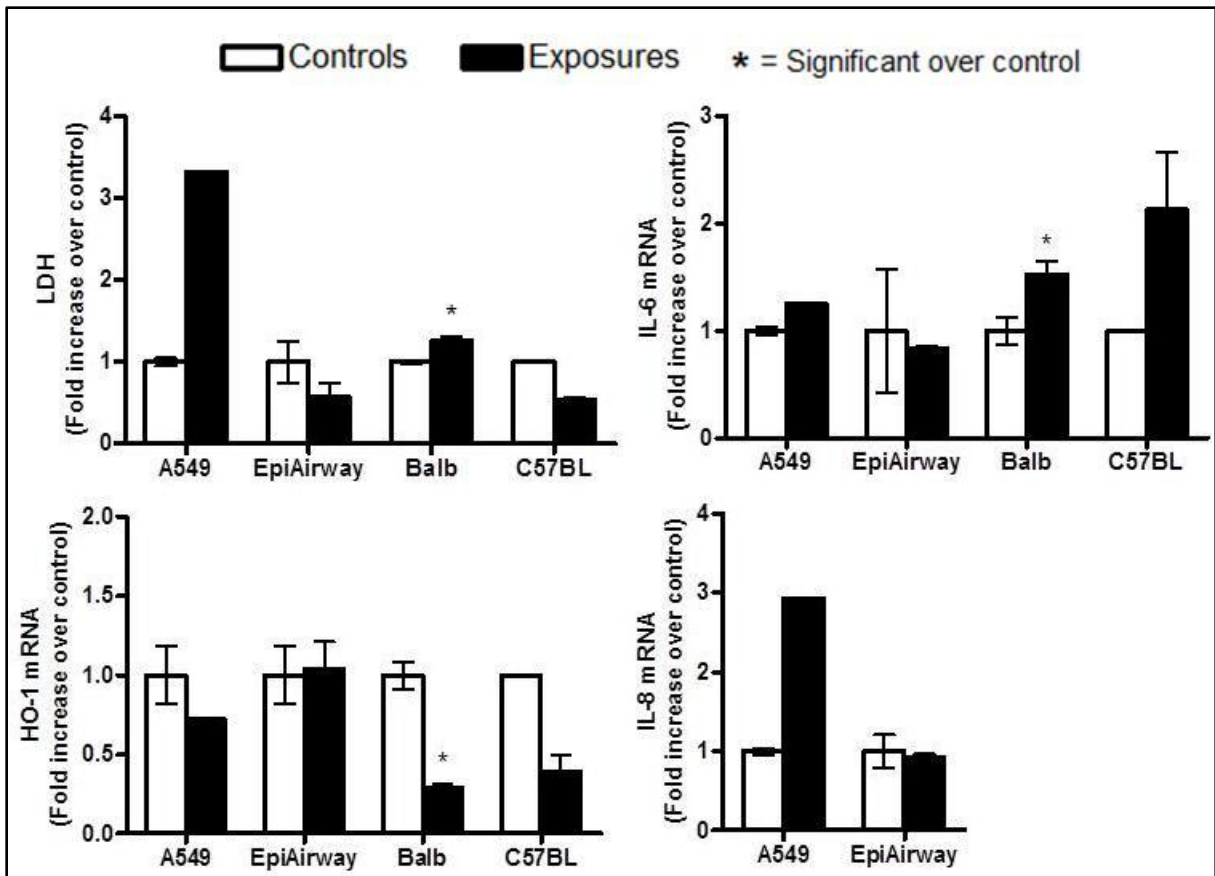


Figure 4-6: Biological analysis of cytotoxicity (LDH), inflammation (IL-6 mRNA and IL-8 mRNA), and oxidative stress (HO-1 mRNA) from A549, EpiAirway, BALB/cJ, and C57BL/6J exposed cell cultures to photochemically-aged diesel exhaust. The * denotes statistical significance ($p < 0.05$).

Conducting this exposure demonstrated that the Gillings Sampler allows the researcher the flexibility to use multiple cell types at once. The results showed that the changes in cytotoxicity, inflammation, and oxidative stress levels induced by air pollution mixtures may be species and strain-dependent. For this reason, it is important to understand the limitations of each *in vitro* model and critical to identify appropriate endpoints and time points for each model.

Exposures to Different Kerosene Concentrations Showed Similar Inflammation levels

Another combustion source was used to generate a residential-like atmosphere. A kerosene lamp was ignited to produce kerosene soot. A549 cells were exposed to 3 different

kerosene soot concentrations to observe the sensitivity of the sampler. Filters were used to collect the kerosene soot from the indoor chamber during the exposure period. By weighing the filters before and after sample collection, it was determined that the cells were exposed to kerosene soot concentrations of 0.6, 1.6 and 6.6 mg/m³. Table 4-2 summarizes the length of time the kerosene lamp was ignited until the desired concentrations were reached, as well as the measured CO, NO, and NO_x for each condition. The number size distribution for all three concentrations can be seen in Figure 4-7. Chromatographs of the measured carbonyls for each of the three different exposures are shown in Figure 4-8.

Table 4-2: Exposure conditions from burning a kerosene lamp for soot generation.

	Exposure to 0.6 mg/m ³	Exposure to 1.6 mg/m ³	Exposure to 6.6 mg/m ³
Burn Time (minutes)	2	4	20
CO (ppm)	0.01	0.02	0.06
NO (ppm)	Below Detection Limit	Below Detection Limit	0.08
NO_x (ppm)	Below Detection Limit	Below Detection Limit	0.23
Theoretical Dose (µg/cm²)	0.288 ± 0.07	0.77 ± 0.19	3.17 ± 0.78

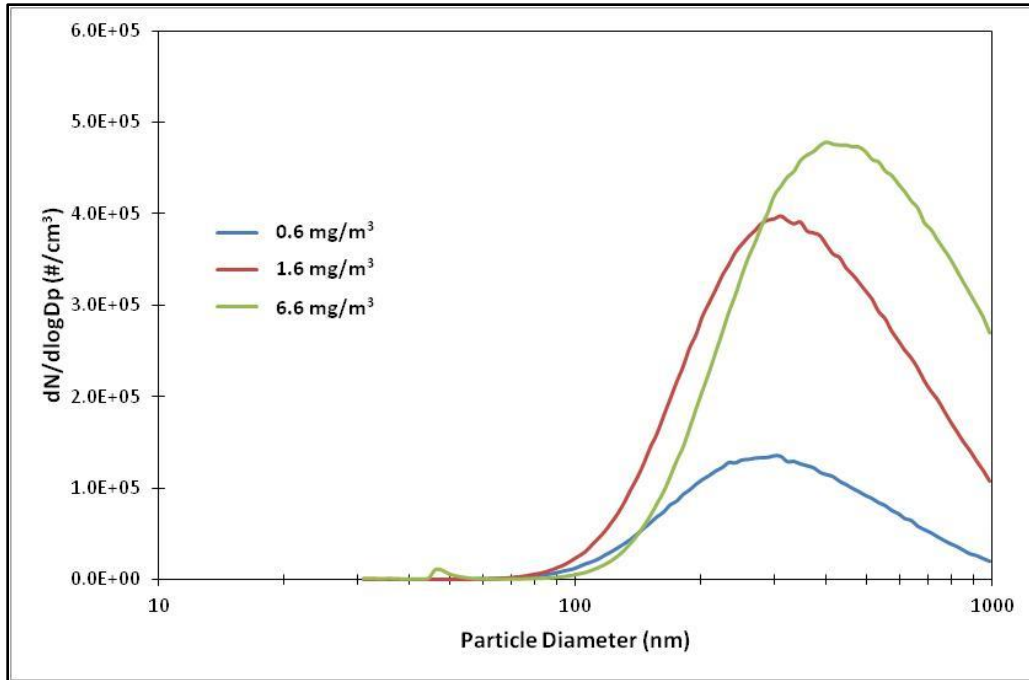


Figure 4-7: Number size distribution of kerosene soot produced from igniting a double-wick kerosene lamp measured with an SMPS for the three concentrations tested.

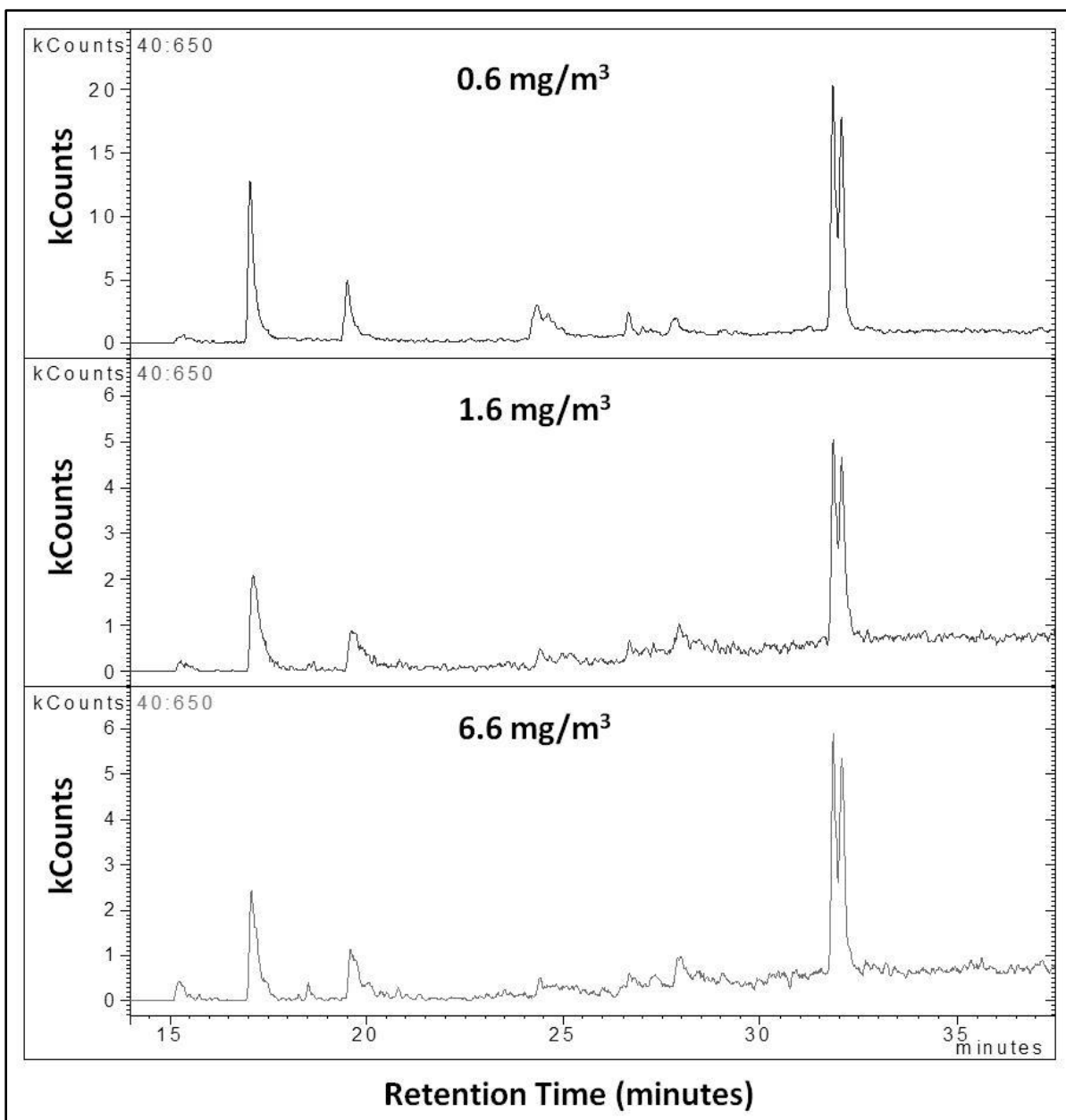


Figure 4-8: GC/MS chromatograph of the measured carbonyls from the kerosene soot sampled from the indoor chamber while cell exposures were being conducted with the Gillings Sampler.

It was expected that the expression levels for all endpoints to increase after exposure to the kerosene soot. This proved true only for IL-8 mRNA levels as a 2-3 fold increase was observed after cells were exposed to kerosene soot (Figure 4-9). The expression levels for IL-6 mRNA and COX-2 mRNA were suppressed in all exposure conditions (Figure 4-9). A possible explanation for the suppression of IL-6 and COX-2 can be attributed to increased

cytotoxicity making the mRNA less stable.^{20, 91} A linear or exponential dose-response relationship was also expected to be observed, however, results showed no differences in the inflammation endpoints analyzed as the dose increased. These data provided insights into a limitation regarding a diminished performance of the particle charging mechanism in the Gillings Sampler.

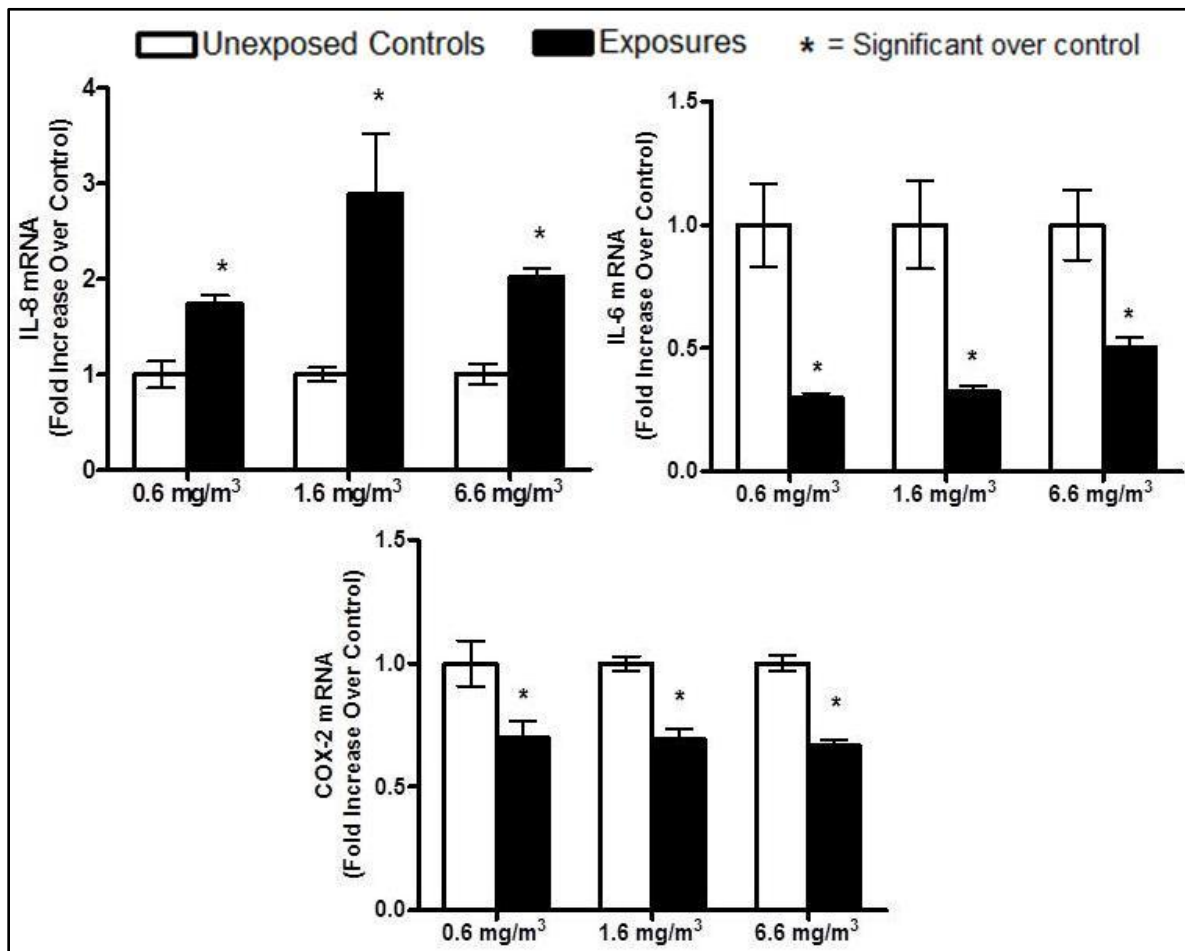


Figure 4-9: Biological analysis of inflammation (IL-6 mRNA, IL-8 mRNA, and COX-2 mRNA) from A549 exposed cell cultures to kerosene soot. Data is presented as fold change over control. The * denotes statistical significance ($p < 0.05$).

Images of unexposed and exposed cells at 9-hours post exposure, before sample collection, were captured with an inverse microscope (Olympus IX71) as was described in

Chapter 3 (Figure 4-10). Changes in cell morphology can be observed after cells have been exposed to the kerosene soot.

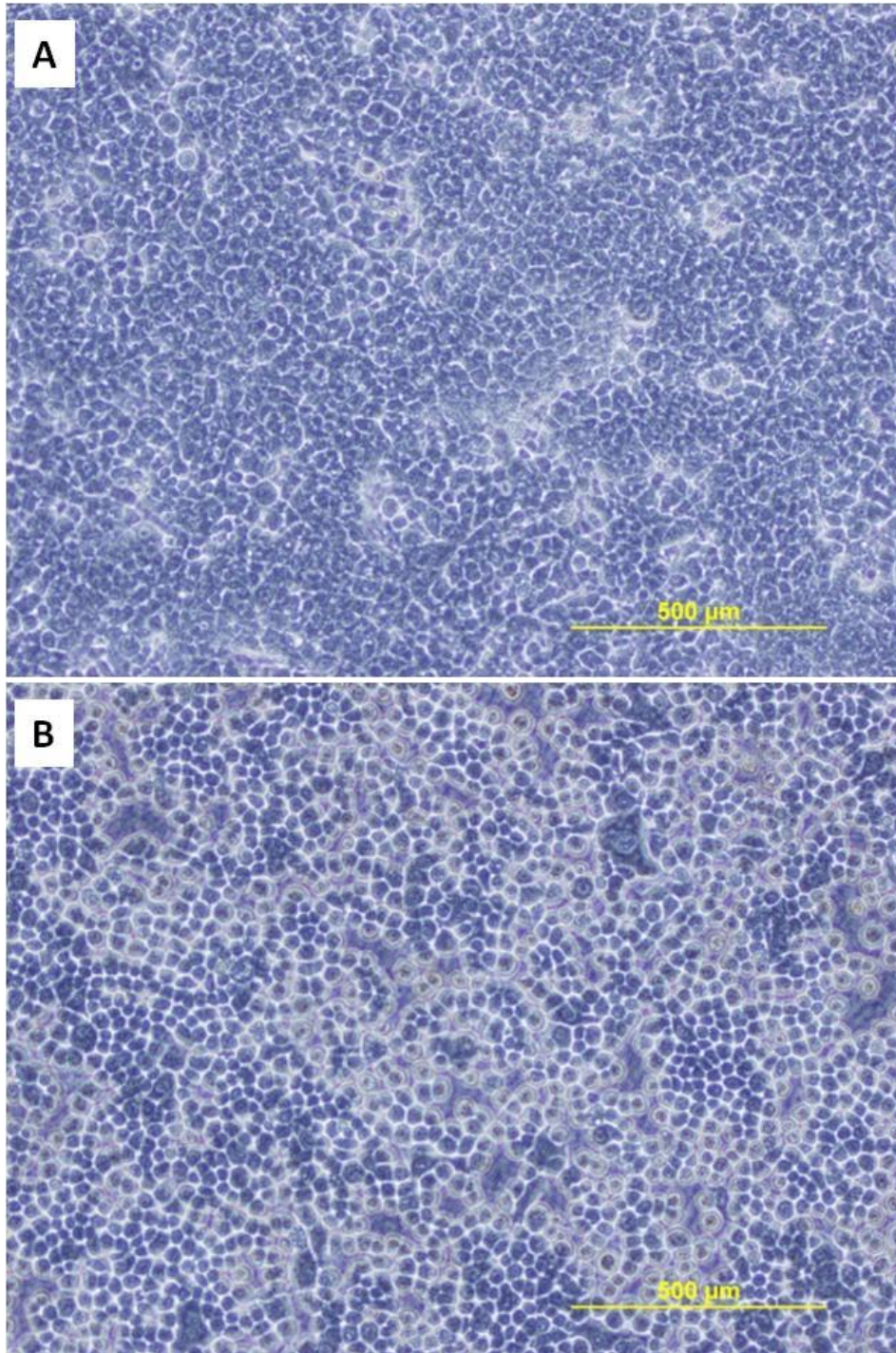


Figure 4-10: Images captured with a 10X objective lens of cells at 9-hours post-exposure for (A) unexposed controls and (B) exposed cells to 0.6 mg/m^3 of kerosene soot. Changes in the cell morphology are observed after cells have been exposed to kerosene soot

For scanning electron microscopy (SEM), unexposed and exposed cell samples were fixed in a buffered primary standard aldehyde fixative (2% glutaraldehyde, 2% paraformaldehyde) at 9-hours post exposure, followed by post-fixation in buffered 1% osmium tetroxide. The samples were rinsed in buffer and dehydrated through a graded series of ethanols (30%, 50%, 75%, 100%, 100%, 100%-10 minutes each). Specimens were subjected to critical point drying in a Bal-Tec CPD030 critical point dryer. The dried samples were mounted on 13 mm aluminum planchets with double-sided carbon adhesive tabs and sputter-coated with gold/palladium in an Anatech Hummer 10.2. Specimens were viewed in a Zeiss Supra 25 FESEM scanning electron microscope at an accelerating voltage of 5 kV and 20 μ m aperture (Carl Zeiss Microscopy, LLC.). SEM analysis was used as an auxiliary tool to observe changes in cell morphology after exposure (Figures 4-11 and 4-12).

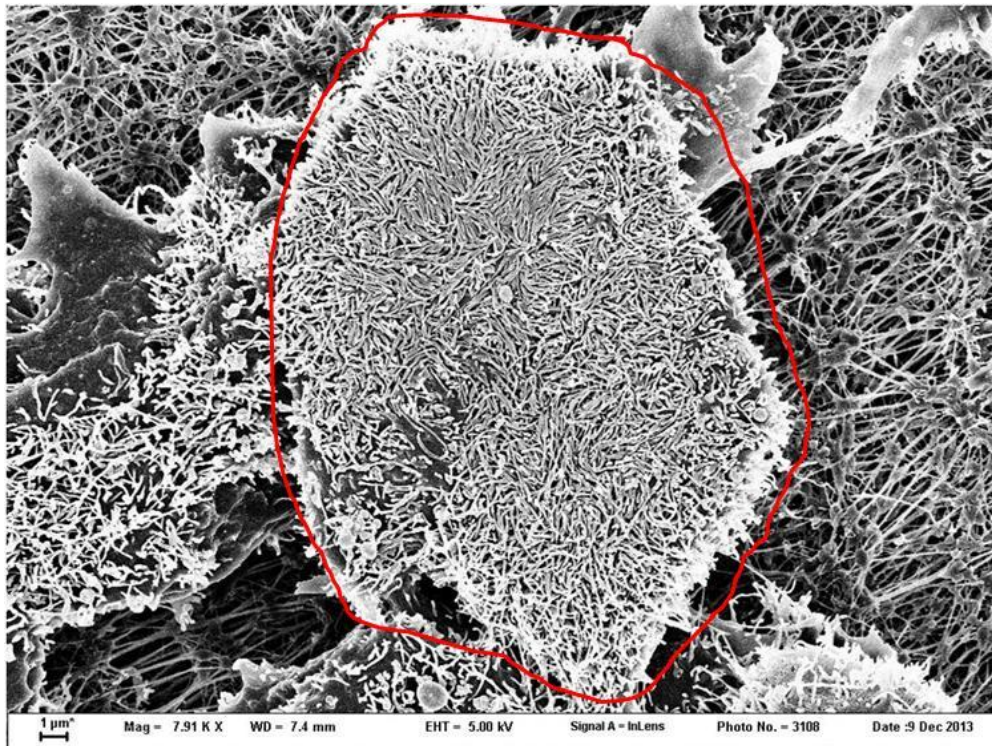


Figure 4-11: Electron micrograph of an unexposed A549 cell, outlined in red, observed under SEM. The "hair-like" membranes seen on the surface of the cell is microvilli, which helps to increase the surface area of the cell and are involved in a variety of functions.

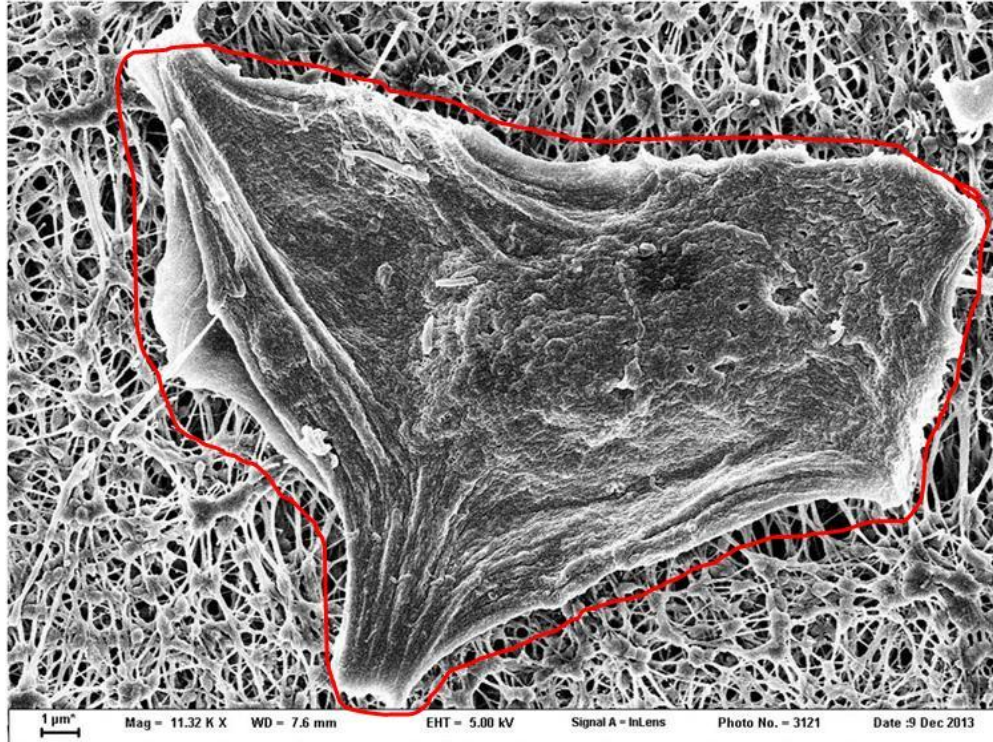


Figure 4-12: Electron micrograph of an exposed A549 cell, outline in red, to kerosene soot observed under SEM. The morphology of the cell has completely changed compared to the unexposed cells.

Electron micrographs of kerosene soot were also captured using TEM grids (Standard Copper with Carbon Film, 400 Mesh, Electron Microscopy Sciences) placed over the deposition plate inside the Gillings Sampler during the kerosene soot exposures. The collected particles were viewed directly on the TEM grid in a Zeiss EM900 TEM at an accelerating voltage of 50 kV (Figure 4-13).

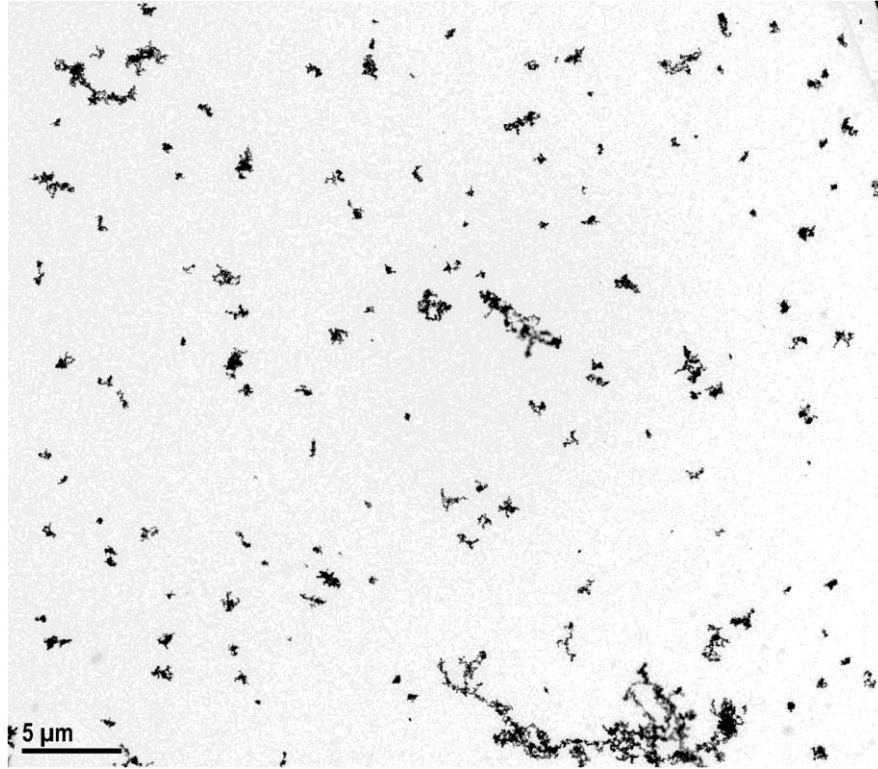


Figure 4-13: TEM micrograph of kerosene soot particles collected on a TEM grid placed on the deposition plate inside the Gillings Sampler during cell exposure.

As described in Chapter 1, a corona wire that is housed in the charging section of the CES is used to produce unipolar ions to electrically charge the sampled particles in the air. The corona current was monitored while the exposures were being conducted, and it was observed that the electrical current applied to the corona wire decreases as particle concentrations increase. The most drastic changes in electrical current occurred at the highest kerosene soot concentration of 6.6 mg/m^3 used. This observation indicated that the corona wire performance is hindered by the higher particle concentrations in the air. As the particles flow over the corona wire housing, they are able to penetrate the slit below the flow path and ultimately deposit on the corona wire surface. Visual inspection of the corona wire after these exposures confirmed that kerosene soot particles had deposited over the corona wire, which lead to a decrease in the corona current, therefore limiting the

production of unipolar ions. Further investigation is needed to determine at what concentrations the performance of the corona wire starts to diminish and if this effect varies depending on the particle type.

Reacting Ozone with Limonene Produced Toxic Levels of Secondary Organic Aerosols

An average SOA concentration of $725 \mu\text{g}/\text{m}^3$, as measured by the SMPS, was produced as a result of reacting 240 ppb of O_3 with 5 mL of limonene. The number size distribution of the SOA produced during each exposure and the chromatographs of the measured carbonyls can be seen in Figures 4-14 and 4-15.

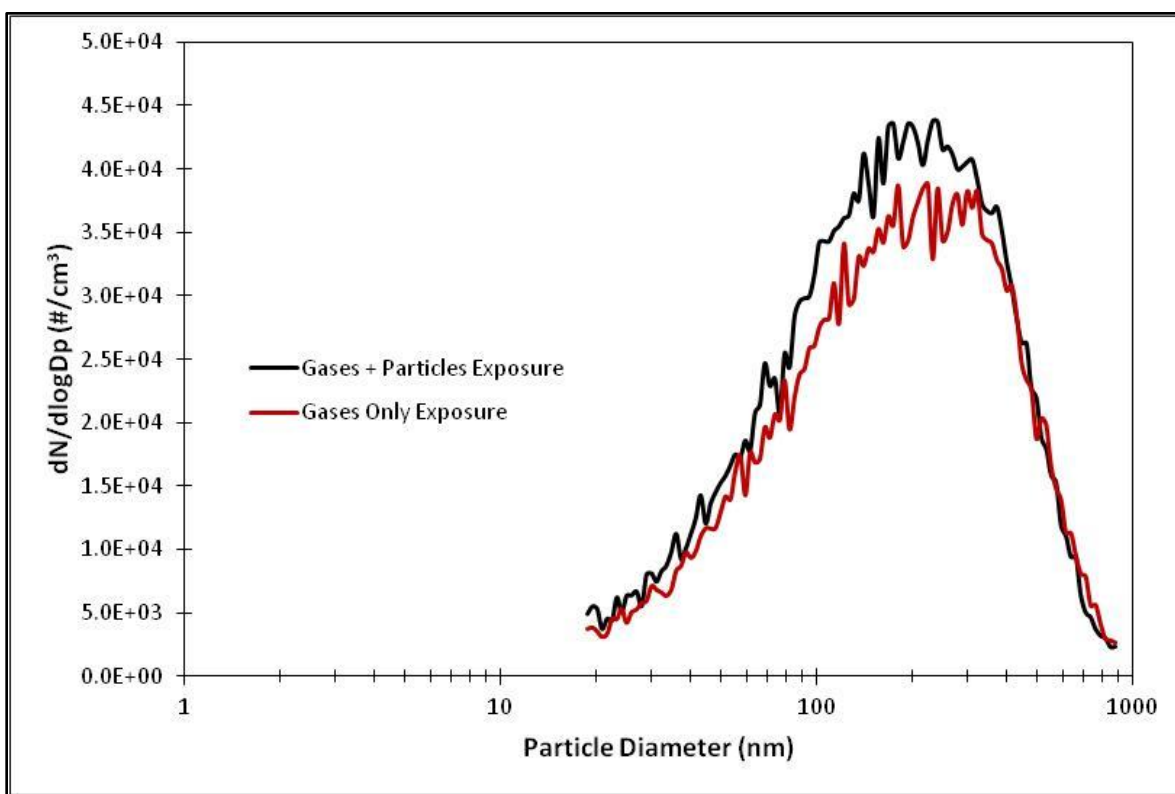


Figure 4-14: Number size distribution of secondary organic aerosols produced from reacting ozone with limonene during the exposures conducted.

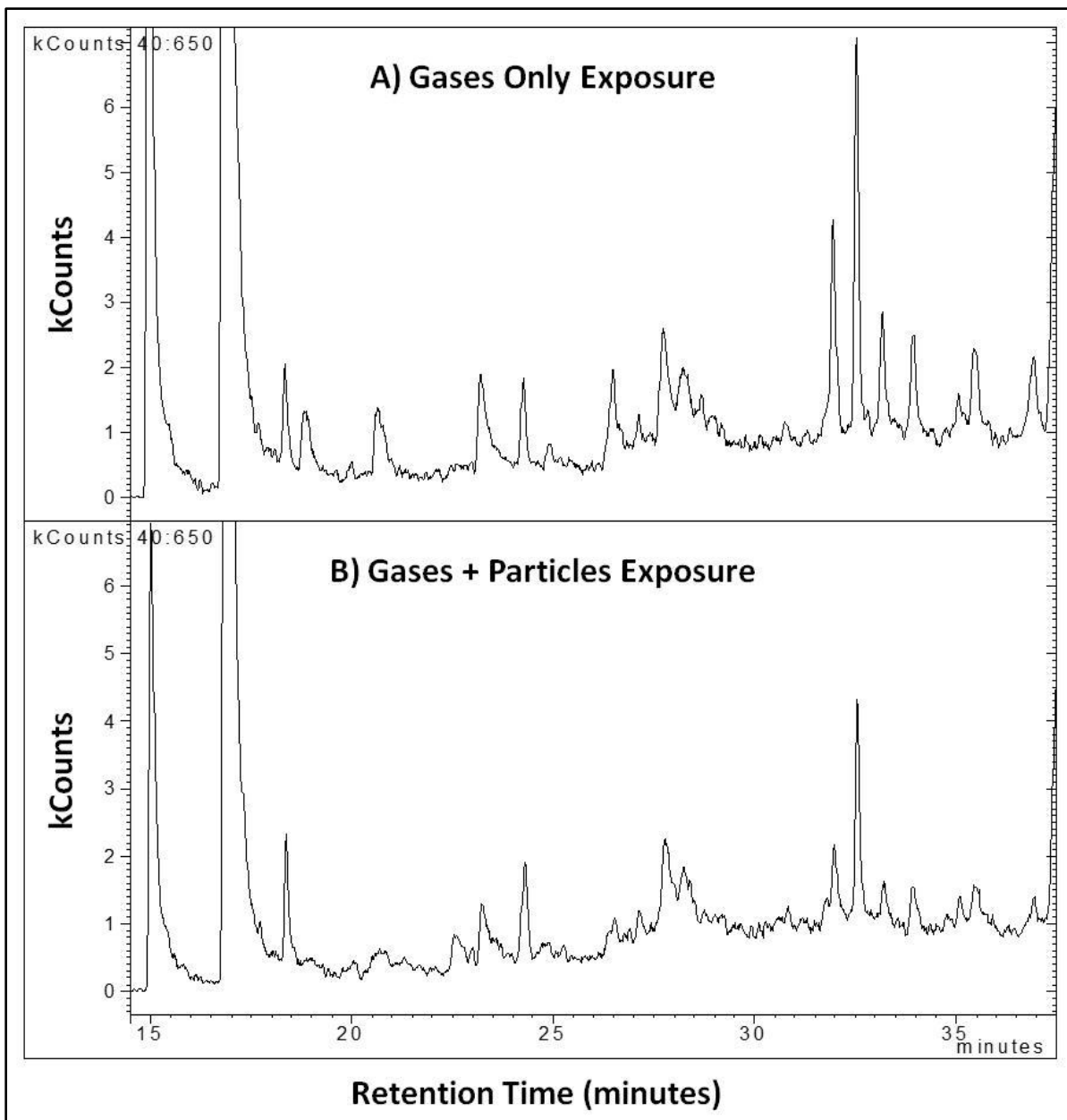


Figure 4-15: GC/MS chromatograph of the measured carbonyls produced from reacting ozone with limonene during the "Gases Only" exposure (top) and "Gases + Particles" exposure (bottom).

A549 cells were first exposed to the test atmosphere by operating the Gillings Sampler without the powering the electric fields to prevent any electrical charging and particle deposition to take place. In doing so, the cells were exposed to the gaseous compounds in the test atmosphere only and therefore any observed toxicity is a result of the gas-particle interaction. Subsequently, a new set of cells were exposed to both the gas- and particle-phase

to observe how the biological response changes when particles are deposited on the cells. In this exposure, an estimated particle dose of $0.35 \pm 0.09 \mu\text{g}/\text{cm}^2$ was delivered to the cells. A large inflammation response with a lower cytotoxicity level was observed when cells were exposed to only the gaseous compounds. Exposing the cells to the whole mixture, by depositing the PM fraction onto the cells, decreased the inflammation response, but the cytotoxicity level increased. These results showed that the gaseous compounds induce high inflammation, while the whole mixture (gases and particles) is more toxic, inducing higher cytotoxicity (Figure 4-16).

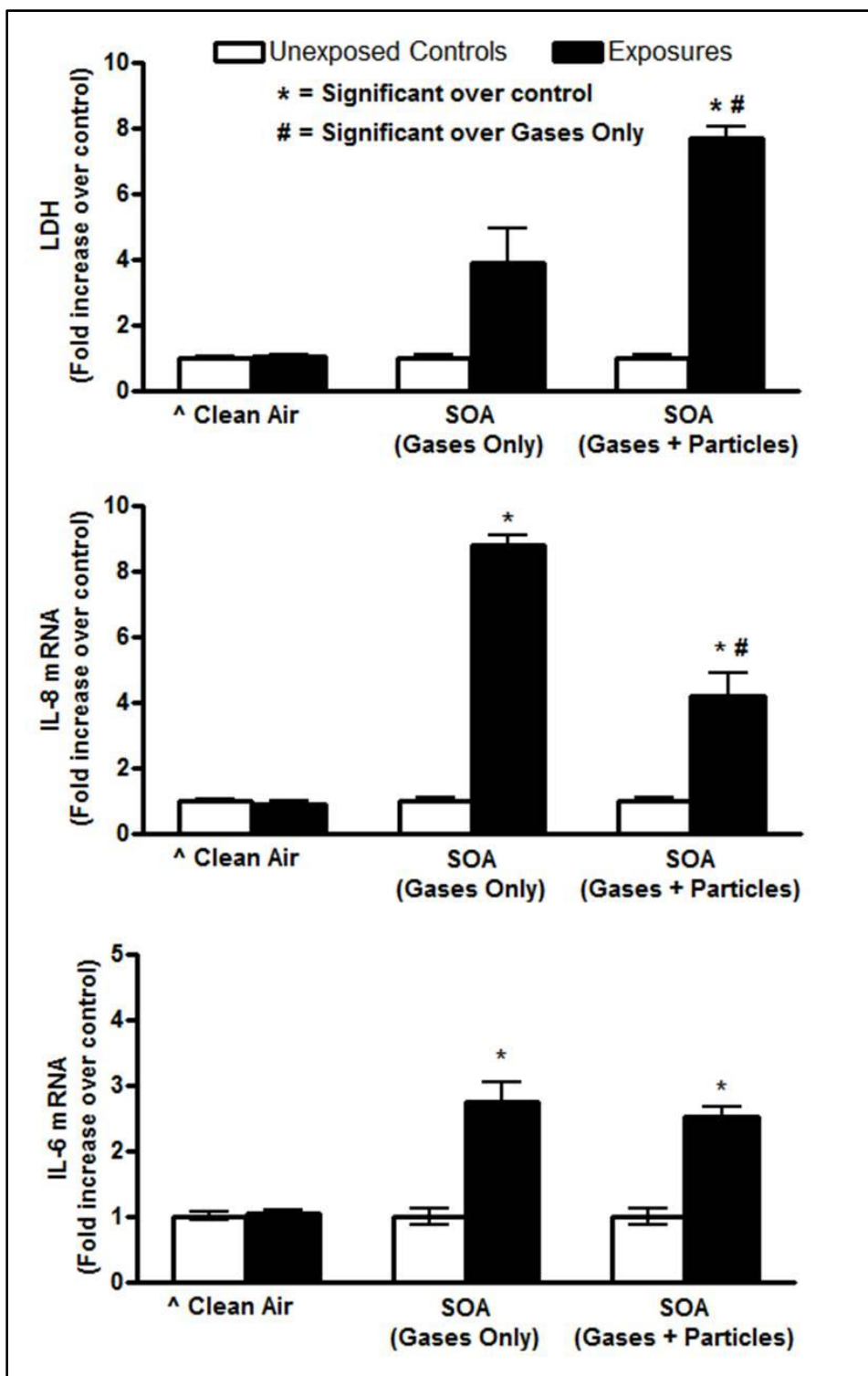


Figure 4-16: Biological analysis of cytotoxicity (LDH) and inflammation (IL-6 mRNA and IL-8 mRNA) from A549 exposed cell cultures to secondary organic aerosols produced from reacting ozone with limonene. The asterisk symbol (*) indicates a statistically significant difference (t-test; $p < 0.05$) over unexposed controls. The pound sign (#) indicates a statistically significant difference (t-test; $p < 0.05$) between the Gases Only exposure and the Gases + Particles exposure. The caret symbol (^) indicates results obtained from the clean air exposures presented in Chapter 2.

Exposing cells to the generated SOA also provided useful insights into the performance of the sampler. I was able to study how biological response changes from exposing cells to the gas-phase components versus the whole pollutant mixture. The results confirmed that the Gillings Sampler can be used to study the toxicity of gas-phase pollutants. This is an important finding because previous studies using the EAVES indicated that the device was a particle-only exposure system in which cells cannot be exposed to gas-phase pollutants.^{19, 20, 48, 49} The enhancements and changes to the design of the Gillings Sampler compared to the EAVES allows the cells to be exposed to the whole mixture and not just the particle-phase compounds. During these exposures, however, the Varian 3400/2000 GC/MS, with both a mass spectrometer (MS) and flame ionization detectors (FID) was not available. Collecting measurements with this GC/MS would have provided more useful data as it could have identified and quantified the species in the air by continuously monitoring gas-phase hydrocarbon compositions of the test atmosphere. This data could have provided better insights into the concentrations the cells were exposed to in the "gases only" exposure. If these concentrations were abnormally high, then it could explain why a toxic effect was observed from the "gases only" compared to previous findings from the EAVES where it was considered a "PM only" exposure system. Another interesting finding showed that measurement of cytokines via ELISA, as measured in Chapter 2, was not possible since the SOA delivered to the cells interferes with the assay (Figure 4-17); similar to the interference observed with the MOA.

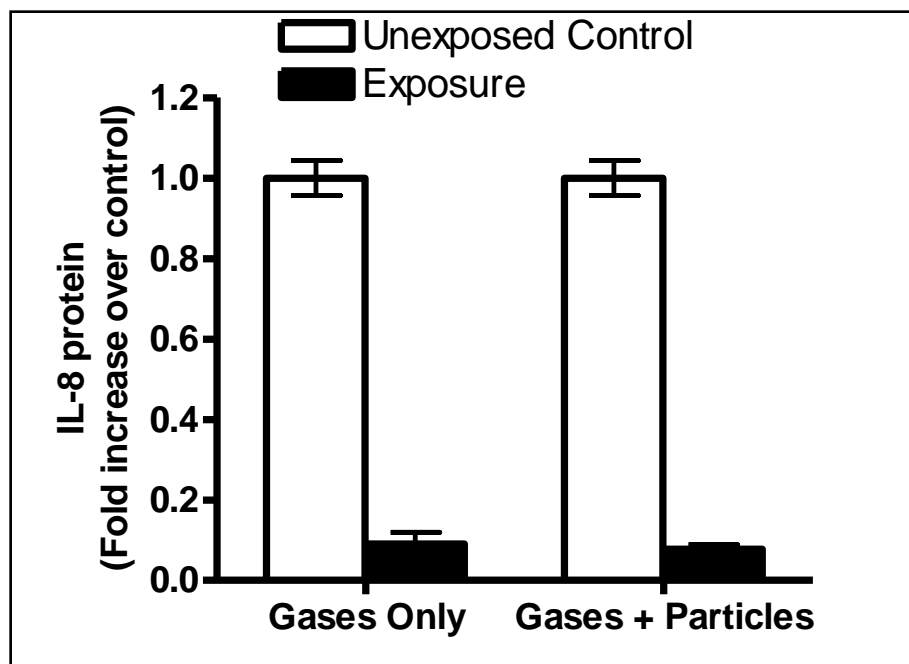


Figure 4-17: IL-8 protein in the supernatant was measured via ELISA in both cell exposures conducted in Chapter 4 to the secondary organic aerosols. Results show that IL-8 protein levels are suppressed after exposure, however these results show interference with the biochemistry of the assay. After conducting qRT-PCR (results shown in Chapter 4), it was observed that IL-8 mRNA levels increased. This indicates that ELISA interference is occurring.

Exposure to ozone alone using the Gillings Sampler does not elicit a biological response

To further investigate the performance of the Gillings Sampler using a gas-phase pollutant, without the presence of PM, two different sets of cells were co-exposed to an average O₃ concentration of 405 ppb from the rooftop chamber using the Gillings Sampler and the GIVES. After biological analysis of the samples was conducted, results from the cells exposed in the Gillings Sampler show that LDH and IL-8 expression levels between unexposed cells and cells exposed to O₃ are not statistically different. When comparing the unexposed cells to cells exposed to O₃ in the GIVES, a 4-5 fold increase of both LDH and IL-8 expression levels are observed (Figure 4-18).

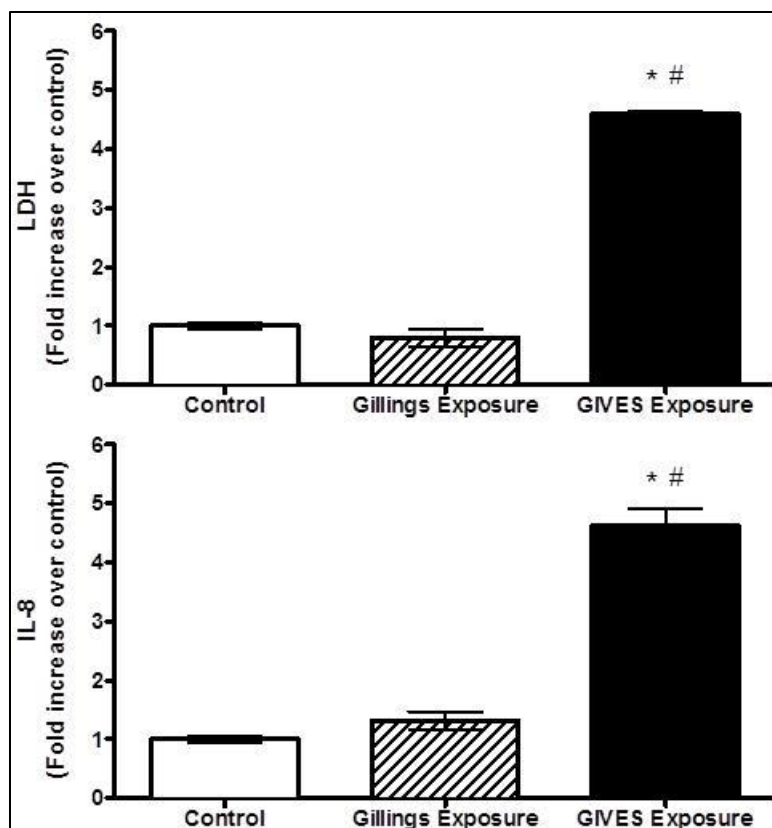


Figure 4-18: Analysis of cytotoxicity (LDH) and inflammation (IL-8 protein) from A549 exposed cell cultures to ozone. The asterisk symbol (*) indicates a statistically significant difference (t-test; $p < 0.05$) over unexposed controls. The pound sign (#) indicates a statistically significant difference (t-test; $p < 0.05$) between the GIVES exposure and the Gillings exposure.

At first glance, these results demonstrate that gas-to-cell interactions that take place during these exposures with high levels of ozone using the Gillings Sampler can have little to no contribution to the overall toxicity observed. These results also seem to agree with previous findings that indicated that the EAVES was a "PM-only" exposure system since the exposed cells only responded to the PM deposits and not the gases.^{19, 20, 48, 49} This lack in sensitivity to 405 ppb of O₃ seems to contradict the results observed after cells were exposed to the gas-phase compounds generated from reacting limonene with ozone, which showed that the Gillings Sampler can induce a biological response from A549 cells after exposure to gaseous pollutants. After further investigation, it was determined that the humidification

system can be a contributing factor to producing false negative results. Additional testing was conducted with O₃ and the humidification system. Results from this test showed that the humidification system is responsible for reducing the O₃ in the air stream as it flows through the system (Figure 4-19). With the current data available, the reason for this observed reduction of O₃ cannot be determined. A possible explanation could be that O₃ loss is a result of water penetrating the humidification system sample line and coating the inside surfaces where the air is sampled through. As a result, it is difficult to speculate what was the true O₃ concentration that the cells were exposed to in the Gillings Sampler since O₃ measurements at the outlet of the sampler were not taken at the time of exposure. Further testing is needed with other pollutants to observe the extent to which the humidification system can alter other air pollutant mixtures.

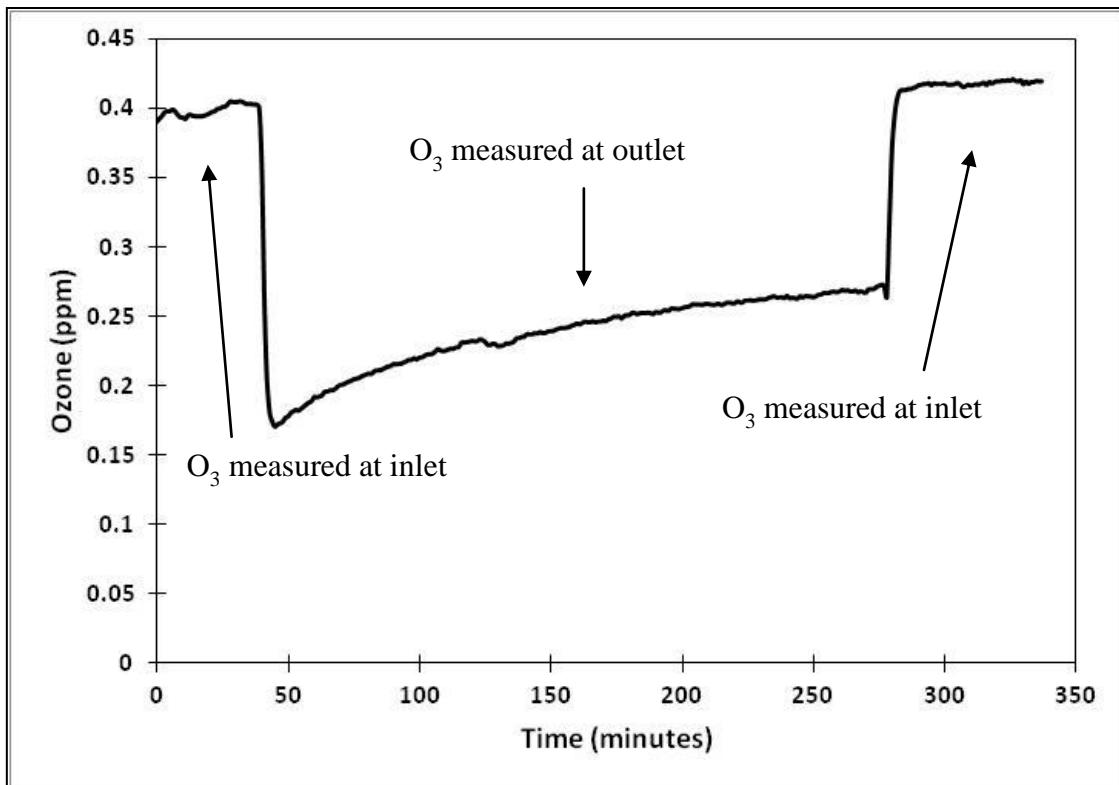


Figure 4-19: Ozone measurements at inlet and outlet of Heated Humidification System. Measurements indicated that ozone concentrations diminish as it flows through the system due to the humid environment present inside.

After observing these results, it is evident that the comparison of the O₃ exposure using the Gillings Sampler and the GIVES is inadequate. While the intent was to co-expose cells using two different exposure systems, each set of cells experienced different exposure conditions. The cells in the GIVES were exposed for 4 hours to an average O₃ concentration of 405 ppb. The GIVES remained inside a tissue culture incubator maintained at 37°C and no humidification system was used. The cells in the Gillings Sampler were exposed to a lower O₃ concentration since the O₃ was sampled through the humidification system at the inlet of the sampler. A more accurate co-exposure should be conducted in the future. To do so, the O₃ concentration should be measured at the outlet of the humidification system to determine the actual O₃ concentration entering the Cell Exposure System (CES). The co-exposed cells in the GIVES should then be exposed to the similar O₃ concentration that was measured entering the CES.

Conclusion

A condensed testing program was used to evaluate the performance of the Gillings Sampler under various testing conditions using various test atmospheres as the pollutant source. The goal of these cell exposures was to evaluate the performance of the Gillings Sampler and observe any potential limitations that have been overlooked or were not anticipated. The test atmospheres used in this study were generated in the laboratory using either smog chambers or bench top reactors. Exposures to these test atmospheres provided useful insights into potential limitations of the sampler that need to be addressed in the future. This study highlighted the advantages and limitations of the Gillings Sampler. In all exposures conducted, the heating and humidification of the Gillings Sampler was successful in maintaining the target RH between 70-80% at all times and its internal temperature at

37°C. Limitations to the type and concentrations of the pollutants were also observed. While more extensive testing is needed to better evaluate the performance of the sampler, sufficient information has been obtained to provide an initial assessment of the sampler. I have shown that the Gillings Sampler is a suitable research tool in future aerosol exposure studies. Careful planning and considerations, however, need to be taken prior to conducting any research studies. If the limitations of the sampler are understood and one can work within the means of the sampler, then the Gillings Sampler can serve as a valuable research tool.

CHAPTER 5: OVERALL CONCLUSIONS, LIMITATIONS, AND FUTURE WORK

Summary of Research Objective

The Gillings Sampler is a second-generation aerosol sampler that uses electrostatics as its principle of operation to expose lung cells to air pollutants at an air-liquid interface. Our research group had previously developed an *in vitro* system named the EAVES by retrofitting a 1967 electrostatic aerosol sampler and housing it inside an incubator at 37°C. The EAVES showed a higher sensitivity compared to the conventional resuspension method of exposing cells under submerged conditions.²⁰ These results propelled us to continue using ALI exposure systems for studying the toxicity of air pollutants. In an effort to enhance the performance and capabilities of the EAVES, it was determined that a new system needed to be developed without the need to retrofit existing instrumentation. In doing so, the Gillings Sampler was designed for ease of manufacturing so that, if desired, mass production could be more feasible.

The Gillings Sampler maintains the features and principle of operation of the EAVES, while new additions to the system serve to enhance its capabilities. A list of design goals was established prior to the design and development phase of the *in vitro* system to have a clear understanding of the final production goal. The objectives for the design and operation of the Gillings Sampler were as follows: 1) use ESP to deposit particles over cells at ALI, 2) use commercially available components for ease of manufacturing and assembly, 3) incorporate a humidification and heating system to remove the need for an incubator, 4) provide the

flexibility to co-expose up to 9 tissue inserts without needing to modify their heights, 5) deposit particles over the entire tissue insert cell growth area, 6) deposit particles across all tissue inserts with minimal variation from insert to insert, 7) do not induce toxicity to the cells from the use of the *in vitro* system, and 8) allow an exposure time of up to 4 hours. This list of design goals is what our research group believed were essential components and characteristics of an ideal *in vitro* system. A series of experiments were conducted to evaluate the performance of the *in vitro* sampler under various environmental conditions in order to determine the limitations of the Gillings Sampler.

Summary of Findings

Chapter 2: The Gillings Sampler - Design and Testing of a Portable In Vitro Aerosol Exposure System

In developing and testing of the Gillings Sampler, I was successful in accomplishing the established goals, as described in Chapter 2. The first 4 objectives focused on the design and manufacturing of the *in vitro* sampler. The use of commercially available components, such as power supplies, heaters, and controllers allowed the Gillings Sampler to be fully capable of maintaining desired air flow humidity and temperature at 37°C. Incorporating the temperature and humidity regulation system increases the potential usage of the Gillings Sampler in a wide range of environmental settings and allows it to be more portable. The interchangeable deposition plates used in the Gillings Sampler were specifically designed for this system to allow co-exposure of multiple commercially available tissue inserts. These interchangeable deposition plates allow researchers the flexibility to conduct time-series studies, co-expose multiple cell types, or simply increase their statistical power with a higher number of samples using the 30 mm Millicell-CM membranes.

The last 4 objectives focused on the operation of Gillings Sampler. To ensure that particle deposition was not localized, infrared PSL (IR-PSL) spheres were deposited on the Millicell-CM membranes and observed with an infrared imaging system. The infrared imaging system showed that IR-PSL spheres were adequately deposited across the entire membrane area. Further testing using fluorescent PSL (YG-PSL) spheres explored the variation in particle deposition from insert to insert and indicated that there exists some variation in mass deposition from insert to insert. Further cell exposure testing (Chapters 3 and 4) showed that there were also some variations when analyzing biological responses. Some variation is expected within replicates, however, when conducting any type of cell exposure. Cell viability testing was conducted and consisted of testing individual components of the Gillings Sampler to demonstrate that the instrument itself did not induce toxicity based on three biological endpoints – cytotoxicity (LDH) and inflammation (IL-6 and IL-8). These tests also served to demonstrate that both operating the Gillings Sampler and conducting exposures for up to 4 hours were possible.

Chapter 3: A Positive Aerosol Control Method for Quality Assurance Testing of In Vitro Exposure Systems

Before attempting to expose cells to a toxic aerosol using the Gillings Sampler, a literature search showed that there is no standardized testing method and aerosol source to determine the efficacy of exposing cells using ALI exposure systems. For this reason, we wanted to develop a positive particle control testing method that can be used to quantify the efficacy of our sampler and facilitate the comparison of the various exposure systems in the future if this method is accepted and widely used by other researchers. The cell type, the aerosol source, and the dose delivered to the cells were three variables that needed to be fixed to develop a consistent and reliable method. The cell type chosen for this method was the

A549 cell line. To have full control of the aerosol, we generated our own aerosol source. To do so, we first established the following criteria: the aerosol should be (a) easy to generate, (b) reproducible in particle size, composition, and concentration (c) maintain a constant concentration during the exposure time, and (d) toxic to cells.

Using the established criteria, I generated a toxic aerosol that elicits an acute biological effect from the cells upon exposure. Mineral oil was nebulized with a Collison nebulizer to generate a mineral oil aerosol (MOA). This non-toxic aerosol became toxic by injecting 25 μL of TOLALD, a toxic VOC, directly into 100 mL of mineral oil before nebulizing. By injecting the toxic VOC directly, I was able to control the toxicity of the aerosol. Three different sets of A549 cells were then exposed to the toxic MOA to demonstrate reproducibility of the method and the biological response. The results showed that exposing cells to MOA with the addition of TOLALD elicits a reproducible biological effect. This simple method contains only one toxic component that is responsible for inducing the observed response, which makes it an easy and reliable system that can aid in the standardization of testing ALI exposure systems. By conducting this reproducible positive aerosol control test on a regular basis, this method can also serve as a quality assurance test to ensure that an exposure system is operating at optimal conditions. This new method has the potential to use alternative toxic components, as demonstrated in Figure 3-8. Individual or multiple compounds can be injected manually into the mineral oil to generate simple or complex mixtures and study their toxicity.

Chapter 4: Performance Testing of the Gillings Sampler under Various Test Atmospheres

In an effort to observe the performance and any potential operational limitations of the Gillings Sampler, a series of cell exposures were conducted under various experimental

conditions that mimic potential real test environments. A condensed testing program that spans several areas of interest in the field of inhalation toxicology was conducted. In this condensed testing program, cells were first exposed to a photochemically-aged DE in the presence of a Synthetic Urban Mixture to represent the pollutants found in the ambient environment. Cells were then exposed to kerosene soot produced from the burning of a double-wick Aladdin® kerosene lamp, which aimed to represent the combustion emissions found in indoor environments as a result of combustion sources – such as cookstoves and liquid-fuel lanterns. Cells were also exposed to SOA produced from reacting an average of 240ppb of O₃ with 5 mL of limonene. This experimental condition represented particulate matter composed of compounds formed from the atmospheric transformation of organic species. Finally, cells were exposed to 400 ppb of O₃ to observe the effects that gaseous pollutants can induce without the presence of PM.

For the photochemically-aged diesel exhaust exposures, a human cell line (A549), human primary cells (EpiAirway) and mouse primary cells (C57BL/6J and BALB/cJ) were exposed simultaneously in the Gillings Sampler, which demonstrated that this exposure system can be used with multiple cell types. The type and magnitude of responses induced by air pollution mixtures may, however, be cell type dependent. Therefore, it is critical to both understand the limitations of each *in vitro* model and identify appropriate endpoints for each cell type. The biological results obtained from the A549 cells were comparable to those observed when A549 cells were previously exposed to photochemically-aged diesel exhaust using the EAVES,¹⁹ which demonstrates that the Gillings Sampler is operating as expected with a complex pollutant mixture.

Exposures to kerosene soot focused on exposing A549 cells only to particle concentrations ranging from 0.6 to 6.6 mg/m³. High particle concentrations were of interest since cooking or burning a lantern indoors can produce similar concentrations. Cells exposed to 0.6 mg/m³ elicited a biological response. At higher concentrations, I expected to see a significantly different biological response, however no differences were observed at the 1.6 and 6.6 mg/m³ concentrations. This observation, while puzzling at first, indicated that there exists an operational constraint in regards to the upper limit of particles concentrations being sampled. At high particle concentrations, the particles begin to interfere with the corona wire in the charging section of the sampler, coating its surfaces and diminishing its ability to generate the unipolar ions needed to electrically charge the particles in the flow path.

Testing of the Gillings Sampler with SOA concentrations of 725 µg/m³ consisted of exposures to A549 cells only. In this application, the cells were exposed to the gaseous compounds only. Subsequently, a new set of cells were exposed to both the gas- and particle-phase to observe how the biological response changes when particles are deposited on the cells. A large inflammation response with a lower cytotoxicity level was observed when cells were exposed to only the gaseous compounds. Exposing the cells to the whole mixture, by depositing the PM fraction onto the cells, decreased the inflammation response, but the cytotoxicity level increased. These results showed that the gaseous compounds induce high inflammation, while the whole mixture (gases and particles) is more toxic, inducing higher cytotoxicity. The 9-hour post-exposure incubation period allows the cells to produce and release the inflammatory markers of toxicity. If early cell death occurs then the cells do not have enough time to produce and release these markers and therefore higher cytotoxicity (LDH) levels will be observed.

To observe how A549 cells respond to a gaseous pollutant without the presence of PM, cells were co-exposed to 400 ppb of O₃ using the Gillings Sampler and the GIVES. Since the GIVES has been used solely as a gas exposure chamber, it was used as a bench mark to determine how the Gillings Sampler compares. Results indicated that exposing the cells to 400 ppb of O₃ using the Gillings Sampler induced no changes in inflammation and cytotoxicity. The results with the GIVES showed a 4-5 fold increase in both inflammation and cytotoxicity. At first glance, it seems the ozone concentration tested here is minimal for the Gillings Sampler and therefore no biological effects were induced. After further investigation, it was determined that the humidification system is responsible for reacting away O₃ from the air stream. As the air stream exits the humidification system, it enters the Cell Exposure System (CES) and at this point the O₃ in the air is diminished significantly. While this humidification system was designed to represent the natural humidification and heating of inhaled air that occurs in human airways, this critical component can alter and react with water soluble pollutants.

Limitations

All cell exposure testing described in Chapters 2 and 3 were conducted using the A549 cell line under controlled conditions using clean air or a one-component toxic aerosol. The Gillings Sampler seemed to be operating exactly as it was designed and as expected. It is understood, however, that these controlled tests are only the beginning of an extensive testing program that new technology, such as the Gillings Sampler, should undergo before it can be considered a research tool that can be used by researchers studying a wide range of airborne pollutants. Due to the limitation of resources and time frame, a condensed testing program that spans several areas of interest in the field of inhalation toxicology was conducted and

described in Chapter 4. The Gillings Sampler was evaluated under various realistic conditions in order to identify any potential problems that otherwise could have not been predicted or detected. Over the course of these tests, several limitations of the Gillings Sampler were identified and will be discussed in greater detail below. I will also address the limitation of resources that prevented further testing to overcome or further explore the sampler's limitations, as well as other cell exposure conditions that could have provided more insights.

Gillings Sampler Limitation 1: Screen Diffusers

As the air enters the CES, two perforated screens are installed to uniformly disperse the air into the charging region (see Figure 1, Chapter 2). The deposition testing conducted with the YG-PSL spheres showed variability in deposition from well-to-well. While some variability was expected, it appears that the screen diffusers are not dispersing the flow uniformly across the entire volume. This was evident when more YG-PSL deposition tests were conducted to observe how the deposition pattern is affected as the pulse-precipitation cycle timing is adjusted. As a reminder, one deposition cycle in this 2-part, pulsed-precipitation pattern consists of having the electric field turned off to allow the precipitation region to be filled with particles, followed by turning on the electric field to force down the particles onto the collection area. In all experiments described in this dissertation, the deposition cycle consisted of having the electric field turned off for 4 seconds followed by 1.5 seconds with the electric field turned on. Based on the volume inside the CES and the 2.2 L/min flow rate used, it was calculated that 4 seconds of having the electric field off was sufficient to entirely "fill up" the volume over the cells. If the time that the electric field is turned off is adjusted, then decreasing this time should prevent

deposition from taking place over the entire deposition area (with no deposition downstream of the deposition plate). When the timing was adjusted, however, the observed deposition pattern did not reflect what was expected (Figure 5-1). Visually, the observed deposition looks similar in all conditions. The deposition efficiencies were calculated as the pulse-precipitation cycles were adjusted (Figure 5-2), though, it was evident that the deposition efficiencies decreased as a result of reducing the time allowed for the sampled air to "fill up" the volume over the cells. While this limitation did not affect any of the tests presented in this dissertation since the same pulse-precipitation cycle was used at all time (electric field off for 4 seconds and on for 1.5 seconds), it is still a concern that should be addressed in the future. A simple solution is to replace the current screens with finer mesh screens and test to see if they disperse the flow better. An alternative is to completely change the inlet head design to allow for better uniform dispersion.

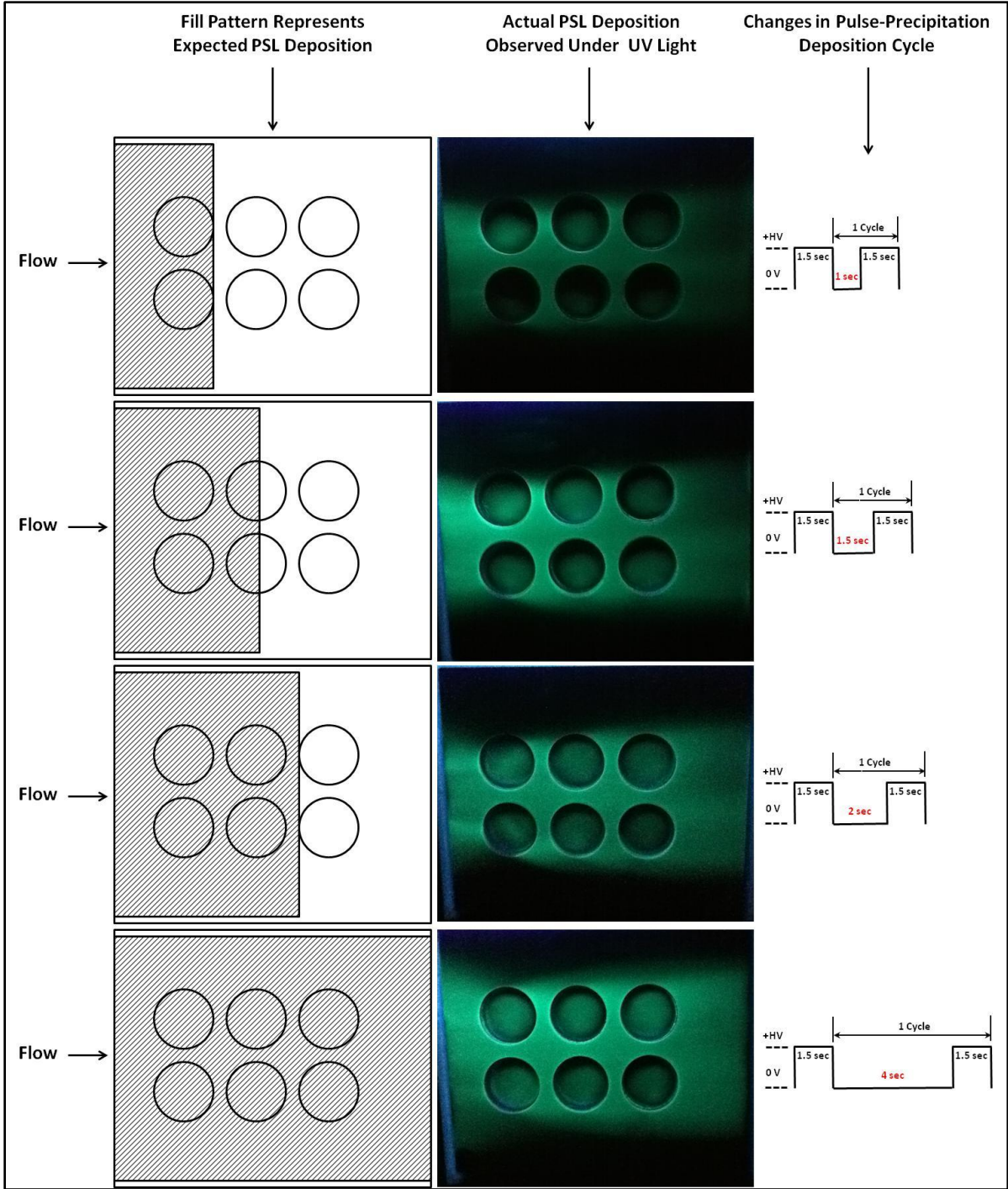


Figure 5-1: Observed YG-PSL deposition versus the expected deposition pattern as the deposition cycle time change.

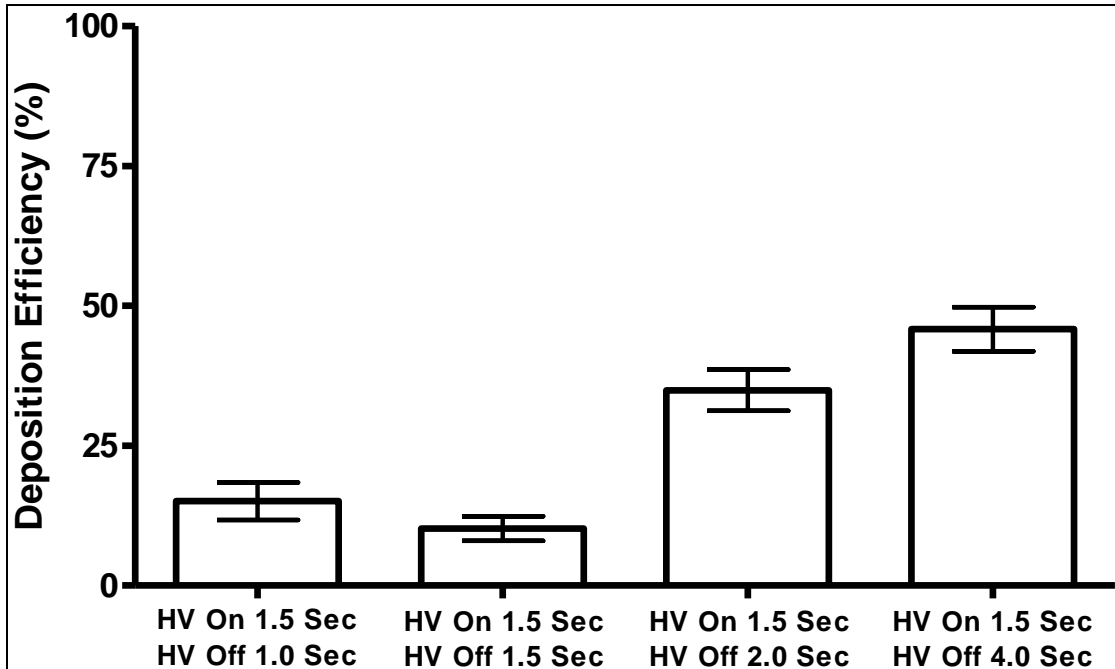


Figure 5-2: Calculated deposition efficiencies using the 6-well deposition plate as the pulse-precipitation cycle times are adjusted. HV = High Voltage in the Cell Exposure System

Gillings Sampler Limitation 2: Deposition Plate

The largest obstacle encountered was designing an appropriate deposition plate. Several designs consisting of various materials were manufactured and tested, however the deposition efficiencies were very low (< 2%). All of these designs were initially intended to be used with 12 mm Snapwell membranes. Due to the complexity and ineffectiveness of these designs, I decided to move away from using the Snapwell membranes. For this reason, the deposition plate was specifically designed to be used with the 30 mm Millicell-CM membranes only. The drawback to this design is that only the large 30 mm membranes can be used and they require about 4 times more cell tissue than the more conventional 12 mm membranes. Also, the current material used to manufacture the final deposition plate is not translucent, therefore cells cannot be observed under a microscope while housed in the deposition plate. All commercially available tissue culture plates are made out of polystyrene and this could be a material that can be tested in future plate designs. Ideally, several

deposition plate designs could have been developed to accommodate for every type of commercially available cell culture membranes (e.g. Transwells, Snapwells, and Millicells). This could be a challenging task since the geometry and dimensions of the various commercially available membranes vary greatly. Several design variations of the deposition plate and how the electric field is generated inside the CES should be explored.

Gillings Sampler Limitation 3: Corona Wire

The charging section of the CES contains a corona wire that produces unipolar ions which are used to electrically charge the incoming particles in the sampled flow. During the kerosene exposures (described in Chapter 4) it was observed that the corona wire performance was hindered by the particle concentration in the air. High particle concentrations in the air can lead to a diminished performance since particles can penetrate the slit below the flow path where the corona wire is housed. These particles can then overload the wire, coating its surface, and limiting the production of ions to electrically charge the particles in the air stream. Low charging of the particles can then lead to lower particle deposition onto the cells. This limitation suggests that the sampler must be used with caution under high particle concentrations. If high concentrations are to be sampled, the air might need to be diluted to prevent the corona wire from malfunctioning. More testing is needed to determine the upper limit of the particle concentrations that can be sampled without any corona wire problems. If needed, the corona wire can also be replaced. Careful consideration and preliminary testing might be needed in the event of using the sampler in conditions where high particle concentrations are common, such as occupational settings. Another alternative to overcome this limitation is to modify the

existing corona wire housing by slightly pressurizing the cavity to prevent any particles from entering the cavity through the slit. This option would require more testing to determine if it is a viable solution.

Gillings Sampler Limitation 4: Heated Humidification System (HHS)

The Heated Humidification System (HHS) was used in all of the cell exposure tests described in this dissertation. The removable humidification system moistens and pre-heats the incoming airflow before it reaches the cells. This system is meant to not only maintain cell viability, but also to represent the pre-heating and humidification of inhaled air that occurs in the human airways. Due to the principle of operation, however, this system should be used with caution as it is believed water accumulates on the inside surfaces causing the sampled pollutants to be titrated. This "limitation" was not anticipated when the system was designed and it became evident when cells were exposed to O₃ in the Gillings Sampler (Chapter 4). When further O₃ measurements were taken upstream and downstream of the HHS, it was clear that O₃ is titrated inside the HHS. To prevent this issue from occurring in the future, a new design for the HHS that does not alter the chemical composition of the sampled air would be needed. While to some researchers, such as atmospheric chemists, would agree that the current humidification system is a "limitation" since it can potentially change the chemical composition and concentrations, others, such as toxicologists, might consider this humidification system a positive feature as the water on the surfaces can resemble the effect of the surfactant in the human airways.

Resource Limitation 1: Design Modifications

As described above, several limitations to the Gillings Sampler were identified. Manufacturing and testing of new designs for the deposition plates, screen diffusers, and the

humidification system are needed, however, manufacturing costs and time prevented me from doing so. As stated above, several deposition plate designs (about 8 different designs) were developed and tested over the course of a year. The Cell Exposure System also required a completely new design than what was initially manufactured. All these modifications were not initially expected and consumed a significant amount of time and budget. Regardless of the limitations encountered, the current design still allowed us to obtain important information on the performance of the Gillings Sampler. While it is not a *perfect* instrument, it is still a valuable research tool that can be optimized in the future.

Resource Limitation 2: In Vitro Models and Biological Analysis

Ideally, each exposure could have benefited from conducting time-course and dose-response studies with multiple endpoints and various cell types. A549 cells were used in all exposures due to their reproducibility, easiness to culture on the Millicell-CM membranes, and short doubling time (22 hours), and their robust biological signal in response to pollutant exposures. While human (EpiAirway) and mouse (C57BL/6J and BALB/cJ) primary cells were tested with the diesel exhaust exposures, the use of these cells for all other exposures was logistically not possible. The EpiAirway cells are commercially available, however it takes 4-5 weeks to receive an order. In addition, other preliminary exposures in our research group conducted using these cells showed that EpiAirway cells did not provide robust biological signals. While the mouse primary cells provided significant biological signals after exposure, their use with more experiments was also logistically difficult. From the time the mice are purchased until the cells are isolated and allowed to fully differentiate, an 8-10 week time span is required. For these reasons, the A549 cells were selected as an adequate cell type to use for the purpose of testing the Gillings Sampler. While another cell line, such

as the BEAS-2B, could have been used, limiting my tests to only A549 cells prevented further variability in the results obtained.

Resource Limitation 3: Instrument and Equipment Availability

During the time the exposures described in Chapter 4 were conducted, the Varian 3400/2000 GC/MS, with both a mass spectrometer (MS) and flame ionization detectors (FID) was not available. The use of this GC/MS would have been ideal since it could have identified and quantified the species in the air by continuously monitoring gas- phase hydrocarbon compositions of the exposure atmospheres. Regardless, not having this data does not take away from the work presented here. The purpose of the tests presented here was to determine if the Gillings Sampler can be used as a screening tool to determine if the test atmosphere elicits a biological response from the cells. These tests did not aim to identify which compound(s) in the air were responsible for inducing the observed toxicity.

While gathering and reviewing all data from the exposures conducted, I realized that more cell exposures could have been conducted to address more concerns and have a more complete testing program. Looking back at Chapter 3, an exposure to the MOA containing TOLALD without depositing the aerosol onto the cells is needed to determine if the TOLALD is off-gassing and eliciting any biological effects. In Chapter 4, a chamber sham exposure (background chamber air) with the indoor chamber should have been conducted to show if the background chamber air contributed to the biological response observed. Also, exposures to the gaseous components of the kerosene soot should have been conducted to observe if these gases contribute to the overall toxicity observed. Due to complications with the Gillings Sampler (contamination of the HHS and electrical malfunctions requiring reconstruction of the HHS), these exposures were not conducted. It is important to note that

the absence of these exposures does not take away from the work presented here. Each experiment conducted has provided useful insights that have helped me assess the performance of the sampler and I don't foresee changes to my conclusions and observations if I was to be able to conduct these missing exposures.

Future Work

While there are some operational limitations with the current version of the Gillings Sampler, further testing can be conducted to provide more insight on how well the sampler works under other various conditions. Further deposition testing of monodispersed YG-PSL spheres and IR-PSL spheres ranging in various sizes from the lower nanometer scale (i.e. 20nm) to micron sized spheres (i.e. 5 μ m) should be conducted. With testing of the various sized PSL spheres, various operational parameters of the Gillings Sampler can be adjusted to observe the effect on deposition efficiencies. The operational parameters that can be adjusted are the electrical current on the corona wire, the frequency and magnitude of oscillating high voltage applied to the charger plate, and the magnitude of the electric field in the precipitation region. An example chart of the extensive particle deposition testing that can be conducted is shown in Figure 5-3.

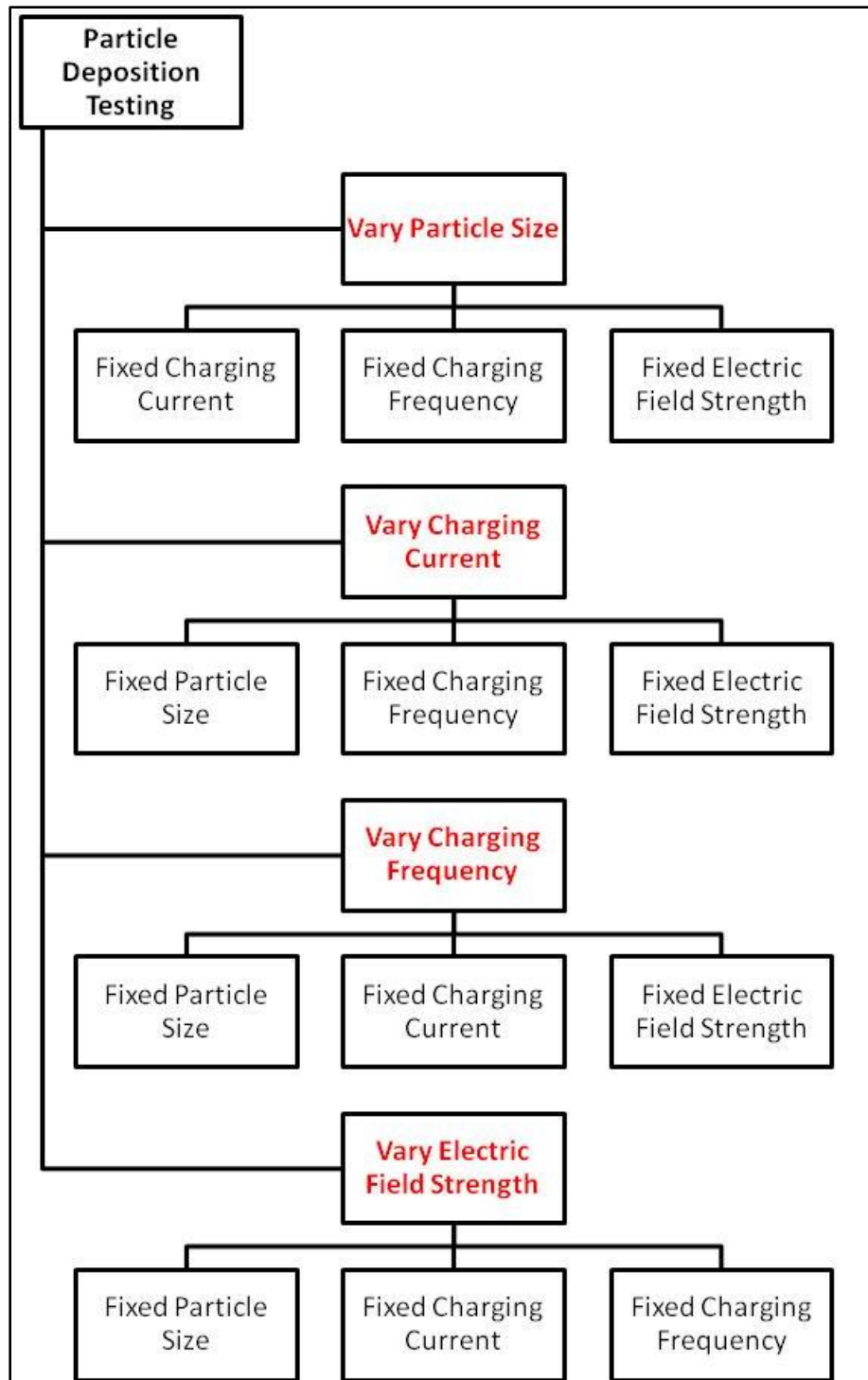


Figure 5-3: Example of suggested deposition testing plan by varying each operational variable. First, testing can be conducted by varying the particle size and fixing the other parameters. In a new set of experiments, the charging current can be varied while maintaining the other parameters fixed. In the next two sets of the experiments the charging frequency and electric field strength can then be changed.

Again, while limitations exist, more performance testing can be conducted with the Gillings Sampler. These tests can serve to obtain preliminary data of various test atmospheres, while also providing more insights into the performance of the sampler. Tests can be conducted with various test atmospheres that can include, but are not limited to, diesel and biodiesel exhaust, biomass fuel emissions, cigarette smoke, bioaerosols, and various nanomaterials. Also, further testing and cell exposures are needed of the mineral oil spiked with a "cocktail mix" that represents a complex mixture. Successful use of the mineral oil as a synthetic, non-toxic aerosol can lead to its use in other applications outside of air pollution exposure. Knowing the constraints of the Gillings Sampler, it can be used as an alternative exposure method to conduct complete inhalation exposures studies.

Based on work presented in this dissertation, and if the Gillings Sampler is to be used for conducting future cell exposure studies, I recommended following the experimental flow chart shown in Figure 5-4. In this experimental procedure, the cells to be used for the research study should first be exposed to clean filtered air as a negative control. By doing so, one can ensure that the Gillings Sampler does not induce toxicity due to possible contamination in the system or any other internal faults. Cells should then be exposed to the mineral oil aerosol with and without a toxic VOC, as described in Chapter 3, and the results from this positive control should be compared to previous mineral oil exposures. This quality assurance test will determine if the Gillings Sampler and exposed cells are providing reliable and reproducible biological data. Finally, cells can then be exposed to the test atmosphere of interest. Following this experimental procedure at the beginning of each research study will ensure that the Gillings Sampler is working at optimal conditions.

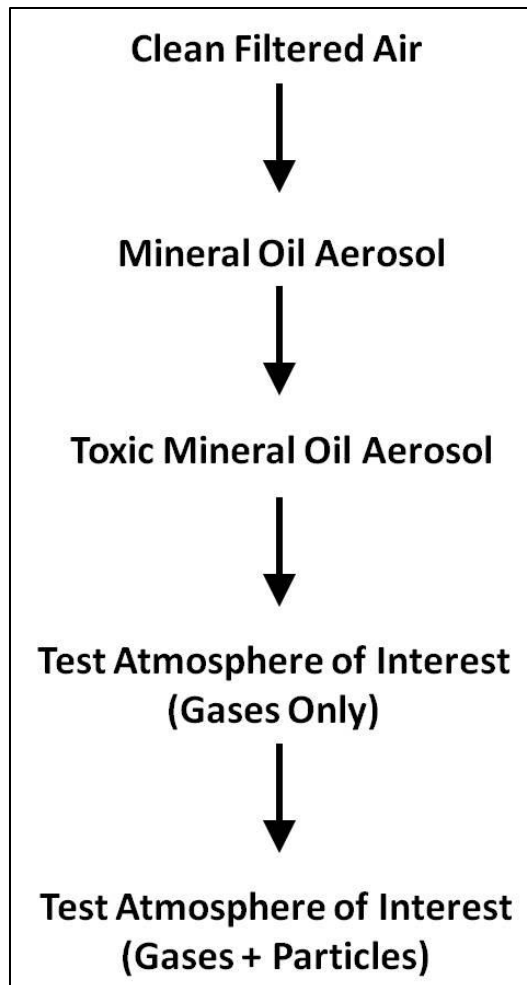


Figure 5-4: Recommended experimental flow chart for conducting future cell exposure studies with the Gillings Sampler.

Overall Conclusion

The Gillings Sampler was developed and tested under various environmental conditions to determine its efficacy in exposing lung cells to air pollutants at ALI by using electrostatics. The Gillings Sampler is intended to be used as an alternative research tool for aerosol *in vitro* exposure studies. While the condensed testing program detailed here does not cover every possible study for which the Gillings Sampler can be used, it represents possible areas of interests that could be further explored in future studies. Over the course of testing the Gillings Sampler under various realistic conditions, several operational problems and

limitations were identified. Although some limitations exist, the final production goal was achieved based on the list of goals that were established prior to the design and development phase of the Gillings Sampler.

As a result of the work presented in this dissertation, several provisional patents on this technology have been obtained. I am a lead inventor in the provisional patent obtained for the design of the deposition plate. I am also a co-inventor in the provisional patent obtained for the design of the heated humidification system. The work presented and the patents obtained contributed to create a start-up company named BioDeptronix, LLC – founded by various principal investigators involved with this work. This company was founded in effort to continue developing and optimizing the Gillings Sampler. Some of the limitations that were identified are already being addressed with the next-generation sampler named QuantAire™. The recommendations for future work presented here will be adapted by BioDeptronix, LLC to develop a commercially available *in vitro* aerosol sampler that can be used by other research groups.

The Gillings Sampler can help meet the needs of the scientific community to better address the link between multi-pollutant exposures and health effects. This new technology can serve as an alternative research tool for aerosol *in vitro* exposure studies, which can help achieve EPA and HEI's strategic plans toward setting standards for multi-pollutant mixtures and next-generation multi-pollutant approaches.^{1,3} Successful development of this innovative technology can help bridge the gap between toxicologist and epidemiologist, and affect policy decision-making by more accurately representing toxic effects and risk of exposure to air pollutants. By being portable and field-ready, the Gillings Sampler can be deployed in particular micro-environments, such as those downwind from an oil refinery. In the

environmental decision making process, measurements obtained from air monitoring stations are used, but these numbers do not entirely represent all the specific air quality conditions that communities have to endure. In future epidemiology studies, several Gillings Samplers can be deployed in locations where epidemiologists have identified a need for further investigation. Occupational settings where high levels of air pollutants are prominent can benefit from a portable aerosol *in vitro* system to monitor the toxic pollutant levels that workers are exposed to on a daily basis. While further testing and optimization is still required to produce a "commercially ready" *in vitro* system, the Gillings Sampler is a stepping-stone in the development of cost-effective *in vitro* technology that can be made accessible to researchers in the near future. Therefore, the Gillings Sampler has the potential to become a valuable research tool for the scientific community, policy makers, and to protect public health.

REFERENCES

1. Board of Scientific Counselors (BOSC). Mid-Cycle Review of the Office of Research and Development's Air Research Program at the U.S. Environmental Protection Agency. U S Environmental Protection Agency. 2008. In.
2. Dominici, F.; Peng, R. D.; Barr, C. D.; Bell, M. L., Protecting human health from air pollution: shifting from a single-pollutant to a multi-pollutant approach. *Epidemiology (Cambridge, Mass.)* **2010**, *21*, (2), 187.
3. Health Effects Institute (HEI). HEI Strategic Plan for Understanding Health Effects of Air Pollution 2010-2015. Boston, MA: HEI; 2010. In.
4. Dockery, D. W.; Pope, C. A., 3rd; Xu, X.; Spengler, J. D.; Ware, J. H.; Fay, M. E.; Ferris, B. G., Jr.; Speizer, F. E., An association between air pollution and mortality in six U.S. cities. *N Engl J Med* **1993**, *329*, (24), 1753-9.
5. Pope, C. A., 3rd; Thun, M. J.; Namboodiri, M. M.; Dockery, D. W.; Evans, J. S.; Speizer, F. E.; Heath, C. W., Jr., Particulate air pollution as a predictor of mortality in a prospective study of U.S. adults. *Am J Respir Crit Care Med* **1995**, *151*, (3 Pt 1), 669-74.
6. Pope, C. A., 3rd; Dockery, D. W., Health effects of fine particulate air pollution: lines that connect. *J Air Waste Manag Assoc* **2006**, *56*, (6), 709-42.
7. Valberg, P. A., Is PM more toxic than the sum of its parts? Risk-assessment toxicity factors vs. PM-mortality "effect functions". *Inhal Toxicol* **2004**, *16 Suppl 1*, 19-29.
8. Dockery, D. W.; Pope, C. A., 3rd; Kanner, R. E.; Martin Villegas, G.; Schwartz, J., Daily changes in oxygen saturation and pulse rate associated with particulate air pollution and barometric pressure. *Res Rep Health Eff Inst* **1999**, (83), 1-19; discussion 21-8.
9. Devlin, R. B.; Frampton, M. L.; Ghio, A. J., In vitro studies: what is their role in toxicology? *Exp Toxicol Pathol* **2005**, *57 Suppl 1*, 183-8.
10. Akhtar, U. S.; Scott, J. A.; Chu, A.; Evans, G. J., In vivo and in vitro assessment of particulate matter toxicology. In *Urban Airborne Particulate Matter*, 2011; pp 427-449.

11. MacClellan, R. O.; Henderson, R. F., *Concepts in inhalation toxicology*. CRC Press: 1995.
12. Holgate, S. T., *Air pollution and health*. Academic Press: San Diego, 1999; p xiv, 1065 p.
13. Salem, H.; Katz, S., *Inhalation toxicology*. In Boca Raton (FL): CRC Press, Taylor & Francis Group: 2006.
14. Cao, D.; Bromberg, P. A.; Samet, J. M., COX-2 expression induced by diesel particles involves chromatin modification and degradation of HDAC1. *American journal of respiratory cell and molecular biology* **2007**, *37*, (2), 232-239.
15. Ristovski, Z. D.; Miljevic, B.; Surawski, N. C.; Morawska, L.; Fong, K. M.; Goh, F.; Yang, I. A., Respiratory health effects of diesel particulate matter. *Respirology* **2012**, *17*, (2), 201-212.
16. Legrand, C.; Bour, J.; Jacob, C.; Capiaumont, J.; Martial, A.; Marc, A.; Wudtke, M.; Kretzmer, G.; Demangel, C.; Duval, D., Lactate dehydrogenase (LDH) activity of the number of dead cells in the medium of cultured eukaryotic cells as marker. *Journal of biotechnology* **1992**, *25*, (3), 231-243.
17. Seagrave, J. C.; McDonald, J. D.; Mauderly, J. L., In vitro versus in vivo exposure to combustion emissions. *Experimental and Toxicologic Pathology* **2005**, *57*, 233-238.
18. Paur, H. R.; Cassee, F. R.; Teeguarden, J.; Fissan, H.; Diabate, S.; Aufderheide, M.; Kreyling, W. G.; Hänninen, O.; Kasper, G.; Riediker, M.; Rothen-Rutishauser, B.; Schmid, O., In-vitro cell exposure studies for the assessment of nanoparticle toxicity in the lung-a dialogue between aerosol science and biology. *Journal of Aerosol Science* **2011**, *42*, (10), 668-692.
19. de Bruijne, K.; Ebersviller, S.; Sexton, K. G.; Lake, S.; Leith, D.; Goodman, R.; Jettens, J.; Walters, G. W.; Doyle-Eisele, M.; Woodside, R.; Jeffries, H. E.; Jaspers, I., Design and testing of electrostatic aerosol in vitro exposure system (EAVES): an alternative exposure system for particles. *Inhal Toxicol* **2009**, *21*, (2), 91-101.
20. Lichtveld, K.; Ebersviller, S. M.; Sexton, K. G.; Vizuete, W.; Jaspers, I.; Jeffries, H., In vitro exposures in diesel exhaust atmospheres: Resuspension of PM from filters versus direct deposition of PM from air. *Environmental Science & Technology* **2012**, *46*, (16), 9062-9070.

21. Tsien, A.; Diaz-Sanchez, D.; Ma, J.; Saxon, A., The Organic Component of Diesel Exhaust Particles and Phenanthrene, a Major Polyaromatic Hydrocarbon Constituent, Enhances IgE Production by IgE-Secreting EBV-Transformed Human B Cells in Vitro. *Toxicology and applied pharmacology* **1997**, *142*, (2), 256-263.
22. Hinds, W. C., *Aerosol technology : properties, behavior, and measurement of airborne particles*. 2nd ed.; Wiley: New York, 1999.
23. McDonald, J. D.; Barr, E. B.; White, R. K.; Chow, J. C.; Schauer, J. J.; Zielinska, B.; Grosjean, E., Generation and characterization of four dilutions of diesel engine exhaust for a subchronic inhalation study. *Environmental Science & Technology* **2004**, *38*, (9), 2513-2522.
24. Li, N.; Kim, S.; Wang, M.; Froines, J.; Sioutas, C.; Nel, A., Use of a stratified oxidative stress model to study the biological effects of ambient concentrated and diesel exhaust particulate matter. *Inhalation toxicology* **2002**, *14*, (5), 459-486.
25. Madden, M. C.; Dailey, L. A.; Stonehuerner, J. G.; Harris, D. B., Responses of cultured human airways epithelial cells treated with diesel exhaust extracts will vary with the engine load. *Journal of Toxicology and Environmental Health Part A* **2003**, *66*, (24), 2281-2297.
26. Jaspers, I.; Ciencewicz, J. M.; Zhang, W.; Brighton, L. E.; Carson, J. L.; Beck, M. A.; Madden, M. C., Diesel exhaust enhances influenza virus infections in respiratory epithelial cells. *Toxicological Sciences* **2005**, *85*, (2), 990-1002.
27. Madden, M. C., Complex issues with examining diesel exhaust toxicity: Is the task getting easier or harder? *Experimental and Toxicologic Pathology* **2008**, *60*, (2), 135-140.
28. Maier, K. L.; Alessandrini, F.; Beck-Speier, I.; Josef Hofer, T. P.; Diabaté, S.; Bitterle, E.; Stöger, T.; Jakob, T.; Behrendt, H.; Horsch, M., Health effects of ambient particulate matter-biological mechanisms and inflammatory responses to in vitro and in vivo particle exposures. *Inhalation toxicology* **2008**, *20*, (3), 319-337.
29. Blank, F.; Rothen-Rutishauser, B. M.; Schurch, S.; Gehr, P., An optimized in vitro model of the respiratory tract wall to study particle cell interactions. *Journal of aerosol medicine* **2006**, *19*, (3), 392-405.

30. Aufderheide, M.; Mohr, U., CULTEX - a new system and technique for the cultivation and exposure of cells at the air/liquid interface. *Experimental and Toxicologic Pathology* **1999**, *51*, (6), 489-490.
31. Aufderheide, M.; Mohr, U., A modified CULTEX® system for the direct exposure of bacteria to inhalable substances. *Experimental and Toxicologic Pathology* **2004**, *55*, (6), 451-454.
32. Lenz, A. G.; Karg, E.; Lentner, B.; Dittrich, V.; Brandenberger, C.; Rothen-Rutishauser, B.; Schulz, H.; Ferron, G. A.; Schmid, O., A dose-controlled system for air-liquid interface cell exposure and application to zinc oxide nanoparticles. *Particle and fibre toxicology* **2009**, *6*, 32.
33. Tippe, A.; Heinzmann, U.; Roth, C., Deposition of fine and ultrafine aerosol particles during exposure at the air/cell interface. *Journal of Aerosol Science* **2002**, *33*, (2), 207-218.
34. Cooney, D. J.; Hickey, A. J., Cellular response to the deposition of diesel exhaust particle aerosols onto human lung cells grown at the air-liquid interface by inertial impaction. *Toxicology In Vitro* **2011**, *25*, (8), 1953-1965.
35. Aufderheide, M.; Halter, B.; Möhle, N.; Hochrainer, D., The CULTEX RFS: A comprehensive technical approach for the in vitro exposure of airway epithelial cells to the particulate matter at the air-liquid interface. *BioMed Research International* **2013**, *2013*, 734137.
36. Savi, M.; Kalberer, M.; Lang, D.; Ryser, M.; Fierz, M.; Gaschen, A.; RicÅåka, J.; Geiser, M., A novel exposure system for the efficient and controlled deposition of aerosol particles onto cell cultures. *Environmental Science & Technology* **2008**, *42*, (15), 5667-5674.
37. Volckens, J.; Dailey, L.; Walters, G.; Devlin, R. B., Direct particle-to-cell deposition of coarse ambient particulate matter increases the production of inflammatory mediators from cultured human airway epithelial cells. *Environmental Science & Technology* **2009**, *43*, (12), 4595-4599.
38. Ning, Z.; Sillanpää, M.; Pakbin, P.; Sioutas, C., Field evaluation of a new particle concentrator-electrostatic precipitator system for measuring chemical and toxicological properties of particulate matter. *Particle and fibre toxicology* **2008**, *5*, (1), 15.

39. Desantes, J.; Margot, X.; Gil, A.; Fuentes, E., Computational study on the deposition of ultrafine particles from Diesel exhaust aerosol. *Journal of Aerosol Science* **2006**, *37*, (12), 1750-1769.
40. Boelter, K. J.; Davidson, J. H., Ozone generation by indoor, electrostatic air cleaners. *Aerosol Sci Tech* **1997**, *27*, (6), 689-708.
41. Whitby, K.; Charlson, R.; Wilson, W.; Stevens, R.; Lee, R. E., The size of suspended particle matter in air. *Science* **1974**, *183*, (4129), 1098-1100.
42. Knutson, E.; Whitby, K., Aerosol classification by electric mobility: apparatus, theory, and applications. *Journal of Aerosol Science* **1975**, *6*, (6), 443-451.
43. *WHO Air Quality Guidelines for Particulate Matter, Ozone, Nitrogen Dioxide and Sulfur Dioxide. Global Update 2005, Summary of Risk Assessment*; World Health Organization: 2006.
44. Cohen, A. J.; Anderson, H. R.; Ostro, B.; Pandey, K. D.; Krzyzanowski, M.; Künzli, N.; Gutschmidt, K.; Pope, A.; Romieu, I.; Samet, J. M., The global burden of disease due to outdoor air pollution. *Journal of Toxicology and Environmental Health, Part A* **2005**, *68*, (13-14), 1301-1307.
45. Strak, M.; Janssen, N. A. H.; Godri, K. J.; Gosens, I.; Mudway, I. S.; Cassee, F. R.; Lebret, E.; Kelly, F. J.; Harrison, R. M.; Brunekreef, B., Respiratory health effects of airborne particulate matter: The role of particle size, composition, and oxidative potential - The RAPTES Project. *Environmental Health Perspectives* **2012**, *120*, (8), 1183.
46. *EPA Air Quality Criteria for Particulate Matter (Final Report, Oct 2004)*; U.S. Environmental Protection Agency: Washington, DC, 2004.
47. Dvorak, A.; Tilley, A.; Shaykhiev, R.; Wang, R.; Crystal, R., Do airway epithelium air-liquid cultures represent the in vivo airway epithelium transcriptome? *American journal of respiratory cell and molecular biology* **2011**, *44*, (4), 465.
48. Ebersviller, S.; Lichtveld, K.; Sexton, K.; Zavala, J.; Lin, Y.; Jaspers, I.; Jeffries, H., Gaseous VOCs rapidly modify particulate matter and its biological effects - Part 1: Simple VOCs and model PM. *Atmos. Chem. Phys.* **2012**, *12*, 12277-12292.
49. Ebersviller, S.; Lichtveld, K.; Sexton, K.; Zavala, J.; Lin, Y.; Jaspers, I.; Jeffries, H., Gaseous VOCs rapidly modify particulate matter and its biological

- effects - Part 2: Complex urban VOCs and model PM. *Atmos. Chem. Phys.* **2012**, *12*, 12293-12312.
50. Morris, J. B.; Shusterman, D., *Toxicology of the nose and upper airways*. Informa Healthcare USA: New York, 2010.
 51. Liu, B. Y. H.; Whitby, K. T.; Yu, H. H. S., Electrostatic aerosol sampler for light and electron microscopy. *Review of Scientific Instruments* **1967**, *38*, (1), 100-102.
 52. Sillanpää, M.; Geller, M. D.; Phuleria, H. C.; Sioutas, C., High collection efficiency electrostatic precipitator for in vitro cell exposure to concentrated ambient particulate matter (PM). *Journal of Aerosol Science* **2008**, *39*, (4), 335-347.
 53. Han, B.; Hudda, N.; Ning, Z.; Kim, Y.-J.; Sioutas, C., Efficient Collection of Atmospheric Aerosols with a Particle Concentrator - Electrostatic Precipitator Sampler. *Aerosol Sci Tech* **2009**, *43*, (8), 757-766.
 54. Jaspers, I.; Flescher, E.; Chen, L., Ozone-induced IL-8 expression and transcription factor binding in respiratory epithelial cells. *American Journal of Physiology-Lung Cellular and Molecular Physiology* **1997**, *272*, (3), L504.
 55. Bosson, J.; Stenfors, N.; Bucht, A.; Helleday, R.; Pourazar, J.; Holgate, S. T.; Kelly, F. J.; Sandstrom, T.; Wilson, S.; Frew, A. J.; Blomberg, A., Ozone-induced bronchial epithelial cytokine expression differs between healthy and asthmatic subjects. *Clin Exp Allergy* **2003**, *33*, (6), 777-82.
 56. Gerritsen, W. B.; Asin, J.; Zanen, P.; van den Bosch, J. M.; Haas, F. J., Markers of inflammation and oxidative stress in exacerbated chronic obstructive pulmonary disease patients. *Respir Med* **2005**, *99*, (1), 84-90.
 57. Holgate, S. T.; Sandstrom, T.; Frew, A. J.; Stenfors, N.; Nordenhall, C.; Salvi, S.; Blomberg, A.; Helleday, R.; Soderberg, M., Health effects of acute exposure to air pollution. Part I: Healthy and asthmatic subjects exposed to diesel exhaust. *Res Rep Health Eff Inst* **2003**, (112), 1-30; discussion 51-67.
 58. Ordonez, C. L.; Shaughnessy, T. E.; Matthay, M. A.; Fahy, J. V., Increased neutrophil numbers and IL-8 levels in airway secretions in acute severe asthma: Clinical and biologic significance. *Am J Respir Crit Care Med* **2000**, *161*, (4 Pt 1), 1185-90.

59. Liu, B. Y. H.; Verma, A. C., Pulse-charging, pulse-precipitating electrostatic aerosol sampler. *Analytical Chemistry* **1968**, *40*, (4), 843-847.
60. Aufderheide, M.; Scheffler, S.; Möhle, N.; Halter, B.; Hochrainer, D., Analytical in vitro approach for studying cyto- and genotoxic effects of particulate airborne material. *Analytical and bioanalytical chemistry* **2011**, *401*, (10), 3213-3220.
61. Anderson, S. E.; Jackson, L. G.; Franko, J.; Wells, J., Evaluation of dicarbonyls generated in a simulated indoor air environment using an in vitro exposure system. *Toxicological Sciences* **2010**, *115*, (2), 453-461.
62. Aufderheide, M.; Mohr, U., CULTEX - an alternative technique for cultivation and exposure of cells of the respiratory tract to airborne pollutants at the air/liquid interface. *Experimental and Toxicologic Pathology* **2000**, *52*, (3), 265-270.
63. Phillips, J.; Kluss, B.; Richter, A.; Massey, E., Exposure of bronchial epithelial cells to whole cigarette smoke: assessment of cellular responses. *Altern Lab Anim* **2005**, *33*, (3), 239-48.
64. Stevens, J.; Zahardis, J.; MacPherson, M.; Mossman, B.; Petrucci, G., A new method for quantifiable and controlled dosage of particulate matter for in vitro studies: The electrostatic particulate dosage and exposure system (EPDExS). *Toxicology in Vitro* **2008**, *22*, (7), 1768-1774.
65. Hawley, B.; Volckens, J., Proinflammatory effects of cookstove emissions on human bronchial epithelial cells. *Indoor air* **2013**, *23*, (1), 4-13.
66. Grosjean, D.; Grosjean, E.; Gertler, A. W., On-road emissions of carbonyls from light-duty and heavy-duty vehicles. *Environmental Science & Technology* **2001**, *35*, (1), 45-53.
67. May, K., The Collison nebulizer: description, performance and application. *Journal of Aerosol Science* **1973**, *4*, (3), 235-243.
68. Doyle, M.; Sexton, K. G.; Jeffries, H.; Bridge, K.; Jaspers, I., Effects of 1,3-butadiene, isoprene, and their photochemical degradation products on human lung cells. *Environ Health Perspect* **2004**, *112*, (15), 1488-95.
69. Doyle, M.; Sexton, K. G.; Jeffries, H.; Jaspers, I., Atmospheric photochemical transformations enhance 1,3-butadiene-induced inflammatory responses in human epithelial cells: The role of ozone and other photochemical degradation products. *Chem Biol Interact* **2007**, *166*, (1-3), 163-9.

70. Sexton, K. G.; Jeffries, H. E.; Jang, M.; Kamens, R. M.; Doyle, M.; Voicu, I.; Jaspers, I., Photochemical products in urban mixtures enhance inflammatory responses in lung cells. *Inhal Toxicol* **2004**, *16 Suppl 1*, 107-14.
71. Kocbach, A.; Totlandsdal, A.; Låg, M.; Refsnes, M.; Schwarze, P., Differential binding of cytokines to environmentally relevant particles: A possible source for misinterpretation of in vitro results? *Toxicology letters* **2008**, *176*, (2), 131-137.
72. Kroll, A.; Pillukat, M. H.; Hahn, D.; Schnekenburger, J., Interference of engineered nanoparticles with in vitro toxicity assays. *Archives of toxicology* **2012**, *86*, (7), 1123-1136.
73. Seagrave, J.; Knall, C.; McDonald, J. D.; Mauderly, J. L., Diesel particulate material binds and concentrates a proinflammatory cytokine that causes neutrophil migration. *Inhalation toxicology* **2004**, *16*, (s1), 93-98.
74. Apple, J.; Vicente, R.; Yarberry, A.; Lohse, N.; Mills, E.; Jacobson, A.; Poppendieck, D., Characterization of particulate matter size distributions and indoor concentrations from kerosene and diesel lamps. *Indoor air* **2010**, *20*, (5), 399-411.
75. Schare, S.; Smith, K. R., Particulate emission rates of simple kerosene lamps. *Energy for Sustainable Development* **1995**, *2*, (2), 32-35.
76. Venn, A. J.; Yemaneberhan, H.; Bekele, Z.; Lewis, S. A.; Parry, E.; Britton, J., Increased risk of allergy associated with the use of kerosene fuel in the home. *American journal of respiratory and critical care medicine* **2001**, *164*, (9), 1660-1664.
77. Wainman, T.; Zhang, J.; Weschler, C. J.; Lioy, P. J., Ozone and limonene in indoor air: a source of submicron particle exposure. *Environmental Health Perspectives* **2000**, *108*, (12), 1139.
78. Anderson, S. E.; Khurshid, S. S.; Jean Meade, B.; Lukomska, E.; Wells, J., Toxicological analysis of limonene reaction products using an in vitro exposure system. *Toxicology in Vitro* **2012**.
79. Sunil, V. R.; Laumbach, R. J.; Patel, K. J.; Turpin, B. J.; Lim, H.-J.; Kipen, H. M.; Laskin, J. D.; Laskin, D. L., Pulmonary effects of inhaled limonene ozone reaction products in elderly rats. *Toxicology and applied pharmacology* **2007**, *222*, (2), 211-220.

80. Devlin, R. B.; Duncan, K. E.; Jardim, M.; Schmitt, M. T.; Rappold, A. G.; Diaz-Sanchez, D., Controlled Exposure of Healthy Young Volunteers to Ozone Causes Cardiovascular Effects Clinical Perspective. *Circulation* **2012**, *126*, (1), 104-111.
81. Devlin, R. B.; McDonnell, W. F.; Mann, R.; Becker, S.; House, D. E.; Schreinemachers, D.; Koren, H. S., Exposure of humans to ambient levels of ozone for 6.6 hours causes cellular and biochemical changes in the lung. *American journal of respiratory cell and molecular biology* **1991**, *4*, (1), 72-81.
82. Triantaphyllopoulos, K.; Hussain, F.; Pinart, M.; Zhang, M.; Li, F.; Adcock, I.; Kirkham, P.; Zhu, J.; Chung, K. F., A model of chronic inflammation and pulmonary emphysema after multiple ozone exposures in mice. *American Journal of Physiology-Lung Cellular and Molecular Physiology* **2011**, *300*, (5), L691-L700.
83. Shore, S. A.; Rivera-Sanchez, Y. M.; Schwartzman, I.; Johnston, R. A., Responses to ozone are increased in obese mice. *J Appl Physiol* **2003**, *95*, (3), 938-945.
84. Devlin, R.; McKinnon, K.; Noah, T.; Becker, S.; Koren, H., Ozone-induced release of cytokines and fibronectin by alveolar macrophages and airway epithelial cells. *American Journal of Physiology-Lung Cellular and Molecular Physiology* **1994**, *266*, (6), L612-L619.
85. Jeffries, H. E., Photochemical air pollution. In *Composition, chemistry, and climate of the atmosphere*, Singh, H., Ed. Van Nostrand-Reinhold.: New York, 1995; pp 308–348.
86. Seaman, V. Y.; Charles, M. J.; Cahill, T. M., A sensitive method for the quantification of acrolein and other volatile carbonyls in ambient air. *Analytical Chemistry* **2006**, *78*, (7), 2405-2412.
87. Liu, X.; Jeffries, H. E.; Sexton, K. G., Atmospheric photochemical degradation of 1, 4-unsaturated dicarbonyls. *Environmental Science & Technology* **1999**, *33*, (23), 4212-4220.
88. Yu, J.; Jeffries, H. E.; Sexton, K. G., Atmospheric photooxidation of alkylbenzenes—I. Carbonyl product analyses. *Atmospheric Environment* **1997**, *31*, (15), 2261-2280.
89. Yu, J.; Jeffries, H. E.; Le Lacheur, R. M., Identifying airborne carbonyl compounds in isoprene atmospheric photooxidation products by their

- PFBHA oximes using gas chromatography/ion trap mass spectrometry. *Environmental Science & Technology* **1995**, 29, (8), 1923-1932.
90. You, Y.; Richer, E. J.; Huang, T.; Brody, S. L., Growth and differentiation of mouse tracheal epithelial cells: selection of a proliferative population. *American Journal of Physiology-Lung Cellular and Molecular Physiology* **2002**, 283, (6), L1315-L1321.
91. Wu, W.; Silbajoris, R. A.; Cao, D.; Bromberg, P. A.; Zhang, Q.; Peden, D. B.; Samet, J. M., Regulation of cyclooxygenase-2 expression by cAMP response element and mRNA stability in a human airway epithelial cell line exposed to zinc. *Toxicology and applied pharmacology* **2008**, 231, (2), 260-266.